Scalable and Practical Probability Density Estimators for Scientific Anomaly Detection

Dan Pelleg

May 2004

CMU-CS-04-134

School of Computer Science
Carnegie Mellon University
Pittsburgh, PA 15213

Submitted in partial fulfillment of the requirements for the degree of Doctor of Philosophy.

This research was sponsored by the National Science Foundation (NSF) under grant no. ACI-0121671 and no. DMS-9873442.

Keywords: Machine Learning, Scientific Discovery, Mixture Models, Probability Density Estimators, Efficient Algorithms

To my parents, Gershon and Ilana.

Acknowledgments

First and foremost, I thank Orna for immeasurable help. Much of it was given under workload that was challenging for both of us. This work would not have been possible without her help.

I am deeply indebted to Andrew Moore. He had guided me intellectually, lent his incredibly sharp insight, and provided so much help outside of his academic duties, that merely calling him “advisor” would be misleading.

I would like to thank Mihai Budiu, Scott Davies, Danny Sleator, Alex Gray, and Larry Wasserman for helpful discussions, and Andy Connolly and Bob Nichol for enlightening discussions and data. Andy Connolly also patiently sat in front of my crude tools and provided valuable expert feedback.

I am grateful to the members of the Auton lab for numerous ideas, brainstorms, and help.

Abstract

Originally, astronomers dealt with stars. Later, with galaxies. Today, large scale cosmological structures are so complex, they must be first reduced into more succinct representations. For example, a universe simulation containing millions of objects is characterized by its halo occupation distribution.

This progression is typical of many disciplines of science, and even resonates in our daily lives. The easier it is for us to collect new data, store it and manage it, the harder it becomes to keep up with what it all means. For that we need to develop tools capable of mining big data sets.

This new generation of data analysis tools must meet the following requirements. They have to be fast and scale well to big data. Their output has to be straightforward to understand and easy to visualize. They need to only ask for the minimum of user input - ideally they would run completely autonomously once given the data.

I focus on clustering. Its main advantage is its generality. Separating data into groups of similar objects reduces the perception problem significantly. In this context, I propose new algorithms and tools to meet the challenges: an extremely fast spatial clustering algorithm, which can also estimate the number of clusters; a novel and highly comprehensible mixture model; a sub-linear learner for dependency trees; and an active learning framework to minimize the burden on a human expert hunting for rare anomalies. I implemented the algorithms and used them with very large data sets in a wide variety of applications, including astrophysics.

Contents

1 Fast K-means **7**

1.1 Introduction 8

1.2 Definitions 9

1.3 Algorithms 14

1.3.1 The Simple Algorithm 19

1.3.2 The "Blacklisting" Algorithm 20

1.4 Implementation 21

1.5 Experimental Results 24

1.5.1 Approximate Clustering 28

1.6 Related Work 32

1.6.1 Improvements over fast mixture-of-Gaussians 34

1.7 Conclusion 35

2 X-means **39**

2.1 Introduction 40

2.2 Definitions 41

2.3 Estimation of K 41

2.3.1 Model Searching 42

2.3.2 BIC Scoring 46

2.3.3 Anderson-Darling Scoring 47

2.3.4 Acceleration 49

2.4 Experimental Results 52

2.5 Conclusion 57

3 Mixtures of Rectangles **61**

3.1 Introduction 62

3.2 The Probabilistic Model and Derivation of the EM Step 63
3.2.1 Tailed Rectangular Distributions 63
3.2.2 Maximum Likelihood Estimation of a Single Tailed Rectangular Distribution 66
3.2.3 EM Search for a Mixture of Tailed Rectangles 67
3.2.4 The Full Algorithm 68
3.2.5 Example 68
3.2.6 Intuition 68
3.3 Experimental Results 68
3.4 Conclusion 80

4 Fast Dependency Tree Construction 81
4.1 Introduction 81
4.2 A Slow Minimum-Spanning Tree Algorithm 83
4.3 Probabilistic Bounds on Mutual Information 84
4.4 The Full Algorithm 92
4.4.1 Algorithm Complexity 93
4.5 Experimental Results 94
4.5.1 Sensitivity Analysis 98
4.5.2 Real Data 101
4.6 Red vs. Blue Rule 102
4.7 Error Analysis 105
4.8 Conclusion 106

5 Active Learning for Anomaly Detection 109
5.1 Introduction 109
5.2 Overview of Hint Selection Methods 113
5.2.1 Choosing Points with Low Likelihood 114
5.2.2 Choosing Ambiguous Points 116
5.2.3 Combining Unlikely and Ambiguous Points 117
5.2.4 The “interleave” Method 117
5.3 Experimental Results 119
5.4 Scalability 124
5.5 Conclusion 126

6 Anomaly Hunting 129

6.1 Background 129

6.2 Indicators and Controls 130

6.3 Case Study 134

6.3.1 Requested Features 135

6.4 Conclusion 136

List of Figures

1.1 K-means example on a 2-D set (1) . . . 10
1.2 K-means example on a 2-D set (2) . . . 11
1.3 K-means example on a 2-D set (3) . . . 12
1.4 K-means example on a 2-D set (4) . . . 13
1.5 Domination with respect to a hyper-rectangle. . . . 17
1.6 Non-domination with respect to a hyper-rectangle. . . . 18
1.7 A recursive procedure to assign cluster memberships. . . . 19
1.8 Visualization of the hyper-rectangles owned by centroids . . . 20
1.9 Blacklisting of centroids . . . 22
1.10 Adding to the black list . . . 23
1.11 Comparative results on simulated data . . . 27
1.12 Effect of dimensionality on the blacklisting algorithm . . . 28
1.13 Effect of number of centroids on the blacklisting algorithm . . . 29
1.14 Effect of number of points on the blacklisting algorithm . . . 29
1.15 Approximated K-means . . . 30
1.16 Runtime of approximate clustering . . . 31
1.17 Distortion of approximate clustering . . . 31

2.1 The X-means algorithm. . . . 42
2.2 X-means example (1) . . . 44
2.3 X-means example (2) . . . 44
2.4 X-means example (3) . . . 45
2.5 X-means example (4) . . . 45
2.6 X-means example (5) . . . 45
2.7 X-means overfitting . . . 48
2.8 Distortion of X-means and K-means . . . 52

2.9 Estimated number of classes 54
2.10 BIC of X-means and K-means 55
2.11 Run times of X-means and K-means 56
2.12 Galaxy cluster sizes 58

3.1 A one-dimensional tailed interval 64
3.2 The 2-dimensional form of a rectangle with tails. 65
3.3 Fitting an interval with tails in one dimension 69
3.4 Fitting a two-dimensional rectangle 70
3.5 Fitting a two-dimensional mixture (1) 71
3.6 Fitting a two-dimensional mixture (2) 72
3.7 A three-component example 73
3.8 Estimated boundaries for the “checkerboard” data 74
3.9 Grid cells used generation of “cube” data 75
3.10 Fit to the “cube” data 76
3.11 Goodness of fit to synthetic mixtures 77
3.12 Fit with an incorrect number of rectangles 78

4.1 The MIST algorithm 85
4.2 MIST example (1) 86
4.3 MIST example (2) 87
4.4 MIST example (3) 88
4.5 MIST example (4) 89
4.6 Data usage 95
4.7 Running time 96
4.8 Log-likelihood (1) 96
4.9 Log-likelihood (2) 97
4.10 The data-generation algorithm 98
4.11 Structure of the generated data for 14 attributes. 98
4.12 Edge usage as a function of noise 99
4.13 Running time as a function of δ and ϵ 100
4.14 Log-likelihood as a function of δ and ϵ 100
4.15 Edge-usage as a function of ϵ 101
4.16 Relative log-likelihood vs. relative time, as a function of ϵ 102

4.17 The Red Edge rule 104
4.18 The Blue Edge rule 104
4.19 Interval estimates 106

5.1 Anomalies (Sloan data). 110
5.2 The active learning loop 111
5.3 Underlying data distribution for the example. 113
5.4 Behavior of the lowlik method 115
5.5 Behavior of the ambig method 116
5.6 Behavior of the interleave method. 117
5.7 Different kinds of detected anomalies 119
5.8 Learning curves for simulated data 121
5.9 Learning curves for the ABALONE set 122
5.10 Learning curves for the SHUTTLE set 123
5.11 Learning curves for the KDD set 123
5.12 Learning curves for the EDSGC set 125
5.13 Learning curves for the SDSS set 125
5.14 Various objects spotted with the anomaly-hunting tool (Sloan data). . 127

6.1 The anomaly hunting application 130
6.2 The object information window 131
6.3 The object explanation window 132
6.4 The scatterplot window 133
6.5 The web window 133
6.6 Ranks of anomalous objects 135

List of Tables

1.1 Comparative results on real data 25
1.2 Comparison against BIRCH 26

2.1 Goodness of X-means fit for synthetic data 53
2.2 Comparison of K-means, BIRCH, and X-means 54

3.1 Clusters for the “mpg” data 78
3.2 Clusters for the “census” data 79

4.1 Results on real data 103

5.1 Properties of data sets 124

Introduction

Whenever we approach the so-called "data mining" problem, we realize it means different things to different people. Scientists and analysts — the consumers of algorithms and of data products — relate to the various *tasks*: pattern recognition, structural organization, regression, anomaly finding, and so on. On top of that, we as computer scientists — producers of algorithms and tools — break it down to its building blocks: statistics, computational complexity, and knowledge management.

On first glance, it would seem this disparity has the potential for many false expectations and impossible requirements. But the truth is that this very tension is what advances research in the field. Here is how it typically happens. A scientist has had access to some source of data, say experiments performed in his lab. Over time he had accumulated a set of tools and techniques to analyze it. But recently, the amount of data has become much larger. Possibly, new internet-based collaboration points give him easy access to the results of other researchers' work. Or perhaps new machinery and methods are producing data orders of magnitude better — and faster — than before. The Sloan Digital Sky Survey is a prime example of this. The goal is to map, in detail, one-quarter of the entire sky. The estimated size of the catalog, due to be completed in 2007, is 200 million objects, including images and spectroscopic data. The database will then encompass 5 terabytes of catalog data, and 25 terabytes of data overall.

The unforeseen outcome of such endeavors is that suddenly, the old tools become useless. It might be because their theoretic complexity is poor and they blow up on large inputs. Or because study of a single experiment is no longer interesting, when one can potentially draw conclusions based on thousands of similar observations. Or because the rate at which new results come exceeds the ability of an expert to internalize it all, as the old summarization and visualization methods are inadequate.

This is the light under which the issues addressed in this work are best viewed. Fundamentally, it deals with the difficulties of computer-literate and resourceful scientists in a new world of abundant data. More concretely, we break this down into several distinct components, each attempting to solve an admittedly small aspect of the problem. The unifying element is the task - *clustering*. Historically, this is a task that does not have a good definition that is both general and statistically rigorous. We offer the intuitive definition of partitioning a given unlabeled data set into groups such that elements in each group are somewhat more similar to each other (in some unspecified measure of similarity) than they are to elements in other groups.[1]

Clustering can help in understanding the nature of a given data set in several ways. First, the membership function by itself is meaningful, as it allows further research involving just the part of the data that is of interest. For example, large-scale cosmology simulations as well as recent astronomical surveys enable computation of the correlation between the number of galaxies in a galaxy cluster, and the amount of dark matter in it ("halo occupation distribution"). But before doing this, the mapping from each galaxy to its owning cluster needs to be established.

A second potentially useful output is the number of clusters, if it is estimated by the algorithm. This can serve as a characteristic of the data. Again we relate to the universe example above for an example. By looking at the distribution of galaxy cluster sizes, one can "profile" a given universe. This is potentially useful when judging if a universe simulated from specific parameters is similar to the observed universe (and also when analyzing the effect of changes to the simulation parameters). Here, the number of clusters — typically in the order of thousands — clearly has to be estimated from the data.

Third, the very description of the clusters defines subregions of the data space. These descriptions can be used to achieve insights into the data. For example, if the regions are convex, one can come up with unseen examples that would be included in a given cluster. This ability can be useful for computer program verification tools which aim to increase test-suite coverage.

Fourth, if the statistical model fitted to the data is a probability density estimator, it can be used in a variety of related tasks. All the models described in this work meet this criterion. Below we show how to use such models in an anomaly-hunting task.

Note that we assume here that clusters form a flat hierarchy. This is somewhat arbitrary, as a huge body of existing work deals with hierarchical clustering and fitting of taxonomies. Much of that work is focused on information retrieval. Therefore, it

[1]Later we weaken this definition even further by considering the extension where each element does not have to fully belong to just one class.

is sufficiently different from the kinds of data analyzed here to be outside the scope of this work.

Clustering is used in a multitude of application areas. Some of them are:

- Large-scale cosmological simulations.
- Astronomical data analysis.
- Bioinformatics.
- Computer architecture.
- Musical information retrieval.
- Verification of computer programs.
- Natural language processing.
- Epidemiology.
- Highway traffic analysis.

Diverse as they are, in all of them we encounter similar phenomena. First, labels for individual samples are rare or nonexistent (and too costly to obtain in the general case). Second, the data is too voluminous to be entirely eyeballed by a human expert. In fact, often it is too voluminous to even process mechanically quickly enough. To illustrate the last point, consider an anomaly-hunting application which asks a human expert for labels for a very small number of examples. Given those, it refines the statistical model using the given examples and the full data set, and the cycle repeats. Regardless of data set size, the computer run needs to finish quickly, or else the expert would lose concentration.

Returning to the historical angle, most of the data analysts are already familiar with some clustering method or another. The problem is that it is too slow on big inputs. Generally, there are three approaches to address the speed issue:

1. Develop new algorithms and data-organization methods, such that the statistical qualities of the data can be approximated quickly. Use the approximated measures to generate output in the same form as the existing algorithms.

2. Develop exact and fast algorithms that output the exact same answer as the original method. Enhance the data organization to support this kind of operation.

3. Develop near-exact algorithms using advanced data organization. Allow a user-defined degree of error, or a probabilistic chance of making a mistake. Typically those parameters will be very small.

The first example of the first approach is BIRCH (Zhang et al., 1995). It is an approximate clusterer optimized for on-disk storage of large data sets. The clusters are grown in a heuristic way. Very little can be said on the quality of the output clusters, or about their difference from those obtained by some other method.

Another example of the first approach is sub-sampling. The idea is simple: randomly select a small population from the input set and run the algorithm of choice on it. A variant of this uses the results together with the original data set as if they were created directly from the original set. For example, one might create clusters based on a small sample, and then use the cluster centroids (or any other meaningful property) to assign class membership to points in the original data.

Often, this approach is taken without much consideration of the statistical consequences. Not surprisingly, they can be severe. For example, the 2-point correlation function is used in cosmology to characterize sets of astronomical objects. It is well-known that for the rich structure observed in our universe, straightforward sub-sampling does not preserve the 2-point correlation function. And the same most likely holds for other measures.

My conclusion is that there is merit in expending the effort to develop schemes that can handle large data without affecting output quality. When this is too hard, we would still like to bound the error in some way. This work aims to show that this goal is achievable.

Below I describe how to accelerate several known algorithms, such that their output can be used in exactly the same way as the output from the respective original published versions. Empirical evaluation shows great speed-ups for many of them — often two orders of magnitude faster than a straightforward implementation, measured on actual data sets used by scientists. In one case the run time is even sub-linear in the input size, and only depends on intrinsic properties of the data.

Chapter 1 looks at the familiar K-means algorithm and shows how it can be accelerated by re-structuring the data. The output is exact (meaning the same as it would be for a non-optimized algorithm). Chapter 2 uses the same fast data structure to build a framework supporting estimation of the number of clusters K. The framework exploits the data structure to accelerate the statistical test used for model selection. It is also general in the sense that it allows a variety of statistical measures for scoring and decision between different models. Chapter 3 takes a detour to look at human comprehensibility. It proposes a new statistical model which lends itself to succinct descriptions of clusters. This description can be read by a domain expert with no knowledge of machine learning, and its predicates can be interpreted directly in the application domain. In Chapter 4 we return to dealing with a well-known statistical algorithm. This time we focus on dependency trees as grown by popular the Chow-Liu algorithm and propose a “probably approximately correct” algorithm to fit them. It can decide to consider just a subset of the data for certain computations, if this can be justified by data data already scanned. In practice, this typically happens very quickly, resulting in large speed-ups. In Chapter 5 we consider the task of anomaly-hunting in large noisy sets, where the classes containing the anomalies are extremely rare. For help, we consult an “oracle” for labels for a very small number of examples, which naturally touches on active learning. This work uses the fast dependency tree learner, however it is not dependent on it and can use other models as components. Finally, in Chapter 6 I describe a visual tool based on these ideas, which enables an expert to interact with the data and find anomalies quickly.

Chapter 1

Fast K-means

Modern cosmology relies on simulation data to validate or disprove theories. For example, a universe of several million objects would be created and evolved over time. The simulation data is then available for large-scale analysis. Historically, such tasks — including clustering — were performed on huge data sets by taking a random sub-sample and applying the technique on hand to the smaller set such that it finishes in a reasonable amount of time. Afterwards the results (say, cluster definitions) are somehow projected back to the original data space.

This kind of approach is impractical for cosmology. The fundamental reason is that the rich structure of the universe cannot be easily down-sampled. For example, the 2-point correlation function is used as a succinct summary of spatial data. It is known that random sampling fails to preserve the properties of the 2-point function. Therefore any astrophysicist would be justified to suspect output from a process that starts by reducing the data in such a destructive way. The right way is to devise ways to process large amounts of data natively.

I present new algorithms for the K-means clustering problem. While being extremely fast, they do not make any kind of approximation. Empirical results show a speedup factor of up to 170 on real astrophysical data, and superiority over the naive algorithm on simulated data. My algorithms scale sub-linearly with respect to the number of points and linearly with the number of clusters. This allows for clustering with tens of thousands of centroids and millions of points using commodity hardware.

1.1 Introduction

Consider a dataset with R records, each having M attributes. Given a constant k, the *clustering* problem is to partition the data into k subsets such that each subset behaves "well" under some measure. For example, we might want to minimize the squared Euclidean distances between points in any subset and their center of mass. The *K-means* algorithm for clustering finds a local optimum of this measure by keeping track of centroids of the subsets, and issuing a large number of nearest-neighbor queries (Gersho & Gray, 1992).

A *kd-tree* is a data structure for storing a finite set of points from a finite-dimensional space (Bentley, 1980). Its usage in very fast EM-based Mixture Model Clustering was shown by Moore (1998). The need for such a fast algorithm arises when conducting massive-scale model selection, and in datasets with a large number of attributes and records. An extreme example is the data which is gathered in the Sloan Digital Sky Survey (SDSS) (SDSS, 1998), where M is about 500 and R is in the tens of millions.

In this chapter, I show that *kd*-trees can be used to reduce the number of nearest-neighbor queries in K-means by using the fact that their nodes can represent a large number of points. I am frequently able to prove for certain nodes of the *kd*-tree statements of the form "any point associated with this node must have X as its nearest neighbor" for some centroid X. This, together with a set of statistics stored in the *kd*-nodes, allows for great reduction in the number of arithmetic operations needed to update the centroids of the clusters.

I have implemented my algorithms and tested their behavior with respect to variations in the number of points, dimensions, and centroids, as measured on synthetic data. I also present results of tests on preliminary SDSS data.

The remainder of this chapter is organized as follows. In Section 1.2 I introduce notation and describe the original K-means algorithm. In Section 1.3 I present my algorithms with proofs of correctness. Section 1.4 elaborates on the finer points of the implementation. Section 1.5 discusses results of experiments on real and simulated data. Section 1.6 discusses related work, and Section 1.7 concludes and suggests ideas for further work.

1.2 Definitions

Throughout this chapter, I denote the number of records by R, the number of dimensions by M and the number of centroids by k.

I first describe the naive K-means algorithm for producing a clustering of the points in the input into k clusters. It is the best known of all clustering algorithms, and literally hundreds of papers about its theory and deployment have appeared in the statistics literature in the last 20 years (Duda & Hart, 1973; Bishop, 1995). It partitions the data points into k subsets such that all points in a given subset "belong" to some centroid. The algorithm keeps track of the centroids of the subsets, and proceeds in iterations. We denote the set of centroids after the i-th iteration by $C^{(i)}$. Before the first iteration the centroids are initialized to arbitrary locations. The algorithm terminates when $C^{(i)}$ and $C^{(i-1)}$ are identical. In each iteration, the following is performed:

1. For each point x, find the centroid in $C^{(i)}$ which is closest to x. Associate x with this centroid.
2. Compute $C^{(i+1)}$ by taking, for each centroid, the center of mass of points associated with this centroid.

Figures 1.1, 1.2 and 1.3 give a graphical demonstration of K-means when run on an example dataset.

My algorithms involve modification of just the code within one iteration. I therefore analyze the cost of a single iteration. The naive K-means described above performs a nearest-neighbor query for each of the R points. During such a query the distances in M-space to k centroids are calculated. Therefore the cost is $O(kMR)$.

One fundamental tool I will use to tackle the problem is the *kd*-tree data-structure. I outline its relevant properties, and from this point on will assume that a *kd*-tree for the input points exists. Further details about *kd*-trees can be found in Moore (1991). I will use a specialized version of *kd*-trees called *mrkd*-trees, for "multi-resolution *kd*-trees" (Deng & Moore, 1995). The properties of *kd*-trees relevant to this work are:

- They are binary trees.
- Each node contains information about all points contained in a hyper-rectangle h. The hyper-rectangle is stored at the node as two M-length boundary vectors

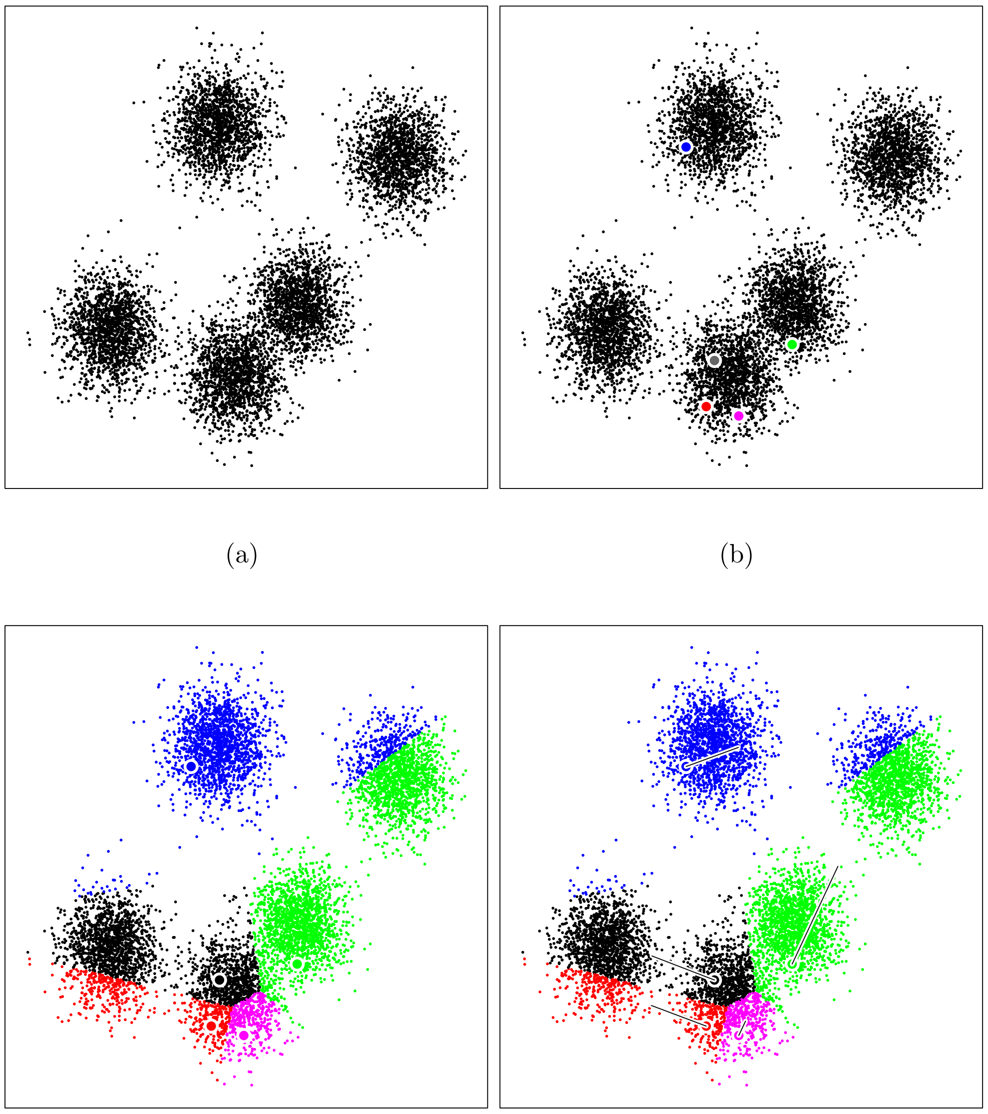

(a) (b)

(c) (d)

Figure 1.1: A 2-D set of 8000 points, drawn from a mixture of 5 spherical Gaussians (a). The 5 initial centroids (b). The partition induced by the centroids (c). For each centroid, the center of mass of points it owns is computed and connected to its current location with a line (d). Note how black and red share the left-hand cluster, and will "race" towards it. (Continued).

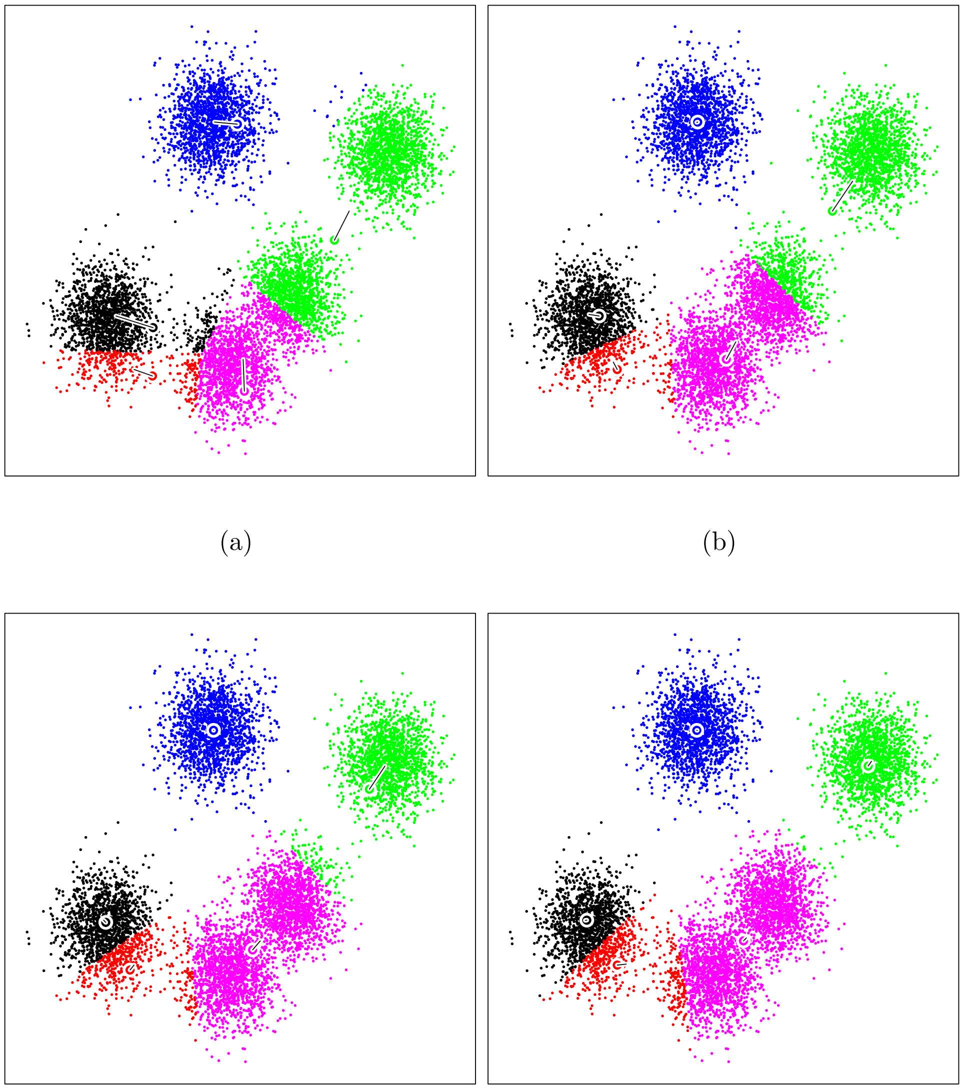

(a) (b) (c) (d)

Figure 1.2: K-means demo (cont'd). After centroid movement, membership is recomputed, and so are the new locations (a). The current boundary between blue and green is on the unpopulated middle ground, which is indicative of good separation. After another iteration, blue and green are nearly settled (b). Pink owns two clusters while red is pushed away from the black cluster (c). Slowly, red starts gaining pink points (d). (Continued).

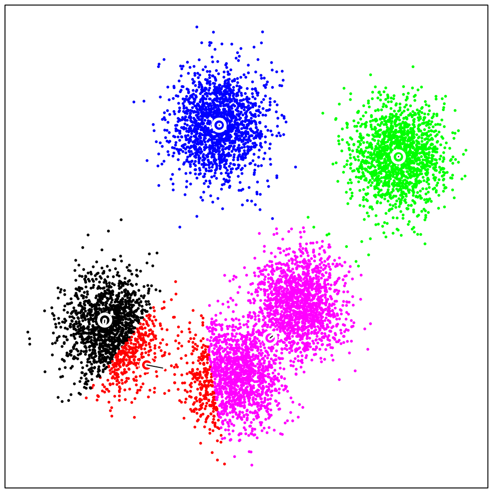

(a)

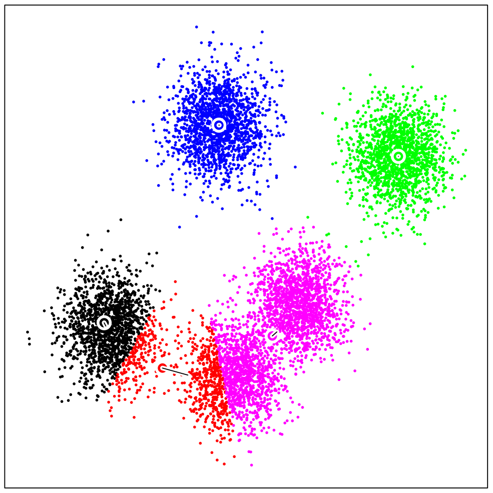

(b)

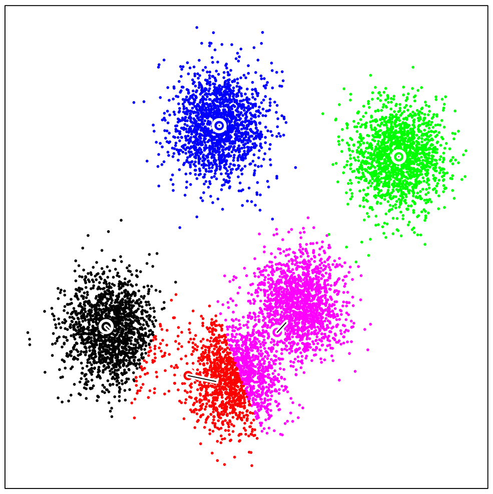

(c)

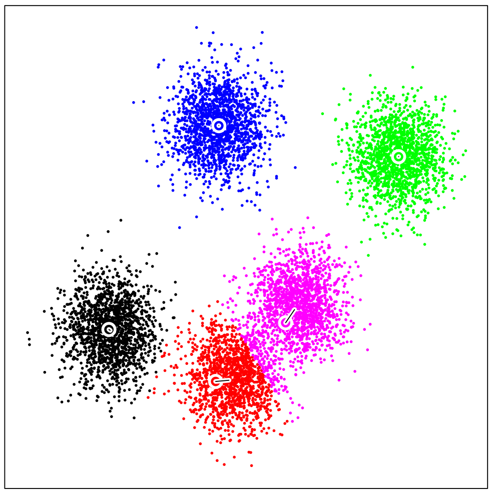

(d)

Figure 1.3: *K*-means demo (cont'd). Red completes the move toward "its" cluster (a-d). (Continued).

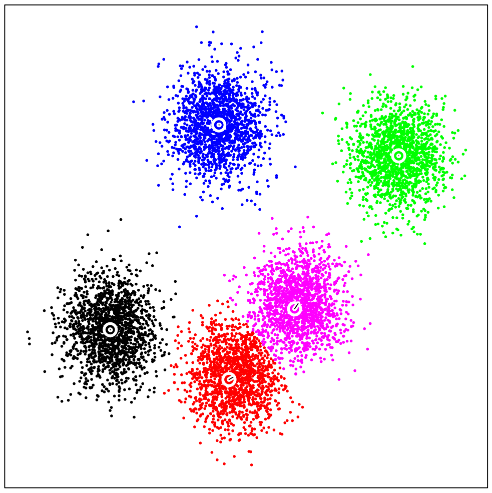

(a)

Figure 1.4: K-means demo (cont'd). The final configuration (a).

$h^{\max}$ and $h^{\min}$. At the node are also stored the number, center of mass, and sum of Euclidean norms, of all points within h. All children of the node represent hyper-rectangles which are contained in h.

- Each non-leaf node has a "split dimension" d and a "split value" v. Its children l (resp. r) represent the hyper-rectangles h_l (h_r), both within h, such that all points in h_l (h_r) have their d-th coordinate value smaller than (at least) v.
- The root node represents the hyper-rectangle which encompasses all of the points.
- Leaf nodes store the actual points.

For two points x, y we denote by $d(x, y)$ their Euclidean distance. For a point x and a hyper-rectangle h we define $\text{closest}(x, h)$ to be the point in h which is closest to x. Note that computing $\text{closest}(x, h)$ can be done in time $O(M)$ due to the following facts:

- If $x \in h$, then x is closest.
- Otherwise, $\text{closest}(x, h)$ is on the boundary of h. This boundary point can be found by clipping each coordinate of x, to lie within h. More precisely this means applying Equation 3.1 in each dimension.

We define the distance $d(x,h)$ between a point x and a hyper-rectangle h to be $d(x, \text{closest}(x,h))$. For a hyper-rectangle h we denote by $\text{width}(h)$ the vector $h^{\max} - h^{\min}$.

Given a clustering ϕ, we denote by $\phi(x)$ the centroid this clustering associates with an arbitrary point x (so for K-means, $\phi(x)$ is simply the centroid closest to x). We then define a measure of quality for ϕ:

$$\text{distortion}_{\phi} = \frac{1}{R} \cdot \sum_{x} d^2(x, \phi(x)) \ , \tag{1.1}$$

where R is the total number of points and x ranges over all input points.

1.3 Algorithms

My algorithms exploit the fact that instead of updating the centroids point by point, a more efficient approach is to update in bulk. This can be done using the known centers of mass and size of groups of points. Specifically, we look at the center-of-mass update from Algorithm 1.2:

$$C_j^{(i+1)} = \frac{\sum_{x \in Q} \vec{x}}{|Q|} \tag{1.2}$$

where j indexes some centroid and Q denotes all the points "belonging" to this centroid (I omit the iteration and centroid indices from Q for clarity). Now consider some partition of Q, that is a set $\{Q_p\}$ such that:

$$\begin{aligned} \bigcup_p Q_p &= Q \\ Q_p \cap Q_j &= \emptyset \ \forall i \neq j \ . \end{aligned}$$

It is obviously true that

$$C_j^{(i+1)} = \frac{\sum_p \sum_{x \in Q_p} \vec{x}}{\sum_p |Q_p|} \ . \tag{1.3}$$

Naturally, the sets Q_p will correspond to nodes in the *kd*-tree. Recall that for those we compute the sums and counts of the included points in advance and store them with the node. Hence the inner summation above reduces to a simple look-up.

The optimization above is not limited to vector sums. Any kind of additive quantity can be computed in the same way. The count is another such measure (the value summed for each point being one). I use it also to compute the distortion. The key equality for this is:

$$\begin{aligned} d^2(x,y) &= (\vec{x}-\vec{y})\cdot(\vec{x}-\vec{y}) \\ &= ||x||^2 - 2x\cdot y + ||y||^2 \ . \end{aligned}$$

In the distortion computation (see Equation 1.1), x ranges over points and $y=\phi(x)$ is the owning centroid. So for a particular subset Q_p such that all points in it belong to the same centroid, y is a constant and can be factored out. Additionally I pre-compute and store $\sum ||x||^2$ for each *kd*-node similarly to the vector sums. I also use a similar technique in obtaining the sets of points which belong to each centroid (as needed by some statistics). For other obtainable statistics see Zhang et al. (1995).

The challenge now shifts to making sure that all of the points in a given hyper-rectangle indeed "belong" to a specific centroid before adding their statistics to it. Below I lay out a framework to support these kinds of assertions. We begin with the notion of an *owner*.

Definition 1 *Given a set of centroids C and a hyper-rectangle h, we define by $\mathit{owner}_C(h)$ a centroid $c \in C$ such that any point in h is closer to c than to any other centroid in C, if such a centroid exists.*

We will omit the subscript C where it is clear from the context. The rest of this section discusses owners and efficient ways to find them. We start by analyzing a property of owners, which, by listing those centroids which *do not* have it, will help us eliminate non-owners from the set of possibilities. Note that $\mathrm{owner}_C(h)$ is not always defined. For example, when two centroids are both *inside* a rectangle, then there exists no unique owner for this rectangle. Therefore the precondition of the following theorem is that there exists a unique owner. The algorithmic consequence is that my method will not always find an owner, and will sometimes be forced to descend the *kd*-tree, thereby splitting the hyper-rectangle in hope to find an owner for the smaller hyper-rectangle. I return to this scenario later. For now I give a necessary condition for an owner.

Theorem 2 *Let C be a set of centroids, and let h be a hyper-rectangle. Let $c \in C$ be $\mathit{owner}_C(h)$. Then:*

$$d(c,h) = \min_{c' \in C} d(c',h) \ .$$

Proof: Assume, for the sake of contradiction, that $c \neq \arg\min_{c' \in C} d(c', h) \equiv c^*$. Then there exists a point in h (namely closest(c^*, h)) which is closer to c' than to c. This is in contradiction to the definition of c as owner(h). $\square$

We distinguish between "shortest" and "minimal" distance. We define *shortest* to be the optimized measure only when it is unique. In contrast, the definition of *minimal* always holds and includes any element which attains the minimum. So there can be multiple minimal elements. But only if there is a single such element, then we say it attains the shortest distance. In these terms, we can say that when looking for owner(h), we should only consider centroids with shortest distance $d(c, h)$. For example, suppose that two (or more) centroids share the minimal distance to h. Then neither can claim to be an owner. This situation arises more often than one would initially expect. In particular, all the centroids inside a given *kd*-node have distance zero to the node.

Theorem 2 narrows down the number of possible owners to either one (if there exists a shortest distance centroid) or zero (otherwise). In the latter case, my algorithm will proceed by splitting the hyper-rectangle. In the former case, all we have is a necessary condition, but it is not sufficient. Consequently we still have to check if this candidate is an owner of the hyper-rectangle in question. As will become clear from the following discussion, this will not always be the case. Let us begin by defining a restricted form of ownership, where just two centroids are involved.

Definition 3 *Given a hyper-rectangle h, and two centroids c^1 and c^2 such that $d(c^1, h) < d(c^2, h)$, we say that c^1* dominates *c^2 with respect to h if every point in h is closer to c^1 than it is to c^2.*

Observe that if some $c \in C$ dominates *all* other centroids with respect to some h, then $c =$ owner(h). A possible (albeit inefficient) way of finding owner(h) if one exists would be to scan all possible pairs of centroids. However, using theorem 2, we can reduce the number of pairs to scan since c^1 is fixed. To prove this approach feasible we need to show that the domination decision problem can be solved efficiently.

Lemma 4 *Given two centroids c^1, c^2, and a hyper-rectangle h such that $d(c^1, h) < d(c^2, h)$, the decision problem "does c^1 dominate c^2 with respect to h?" can be answered in $O(M)$ time.*

Proof: Observe the decision line L_{12} composed of all points which are equidistant to c^1 and c^2 (see Figures 1.5 and 1.6). If c^1 and h are both fully contained in one half-

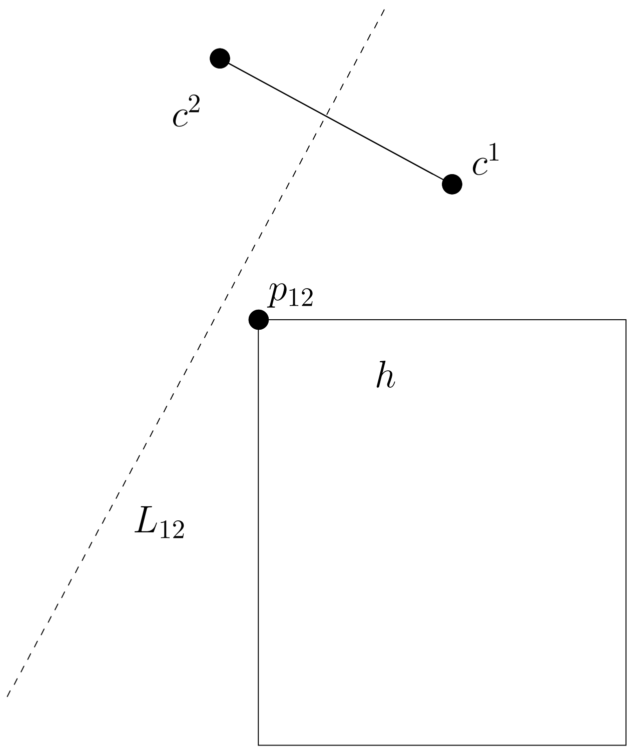

Figure 1.5: Domination with respect to a hyper-rectangle.
L_{12} is the decision line between centroids c^1 and c^2. p_{12} is the extreme point in h in the direction $c^2 - c^1$, . Since p_{12} is on the same side of L_{12} as c^1, c^1 dominates c^2 with respect to the hyper-rectangle h.

space defined by L, then c^1 dominates c^2. The converse is also true; consider a point $x \in h$ such that it is not in the same half-space of L_{13} as c^1, then $d(c^1, x) > d(c^3, x)$ and c^1 does not dominate c^3. It is left to show that finding whether c^1 and h are contained in the same half-space of L can be done efficiently. Consider the vector $\vec{v} \equiv c^2 - c^1$. Let p be a point in h which maximizes the value of the inner product $\langle v, p \rangle$. This is the extreme point in h in the direction $\vec{v}$ (in other words, p is the closest one can get to L, within h). Note that $\vec{v}$ is perpendicular to $\vec{L}$. If p is closer to c^1 than it is to c^2, then so is any point in h. If not, p is a proof that c^1 does not dominate c^2.

Furthermore, the linear program "maximize $\langle v, p \rangle$ such that $p \in h$" can be solved in time $O(M)$. Again we notice the extreme point is a corner of h. The LP solution is attained by, for each coordinate i, choosing p_i to be $h_i^{\max}$ if $c_i^2 > c_i^1$, and $h_i^{\min}$ otherwise. $\square$

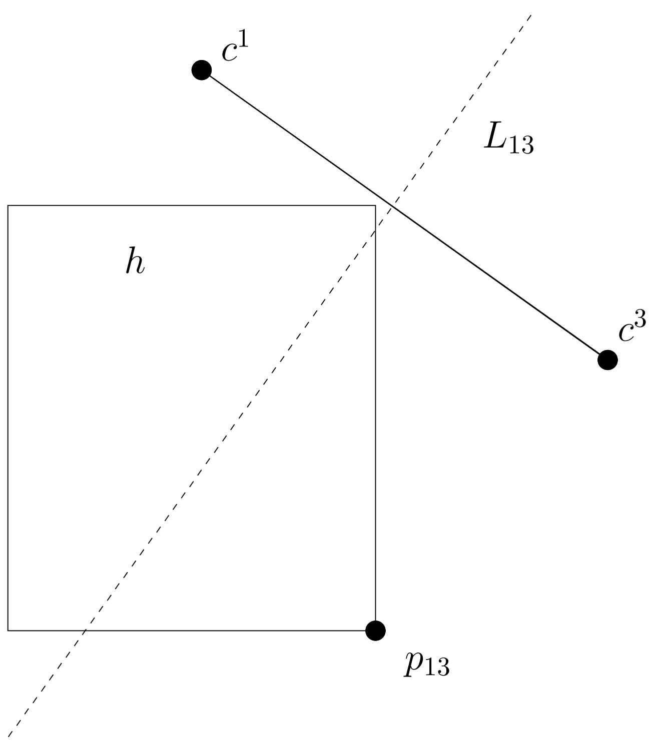

Figure 1.6: Non-domination with respect to a hyper-rectangle. L_{13} is the decision line between c^1 and c^3. p_{13} is the extreme point in h in the direction $c^3 - c^1$. Since p_{13} is *not* on the same side of L_{13} as c^1, c^1 does not dominate c^3.

```
Update($h, C$):
  1. If $h$ is a leaf:
      (a) For each data point in $h$, find the closest centroid to it
          and update the counters for that centroid.
      (b) Return.
  2. Compute $d(c, h)$ for all centroids $c$. If there exists one centroid
     $c$ with shortest distance:
          If for all other centroids $c'$, $c$ dominates $c'$ with respect to
          $h$ (so we have established $c = \text{owner}(h)$):
          (a) Update counters for $c$ using the data in $h$.
          (b) Return.
  3. Call Update($h_l, C$).
  4. Call Update($h_r, C$).
```

Figure 1.7: A recursive procedure to assign cluster memberships.

1.3.1 The Simple Algorithm

I now describe a procedure to update the centroids in $C^{(i)}$. It will take into consideration an additional parameter, a hyper-rectangle h such that all points in h affect the new centroids. The procedure is recursive, with the initial value of h being the universal hyper-rectangle with all of the input points in it. If the procedure can find owner(h), it updates its counters using the center of mass and number of points which are stored in the *kd*-node corresponding to h (I will frequently interchange h with the corresponding *kd*-node). Otherwise, it splits h by recursively calling itself with the children of h. Pseudo-code for this procedure is in Figure 1.7. The correctness follows from the discussion above.

We would not expect my Update procedure to prune in the case that h is the universal set of all input points (since all centroids are contained in it, and therefore no shortest-distance centroid exists). We also notice that if the hyper-rectangles were split again and again so that the procedure is dealing just with leaves, this method would be identical to the original K-means. In fact, this implementation will be

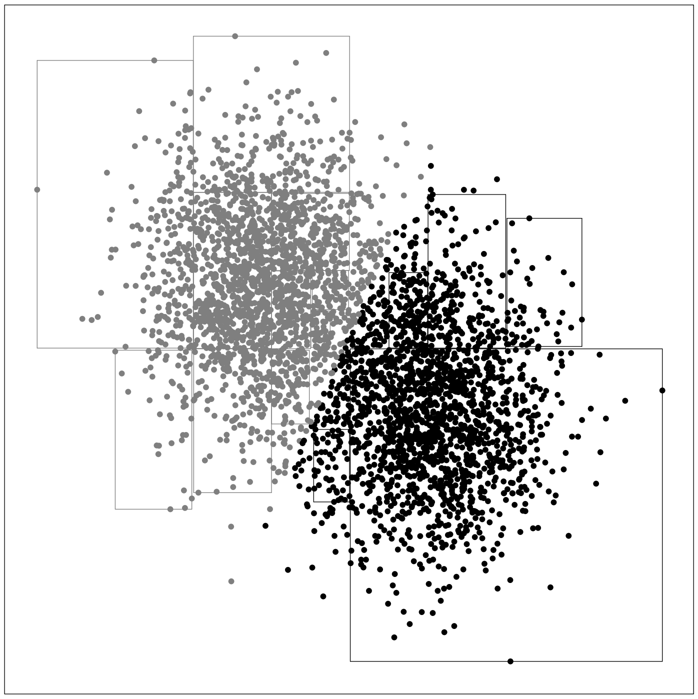

Figure 1.8: Visualization of the hyper-rectangles owned by centroids. The entire two-dimensional dataset is drawn as points in the plane. All points that "belong" to a specific centroid are colored the same color (here, K=2). The rectangles for which it was possible to prove that belong to specific centroids are also drawn. Points outside of rectangles had to be determined in the slow method (by scanning each centroid). Points within rectangles were not considered by the algorithm. Instead, their number and center of mass are stored together with the rectangle and are used to update the centroid coordinates.

more expensive because of the redundant overhead. Therefore our hope is that large enough hyper-rectangles will be owned by a single centroid to make this approach worthwhile. See Figure 1.8 for a visualization of the procedure in operation.

1.3.2 The "Blacklisting" Algorithm

My next algorithm is a refinement of the simple algorithm. The idea is to identify those centroids which will definitely *not* be owners of the hyper-rectangle h. If we can show this is true for some centroid c, there is no point in checking c for any of the descendants of h, hence the term "blacklisting". Let c^1 be a minimal-distance centroid to h, and let c^2 be any centroid such that $d(c^2, h) > d(c^1, h)$. If c^1 dominates c^2 with respect to h, we have two possibilities. One, that $c^1 = \text{owner}(h)$. This is the good case since we do not need any more computation. The other option is that we have not identified an owner for this node. The slow algorithm would have given up at this point and restarted a computation for the children of h. For the blacklisting version, we make use of the following.

Lemma 5 *Given two centroids c^1 and c^2 such that c^1 dominates c^2 with respect to a hyper-rectangle h, c^1 also dominates c^2 with respect to any $h' \subseteq h$.*

Proof: Immediate from Definition 3. $\square$

Theorem 6 *Given two centroids c^1 and c^2 such that c^1 dominates c^2 with respect to a kd-node h, it is not necessary to consider c^2 for the purpose of determining $\text{owner}_C(h')$ for any descendant of h.*

Proof: Recall that each *kd*-node fully contains any of its descendants. Let h' be a descendant of h. From Lemma 5 we get that c^1 dominates c^2 with respect to h'. Therefore c^2 cannot be $\text{owner}_C(h')$. $\square$

The blacklisting version makes use of Theorem 6 by removing c^2 from the list of candidates. The list of prospective owners thus shrinks until it reaches a size of 1. At this point we declare the only remaining centroid the owner of the current node h. Again, we hope this happens before h is a leaf node, to maximize the savings. But even if it does not, we still save work by not considering any centroid in the blacklist. Figure 1.9 shows how the blacklist evolves during a traversal of an example *kd*-tree. For a typical run with 30000 points and 100 centroids, I measured that blacklisting algorithm calculates distances from points to centroids about 270000 times in each iteration. This, plus the overhead, is to be compared with the 3 million distances the naive algorithm has to calculate.

1.4 Implementation

The implementation uses the following architecture for flexibility. The tree-traversal code is generic, and provides hooks for the following actions and predicates:

- Action to perform when discovering a point belongs to some centroid.

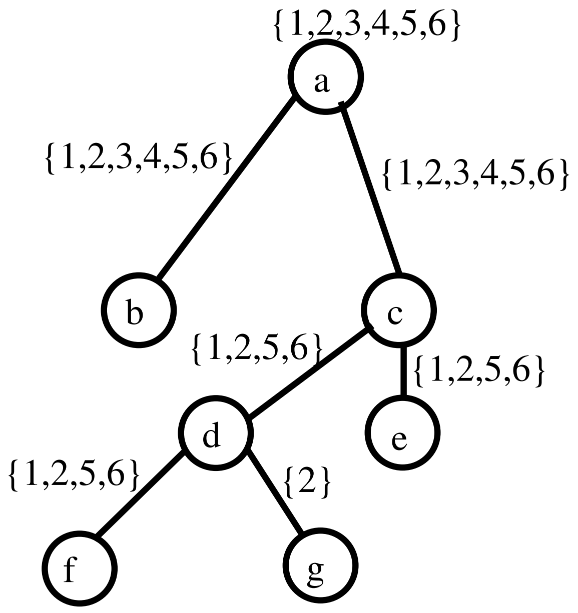

Figure 1.9: Blacklisting of centroids. The root node *a* has to consider all of the six centroids. They are passed to its children *b* and *c*. Node *b* does not manage to eliminate any, but *c* eliminates centroids 3 and 4 (see Figure 1.10). Consequently a shorter list is passed down to its children *d* and *e*, and so on. Node *g* manages to shorten the list to a single centroid, therefore it is wholly owned by it. When a leaf node cannot shorten the list to length one, distances for each point and remaining centroid are computed.

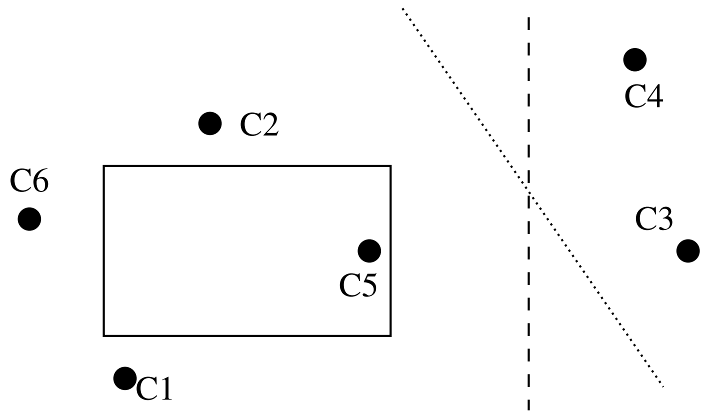

Figure 1.10: Adding to the black list. An example configuration consistent with the blacklisting for node c in Figure 1.9. Centroid $c5$ is closet to the kd-node in question. The two boundary lines prove that it dominates $c3$ and $c4$ respectively with respect to the node. Therefore $c3$ and $c4$ can be eliminated from future searches.

- Action to perform when discovering a whole kd-node belongs to some centroid.
- Predicate for pruning the search at this node and not traversing its descendants.

This framework proved useful in supporting many kinds of operations on the kd-trees. Among them:

- Maintaining vector sums and counts for center-of-mass calculations.
- Maintaining second moment sums for distortion calculations.
- Output of membership lists.
- Localized K-means runs (see Chapter 2).

Another optimization relates to the locality of changes in centroid locations. Often, some regions of the data will stabilize faster than others, in the sense that centroids in them will reach their final locations much sooner. For example, see how in Figure 1.3 (a–d), the top two centroids do not move at all while the bottom centroids still exchange data points. The opportunity here is to save computation by re-using membership information from previous iterations.

The way to achieve this is by storing the results of computations for future use. This is done at the kd-node level. For example, we might record that in a given node, there were two specific centroids competing for the points, as well the total contribution to the accumulated moments due to the node for each of the centroids. This is done during the traversal by considering the values for the accumulators before and after the node is processed. The difference is stored in the node, along with the list of competitors. If, during a subsequent traversal, the competitor list is the same as it is in the cache for this node, the stored statistics are added to the running accumulators instead of traversing the node. There is a small limit to the length of the competitor list, to save memory and to ensure that caching is done only at local regions.

A pre-assumption of this caching scheme is that centroid identifiers are indicative of their location. Assume that we cache the effect some node would have on centroids numbers 3 and 5. Before the next iteration, one or both of them moves slightly. On the next iteration, we could still have 3 and 5 as the only competitors for the node. However matching on the identifiers 3 and 5 and using old information would be wrong, since the new locations can shift the balance between them considerably.

We therefore use a write-once data structure to store centroids. It supports insert and delete operations, but not update. Whenever a centroid moves, we delete its old identifier and insert a new item. This way, a match in identifiers guarantees both elements are indeed equal.

1.5 Experimental Results

I have conducted experiments on both real and randomly-generated data. The real data is preliminary SDSS data with some 400,000 celestial objects. The synthetic data covers a wide range of parameters that might affect the performance of the algorithms. Some of the measures are comparative, and measure the performance of my algorithms against the naive algorithm, and against the BIRCH (Zhang et al., 1995) algorithm. Others simply test the behavior of my fast algorithm on different inputs.

The real data is a two-dimensional data set, containing the X and Y coordinates of objects observed by a telescope. There were 433,208 such objects in my data set. Note that "clustering" in this domain has a well-known astrophysical meaning of clusters of galaxies, etc. Such clustering, however, is somewhat insignificant in a two-dimensional domain since the physical placement of the objects is in 3-space. The results are shown in Table 1.1. The main conclusion is that the blacklisting algorithm executes 25 to 176 times faster than the naive algorithm, depending on the number of points.

points	blacklisting	naive	speedup
50000	2.02	52.22	25.9
100000	2.16	134.82	62.3
200000	2.97	223.84	75.3
300000	1.87	328.80	176.3
433208	3.41	465.24	136.6

Table 1.1: Comparative results on real data. Run-times of the naive and blacklisting algorithm, in seconds per iteration. Run-times of the naive algorithms also shown as their ratio to the running time of the blacklisting algorithm, and as a function of number of points. Results were obtained on random samples from the 2-D “petro” file using 5000 centroids.

In addition, I have conducted experiments with the BIRCH algorithm (Zhang et al., 1995). It is similar to my approach in that it keeps a tree of nodes representing sets of data points, together with sufficient statistics. The experiment was conducted as follows. I let BIRCH run through phases 1 through 4 and terminate, measuring the total run-time. This is normal mode of operation for BIRCH. Then I ran my K-means algorithm for as many iterations as possible, given this time limit. I then measured the distortion of the clustering output by both algorithms. The results are in Table 1.2. In seven experiments out of ten, the blacklisting algorithm produced better (i.e., lower distortion) results. These experiments include randomly generated data files originally used as a test-case in Zhang et al. (1995), random data files generated by me, and real data.

The synthetic experiments were conducted in the following manner. First, a data set was generated using 72 randomly-selected points (class centers). For each data point, a class was first selected at random. Then, the point coordinates were chosen independently under a Gaussian distribution with mean at the class center, and deviation σ equal to the number of dimensions times 0.025. One data set contained $200,000$ points drawn this way. The naive, hyperplane-based, and blacklisting algorithms were run on this data set and measured for speed. Notice that all three algorithms generate exactly the same set of centroids in each iteration, so the number of iterations for all three of them is identical, given the data set. This experiment was repeated 30 times and averages were taken. The number of dimensions varied from 2 to 16. The number of clusters each algorithm was requested to find was 72. The results are shown in Figure 1.11. The main observation is that for this data, the blacklisting algorithm is faster than the naive approach in 2 to 6 dimensions, with speedup of up to 27-fold in two dimensions. In higher dimensions it is slower. My

dataset	form	points	K	blacklisting distortion	BIRCH distortion	BIRCH, relative
1	grid	100000	100	1.85	**1.76**	0.95
2	sine	100000	100	2.44	**1.99**	0.82
3	random	100000	100	**6.98**	8.98	1.29
4	random	200000	250	**7.94e-4**	9.78e-4	1.23
5	random	200000	250	**8.03e-4**	1.01e-3	1.25
6	random	200000	250	**7.91e-4**	1.00e-3	1.27
7	real	100000	1000	3.59e-2	**3.17e-2**	0.88
8	real	200000	1000	**3.40e-2**	3.51e-2	1.03
9	real	300000	1000	**3.73e-2**	4.19e-2	1.12
10	real	433208	1000	**3.37e-2**	4.08e-2	1.21

Table 1.2: Comparison against BIRCH. The distortion for the blacklisting and BIRCH algorithms, given equal run-time, is shown. Six of the datasets are simulated and 4 are real ("petro" data from SDSS). Datasets 1–3 are as published in Zhang et al. (1995). Datasets 4–6 were generated randomly as described. For generated datasets, the number of classes in the original distribution is also the number of centroids reported to both algorithms. The last column shows the BIRCH output distortion divided by the blacklisting output distortion (i.e., if it is larger than 1 than BIRCH is performing worse).

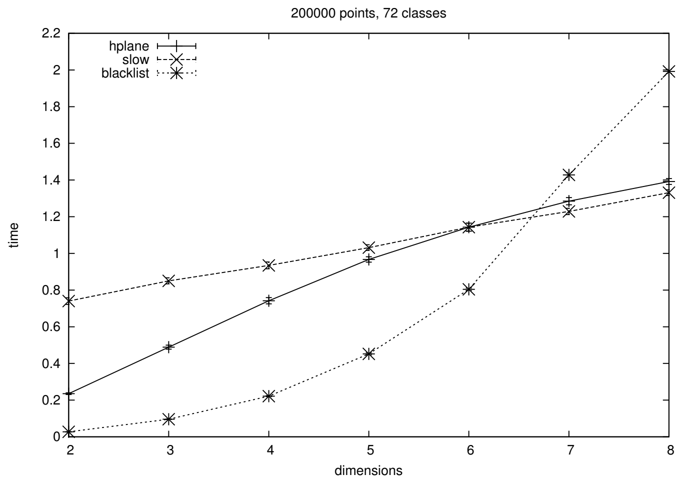

Figure 1.11: Comparative results on simulated data. Running time, in seconds, is shown as the number of dimensions varies. Each line stands for a different algorithm: the naive algorithm ("slow"), my simple algorithm ("hplane"), and the blacklisting algorithm ("black").

simple algorithm is slower, but still faster than the naive approach. In 8 or more dimensions blacklisting is slowest, due to overhead, and naive and simple are approximately the same (results not shown). Note this graph can be "stretched" so that blacklisting is still faster in higher dimensions, by increasing the number of points.

Another interesting experiment to perform is to measure the sensitivity of my algorithms to changes in the number of points, centroids, and dimensions. It is known, by direct analysis, that the naive algorithm has linear dependence on these. It is also known that *kd*-trees tend to suffer from high dimensionality. In fact, I have just established that in the comparison to the naive algorithm. See Moore (1991) as well. To this end, another set of experiments was performed. The experiments used generated data as described earlier (only with 30000 points). But, only the blacklisting algorithm was used to cluster the data and the running time was measured. In this experiment set, the number of dimensions varied from 1 to 8 and the number of centroids the program was requested to generate varied from 10 to 80 in steps of 10. The results are shown in Figure 1.12. The number of dimensions seems to have a super-linear effect on the blacklisting algorithm. This worsens as the number of centroids increases.

Shown in Figure 1.13 is the effect of the number of centroids on the blacklisting algorithm. The run-time was measured for the blacklisting algorithm clustering

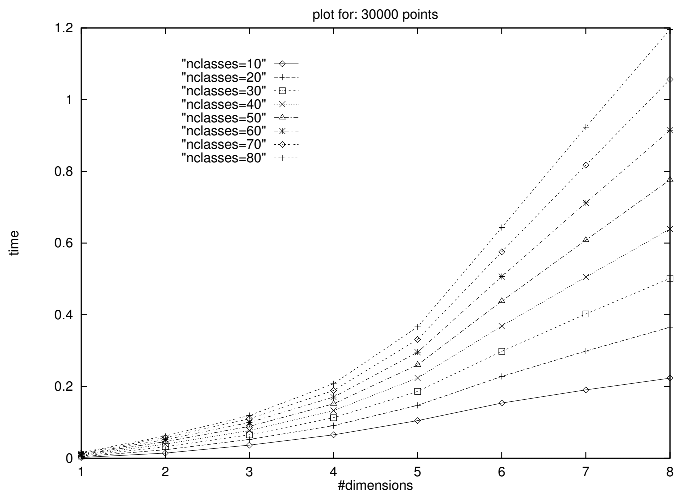

Figure 1.12: Effect of dimensionality on the blacklisting algorithm. Running time, in seconds per iteration, is shown as the number of dimensions varies. Each line shows results for a different number of classes (centroids).

random subsets of varying size from the astronomical data, with 50, 500, and 5000 centroids. We see that the number of centroids has a linear effect on the algorithm. This result was confirmed on simulated data (data not shown).

In Figure 1.14 the same results are shown, now using the number of points for the X axis. We see a very small increase in run-time as the number of points increases.

1.5.1 Approximate Clustering

Another way to accelerate clustering is to prune the search when only small error is likely to be incurred. See Figure 1.15. We do this by not descending down the kd-tree when a "small-error" criterion holds for a specific node. We then assume that the points of this node (and its hyper-rectangle h) are divided evenly among all current competitors (meaning all those centroid not currently blacklisted). For each such competing centroid c, we update its location as if the relative number of points are all located at closest(c, h). Our pruning criterion is:

$$n \cdot \sum_{j=1}^{M} \left(\frac{\mathrm{width}(h)_j}{\mathrm{width}(U)_j} \right)^2 \leq d^i$$

where n denotes the number of points in h, U is the "universal" hyper-rectangle, i is the iteration number, and d is a constant, typically set to 0.8. The idea is to

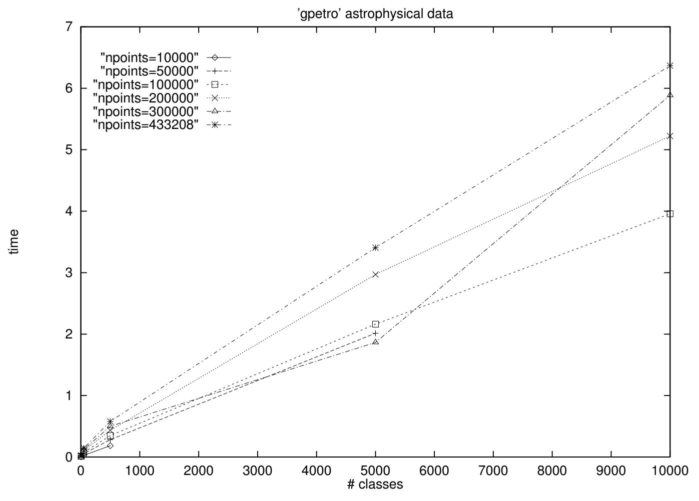

Figure 1.13: Effect of number of centroids on the blacklisting algorithm. Running time, in seconds per iteration, is shown as the number of classes (centroids) varies. Each line shows results for a different number of random points from the original file.

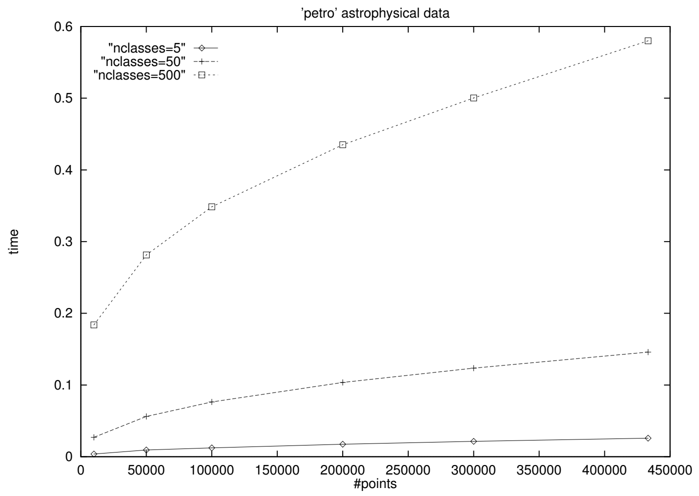

Figure 1.14: Effect of number of points on the blacklisting algorithm. Running time, in seconds per iteration, is shown as the number of points varies. Each line shows results for a different number of classes.

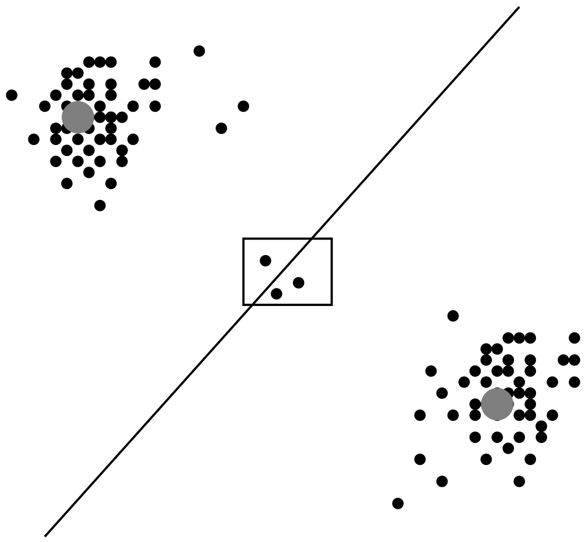

Figure 1.15: Illustration of approximated K-means. Two centroids are shown in gray. Also shown is the decision line between them. A kd-node intersects the line and contains very few points. The overall effect of node on the centroid locations can be approximated without examining individual points.

(heuristically) bound the error contribution from any given node. The exponent i dictates a "cooling schedule" where at the first few iterations it is allowed to make bigger mistakes than later on. So at the beginning the clustering is approximate and fast. But in subsequent iterations it becomes more and more accurate. Note that in later iterations we have a better chance of hitting cached nodes, so this does not necessarily imply a slowdown.

I have conducted experiments with approximate clustering using simulated data. Again, the results shown are averages over 30 random datasets. Figure 1.16 shows the effect approximate clustering has on the run-time of the algorithm. We notice it runs faster than the blacklisting algorithm, with larger speedups as the number of points increases. It is about 25% faster for 10,000 points, and twice as fast $50,000$ points or more. As for the quality of the output, Figure 1.17 shows the distortion of the clustering of both algorithms. The distortion of the approximate method is at most 1% more than the blacklisting clustering distortion (which is exact).

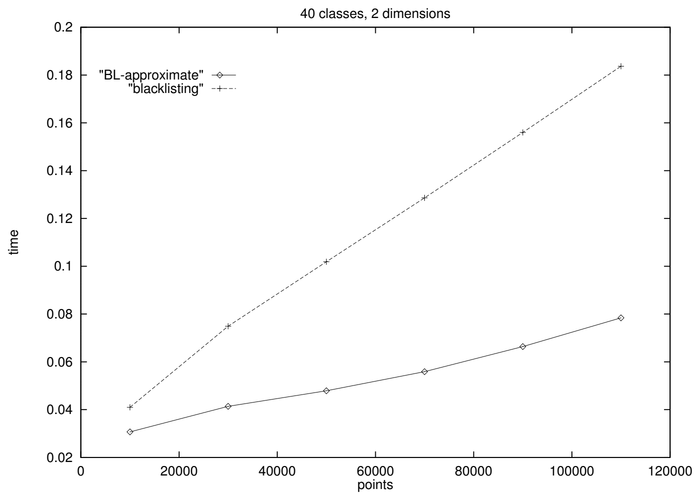

Figure 1.16: Runtime of approximate clustering Running time, in seconds per iteration, is shown as the number of points varies. Each line stands for a different algorithm.

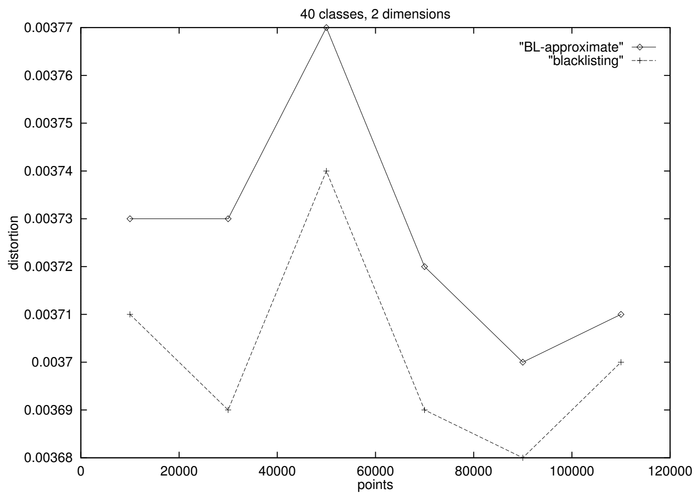

Figure 1.17: Distortion for approximate and exact clustering. Each line stands for a different algorithm.

1.6 Related Work

The K-means algorithm is known to converge to a local minimum of the distortion measure. It is also known to be too slow for practical databases.[1] Much of the related work does not attempt to confront the algorithmic issues directly. Instead, different methods of subsampling and approximation are proposed. A way to obtain a small "balanced" sample of points by sampling from the leaves of a R^* tree is shown in Ester et al. (1995). In Ng and Han (1994), a simulated-annealing approach is suggested to direct the search in the space of possible partitions of the input points. It is also possible to tackle the problem in the deterministic annealing framework (Hofmann & Buhmann, 1997; Ueda & Nakano, 1998). This is generally believed to be a robust method. However the author is not aware of any work to improve its run-time performance or to provide a detailed comparison with standard K-means.

The BIRCH algorithm (Zhang et al., 1995) was designed to optimize disk access. It can operate with a single linear scan of the input, although a recommended refinement step requires a few more scans. The idea is to insert the points into a balanced tree ("CF tree"). The nodes in the tree represent sets of data points and store sufficient statistics for them much like *kd*-nodes here. However the nodes boundaries are not axis-aligned and in general resemble ball trees (Moore, 2000). The rules for point insertion, node splitting and node merging are heuristic and depend on many parameters. The original paper lists no less than 14 parameters that control the output, some of which are high-level algorithms in themselves. Needless to say, BIRCH offers very few guarantees on the quality of its clusters. The authors even note that it is possible for a copy of a point to end up in a node which is different than the one storing the original.

Moreover a key property for the CF trees is that they do not include "outliers". The definition of those is, again, imprecise and dependent on input order. This makes the CF trees unsuitable to use for anomaly-hunting tasks.

BIRCH is useful in quickly finding clusters when they are generally spherical and well-separated. In this sense it has the same appeal as K-means. In contrast, it trades off simplicity of definitions and objective functions for optimizing I/O access patterns.

Follow-up work to BIRCH by Bradley et al. (1998) uses a flat collection of sufficient statistics sets instead of the CF tree. It adds sets for dense regions which are

[1]Another view is that since K-means is one of the few clustering algorithms which has a low linear complexity in R, there is much interest in making it efficient for big data sets.

not always tied to the same centroid, but when they change their owner they do so together. Another noteworthy idea is the use of a "worst-case" criterion to estimate if a point is likely to never change its owner. Unfortunately many details are missing, and again the user is expected to specify many parameters. This work only evaluates the quality of the proposed method against a version of K-means which works on a random sample of the data. No run time analysis is given.

Further improvements are made by Farnstrom et al. (2000). They analyze the work of Bradley et al. (1998) and note that many of the improvements in fact hurt the run time. They simplify the data structure and eliminate many user-supplied parameters. By doing this they were able to reduce the run time from several times slower than standard K-means, to about twice as fast on some datasets. Since an inner loop of this algorithm runs K-means on an in-core sample of the data, it can still take advantage of the work presented here.

A different approach to K-means is suggested by Domingos and Hulten (2001a). They develop a "Probably Approximately Correct" version of K-means that can determine when it has seen enough data points to be confident that the output clusters do not differ by much from ones obtained from infinite data. This is reminiscent of the algorithm I present for dependency trees in Chapter 4 (and indeed, both were inspired by the same work). Their results for K-means are promising.

Another approach to exact acceleration is taken by Elkan (2003). He shows how to use the triangle inequality for both upper and lower bounds on distances between points and centroids to save distance computations. Large speed-ups for synthetic and real data with large M and k are reported. The algorithm is still linear in R. Additionally it requires $O(K^2)$ inter-centroid distance computations which in some cases may be prohibitively high. This work also contains a related work section which brings together previous publications from many different research communities.

More exact acceleration can be found in Moore (2000). That work builds metric trees in a unique way and then decorates them with cached sufficient statistics. This results in a data structure that can use the triangle inequality to prune away big subsets of points and centroids. Large speedups are demonstrated for blacklisting K-means, as well as for kernel regression, locally weighted regression, mixture modeling and Bayes Net learning.

Recall that K-means starts from a set of arbitrary starting locations for the centroids. But once they are given, it is fully deterministic. A bad choice of initial centroids can have a great impact on both performance and distortion. Bradley and Fayyad (1998) discuss ways to refine the selection of starting centroids through repeated sub-sampling and smoothing.

Over the years several modifications to K-means were proposed (Zhang et al., 2000; Kearns et al., 1997; Hamerly & Elkan, 2002; Bezdek, 1981). They try to address the "winner takes all" approach of K-means where only one centroid is affected by each point. The claim is that smoother functions are easier to optimize. For example, imagine a centroid which is away from its optimal location, but the region between the current and target location is sparse. Hard assignment will require the centroid to somehow "leap" over the sparse region, but does not give it a way to "know" about the distant points. In contrast, soft assignment that gives the centroid low-weight versions of the distant points might direct the movement correctly. Hamerly and Elkan (2002) show that the best performer among the surveyed methods is K-harmonic means (Zhang et al., 2000). It remains an open question if any of these methods can be accelerated in a similar manner to this work. One hybrid approach, suggested by Zhang et al. (2000), is to run a few iterations of K-harmonic means to get over the potentially bad initialization stage, and then feed the output as initialization points to the faster K-means algorithm, which is known to behave well with good initialization points. It remains to be seen if distance-based proofs can be used for algorithms that do not follow the "winner takes all" rule.

Originally, *kd*-trees were used to accelerate nearest-neighbor queries. We could, therefore, use them in the K-means inner loop transparently. For this method to work we will need to store the *centroids* in the *kd*-tree. So whatever savings we achieve, they will be a function of the number of centroids, and not of the (necessarily larger) number of points. The number of queries will remain R. Moreover, the centroids move between iterations, and a naive implementation would have to rebuild the *kd*-tree whenever this happens. My methods, in contrast, store the entire *dataset* in the *kd*-tree.

The blacklisting idea was published simultaneously and independently by AlSabti et al. (1999). I stumbled on that paper by chance a while after publication of this work. Their presentation lacks the geometric proofs, but otherwise seems equivalent. Elements missing from that work with respect to this one are exhaustive experimentation, and stable-state caching as in Section 1.4.

1.6.1 Improvements over fast mixture-of-Gaussians

At first glance, this work might seem like a specialization of Moore (1998). Both are similar in that they utilize multiresolution *kd*-trees. Also, they both implement an

EM procedure for a Gaussian mixture model, and they both gain significant speedups. To counter that, I list the improvements specific to this work. First, the idea of blacklisting is novel. Moreover, it cannot be easily applied to the soft-membership model of mixture of general Gaussians. In that framework, each point always affects all of the centroids. Because the effect of the points furthest away from a centroid is small, the general Gaussians algorithm may decide to ignore them by pruning branches of the *kd*-tree. This introduces approximation into the calculation. In contrast, K-means is a hard-membership model and blacklisting only eliminates the points which provably do not belong to a centroid. Therefore my algorithm is exact.

Second, I introduce node caching. It saves a lot of work in regions of the space which are quiescent. This is a frequent occurrence in late iterations. It appears that this idea can be retrofitted to the general Gaussians method.

Third, I provide two alternative implementations. One of them only uses geometric proofs without blacklisting. It is shown in Figure 1.11. It is actually closer in spirit to the ideas presented in Moore (1998). We can see that it behaves qualitatively differently than the blacklisting version as the number of dimensions grows. Notice how there are occasions where it is faster to avoid blacklisting. The exact cross-over point shown is around seven dimensions, but in practice will depend on the properties of the data.

1.7 Conclusion

The main message of this chapter is that the well-known K-means algorithm need not necessarily be considered an impractically slow algorithm, even with many records and centroids. I have described, analyzed and given empirical results for a new fast implementation of K-means. I have shown how a *kd*-tree of all the data points, decorated with extra statistics, can be traversed with a new, extremely cheap, pruning test at each node. Another new technique—blacklisting—gives a many-fold additional speed-up, both in theory and empirically.

For datasets too large to fit in main memory, the same traversal and black-listing approaches could be applied to an on-disk structure such as an R-tree, permitting exact K-means to be tractable even for many billions of records.

This method performs badly in high dimensions. This is a fundamental shortcoming of the *kd*-tree: in each subsequent level it merely splits the data according to one dimension. But this does not imply the work presented here is only useful on toy problems, for several reasons. First, there are multiple domains where only a few dimensions are needed. Of these come to mind astrophysics, geo-spatial-data, and controls. Second, it is possible to first project the data onto a low-dimensional space, and cluster the projected data.[2] In fact there is evidence that such a preprocessing step might make the clusters more spherical and hence easier to work with. Moreover, even a simple approach such as random projection is sufficient to obtain very good results — in some cases evading problems which trip a more complex method such as PCA (Dasgupta, 2000). Third, much of the principles here carry over to data structures better suited for high dimensional data, such as metric trees (Moore, 2000).

Unlike previous approaches (such as the *mrkd*-trees for EM in Moore (1998)) this new algorithm scales very well with the number of centroids, permitting clustering with tens of thousands of centroids. The need for this kind of performance arises in cosmology data where a very large number of astronomical objects are examined or simulated. The structure of large-scale regions of space is summarized in a succinct representation such as the halo occupation distribution (HOD). Assigning cluster membership for each galaxy is a precondition to computing the necessary statistic.

My implementation for K-means (shared with the K-means code described in the following Chapter) is available for researchers[3] and was downloaded by over 200 users as of March 2004. Among others, it was used in the following applications:

- cDNA microarray data. K-means is run repeatedly on a small subset of the total data (Bainbridge, 2004).
- DNA microarray gene expression levels (Ballini, 2003; Qian, 2001).
- Music information retrieval (Zissimopoulos, 2003).
- Financial data analysis (Kallur, 2003).
- Prediction of functional RNA genes in genomic sequences. The data is clustered for the purpose of drawing negative examples for the training set. There are about 700 clusters and more than a million data points (Meraz, 2002).
- Multi-objective optimization with evolutionary algorithms (Koch, 2002).
- Molecular biology (Zhang, 2000).

[2]There are several ways to transfer the resulting clustering back to the original domain. For example one can use the class labels to seed a single iteration of an EM fit in the original space.

[3]See `http://www.pelleg.org/kmeans`.

K-means is a well-established algorithm that has prospered for many years as a clustering algorithm workhorse. Additionally, it is often used to help find starting clusters for more sophisticated iterative methods such as mixture models. The techniques in this chapter can make such preprocessing steps efficient. Finally, with fast K-means, we can afford to run the algorithm many times in the time it would usually take to run it once. This allows automatic selection of k, or subsets of attributes upon which to cluster, to become a tractable, real-time operation. The following chapter develops this idea further.

Chapter 2

X-means

K-means is well-established as a general clustering solution. It is popularly recommended as the first thing to try, given a new data set. In the last chapter I showed how to make it scale so it can run on huge data. But in many contexts, it cannot be immediately used because it requires the user to specify the number of clusters K. Users who are well acquainted with the data have no problem knowing what K is: this is typical of clustering in some well researched area where plenty of prior knowledge exists (a biologist, for example, frequently knows how many different species are represented in the data and can safely assume this will reflect in the clustering). But this is not always the case. For example, a computer architect may profile a running program by monitoring its execution. The instructions are grouped, and similar groups are bundled together to form units of similar execution patterns, or program phases. It is impossible to know in advance what — and how many — phases an arbitrary program will go through when run on an arbitrary input. This calls for a framework to support automatic estimation of K.

Statistical measures to score different models abound. They usually include two terms. One increases as the fit is improved and the data modeled more accurately. It is necessary to have this. However, it can be trivially optimized by tweaking the model and making it more and more complex. Therefore a second penalty term, which favors simpler models, is normally added.

We leave aside the statistical debate on which scoring function is "best". Our focus is how to efficiently compute the score once such a function is chosen. In particular we want to apply it to K-means clusters. We want it to scale as well as K-means itself. Additionally, we want an practical way to search over many models. Without it, we would need to exhaustively search a very large space (for K-means this entails blindly trying many different values for K).

Building on the last chapter, I introduce a new algorithm that efficiently searches the space of cluster locations and number of clusters to optimize a clustering quality measure. The innovations include two new ways of exploiting cached sufficient statistics and a new very efficient test that in one K-means sweep selects the most promising subset of classes for refinement. This gives rise to a fast, statistically founded algorithm that outputs both the number of classes and their parameters. Experiments show this technique reveals the true number of classes in the underlying distribution, and that it is much faster than repeatedly using accelerated K-means for different values of K.

2.1 Introduction

K-means (Duda & Hart, 1973; Bishop, 1995) has long been the workhorse for metric data. Its attractiveness lies in its simplicity, and in its local-minimum convergence properties. It has, however, three main shortcomings. One, it is slow and scales poorly with respect to the time it takes to complete each iteration. Two, the number of clusters K has to be supplied by the user. Three, when confined to run with a fixed value of K it empirically finds worse local optima than when it can dynamically alter K. This chapter offers solutions for these problems. Speed is greatly improved by embedding the dataset in a multi-resolution *kd*-tree as described in Chapter 1. This fast algorithm is used as a building-block in what I call "X-means": a new algorithm that quickly estimates K. It goes into action after each run of K-means, making local decisions about which subset of the current centroids should split themselves in order to better fit the data. The splitting decision is done by computing the Bayesian Information Criterion (BIC). I show how the blacklisting method naturally extends to ensure that obtaining the BIC values for all current centers and their tentative offspring costs no more than a single K-means iteration. I further enhance computation by caching stable-state information and eliminating the need to re-compute it.

I have experimented with X-means against a more traditional method that estimates the number of clusters by guessing K. X-means consistently produced better clustering on both synthetic and real data, with respect to BIC. It also runs much faster, even when the baseline is my accelerated blacklisting K-means.

The rest of the chapter is organized as follows. In Section 2.2 I discuss prior work and introduce notation. My algorithms are presented in Section 2.3, which briefly discusses blacklisting and outlines fast BIC computation. It also expands on BIC and touches on alternative goodness-of-fit measures. I show experimental results in Section 2.4, and conclude in Section 2.5.

2.2 Definitions

I first briefly describe the naive K-means algorithm for producing a clustering of the points in the input into K clusters. It partitions the data points into K subsets such that all points in a given subset "belong" to some center. The algorithm keeps track of the centroids of the subsets, and proceeds in iterations. Before the first iteration the centroids are initialized to arbitrary values. The algorithm terminates when the centroid locations stay fixed during an iteration. For a more detailed description and a literature survey refer to Chapter 1.

For the remainder of this paper we denote by μ_j the coordinates of the j-th centroid. We will use the notation (i) to denote the index of the centroid which is closest to the i-th data point. For example, $\mu_{(i)}$ is the centroid associated by the i-th point during an iteration. D is the input set of points, and $D_i \subseteq D$ is the set of points that have μ_i as their closest centroid. We let $R = |D|$ and $R_i = |D_i|$. The number of dimensions is M, and the Gaussian covariance matrix is $\Sigma = \mathrm{diag}(\sigma^2)$.

2.3 Estimation of K

The algorithm as it was described up to this point can only be used to perform K-means where K is fixed and supplied by the user. This is a reasonable requirement if K is small or if a strong prior exists. For example, a biologist might collect measurements on seven different species of an organism, and then run K-means with K set to 7. But in many other applications, we do not have this privilege. For example, a computer program execution can be traced and the instructions grouped into blocks (Sherwood et al., 2002). Now we would like to group the blocks and define different phases of the program execution. The number of phases for an arbitrary program it unknown in advance, and needs to be estimated as well.

We proceed now to demonstrate how to efficiently search for the best K. The framework now changes so the user only specifies a range in which the true K reasonably lies[1], and the output is not only the set of centroids, but also a value for K in this range which scores best by some model selection criterion. Note that using the

[1]We allow the range to be $[2..R]$, but in practice much better bounds can be given.

X-means:

1. **Improve-Params**
2. **Improve-Structure**
3. If $K > K_{\max}$ stop and report the best-scoring model found during the search. Else, Goto 1.

Figure 2.1: The X-means algorithm.

inherent objective function in K-means, namely the distortion, favors models with large K. Indeed, it is possible to reach its absolute minimum of zero by having a cluster for each data point (located on the point). Clearly the number of clusters needs to be considered as well to reject these kinds of models. There are several measures that aim to achieve this, with no single one being universally best. I choose to focus on the BIC for the rest of this discussion (see Section 2.3.2). But there is very little in this work that is BIC-specific. The implementation supports "plugging-in" of other measures in a straightforward way, and includes one other optional scoring function (see Section 2.3.3).

We first describe the process conceptually, without paying much attention to the algorithmic details. Next, we derive the statistical tests used for scoring different structures. We then come back to the high-level description of the algorithm and show how it can be implemented efficiently using ideas deriving from blacklisting and the sufficient statistics stored in the *kd*-tree nodes.

2.3.1 Model Searching

In essence, the algorithm starts with K equal to the lower bound of the given range and continues to add centroids where they are needed until the upper bound is reached. During this process, the centroid set that achieves the best score is recorded, and this is the one that is finally output. Recall that theoretically, the score function is not guaranteed to be monotone in K. Additionally, in practice it rarely is (and is rarely smooth).

The algorithm is described in Figure 2.1. It uses an unspecified scoring function that trades goodness-of-fit for complexity. This is discussed further in Section 2.3.2.

The **Improve-Params** operation is simple: it consists of running conventional

K-means to convergence.

The **Improve-Structure** operation finds out if and where new centroids should appear. This is achieved by letting some centroids split in two. How can we decide what to split? We begin by describing and dismissing two obvious strategies, after which I will combine their strengths and avoid their weaknesses in my X-means strategy.

Splitting idea 1: One at a time. The first idea would be to pick one centroid, produce a new centroid nearby, run K-means to completion and see if the resulting model scores better. If it does, accept the new centroid. If it doesn't, return to the previous structure. But this will need $O(K_{\max})$ **Improve-Params** steps until X-means is complete. This begs the question of how to choose which centroid is most deserving to give birth. Having answered that we face another issue: if it doesn't improve the score what should be tried next? Perhaps all centroids could be tested in this way (and then we stick with the best) but since each test needs a run of K-means that would be an extremely expensive operation for adding only one centroid.

Splitting idea 2: Try half the centroids. Simply choose (say) half the centroids according to some heuristic criterion for how promising they are to split. Split them, run K-means, and see if the resulting model scores better than the original. If so accept the split. This is a much more aggressive structure improvement, requiring only $O(\log K_{\max})$ **Improve-Params** steps until X-means completes. But what should the heuristic criterion be? Size of region owned by centroid? Distortion due to centroid? Furthermore, we will miss the chance to improve in cases when one or two centroids need to split but the rest do not.

My solution achieves the benefits of ideas 1 and 2, but avoids the drawbacks and can be turned into an extremely fast operation (as we will see in Section 2.3.4). I will explain by means of an example.

Figure 2.2 shows a stable K-means solution with 3 centroids. The boundaries of the regions owned by each centroid are also shown. The structure improvement operation begins by splitting each centroid into two children (Figure 2.3). They are moved a distance proportional to the size of the region in opposite directions along a randomly chosen vector. Next, in each parent region we run a local K-means (with $K = 2$) for each pair of children. It is local in that the children are fighting each other for the points in the parent's region: no others. Figure 2.4 shows the first step of all

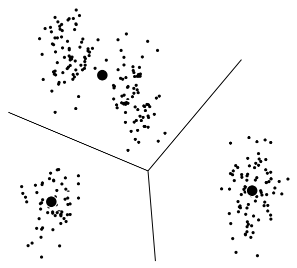

Figure 2.2: The result of running K-means with three centroids.

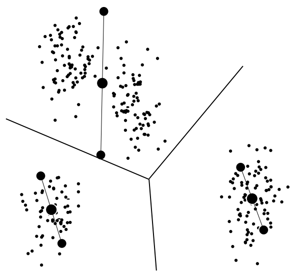

Figure 2.3: Each original centroid splits into two children.

three local 2-means runs. Figure 2.5 shows where all the children eventually end up after all local 2-means have terminated.

This initial placement of child centers is somewhat arbitrary. The hope is that during the local 2-means run the centers will move to a better place. And in practice they frequently do. In theory one could use a more sophisticated approach for this, such as considering the principal components of points in the local region.

At this point a model selection test is performed on all pairs of children. In each case the test asks "is there evidence that the two children are modeling real structure here, or would the original parent model the distribution equally well"? The next section gives the details of one such test for K-means. According to the outcome of the test, either the parent or its offspring are killed. The hope is that centroids that already own a set of points which form a cluster in the true underlying distribution will not be modified by this process (that is, they will outlive their children). On the other hand, regions of the space which are not represented well by the current centroids will receive more attention by increasing the number of centroids in them. Figure 2.6 shows what happens after this test has been applied to the three pairs of children in Figure 2.5.

Therefore our search space covers all possible 2^K post-splitting configurations,

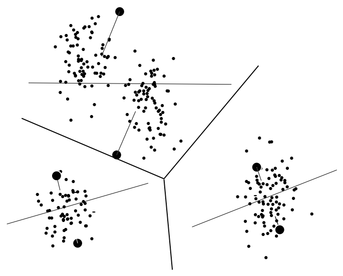

Figure 2.4: The first step of parallel local 2-means. The line coming out of each centroid shows where it moves to.

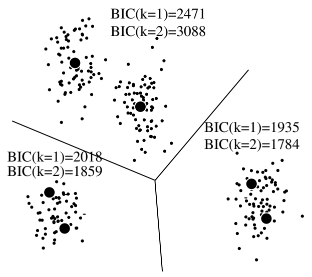

Figure 2.5: The result after all parallel 2-means have terminated.

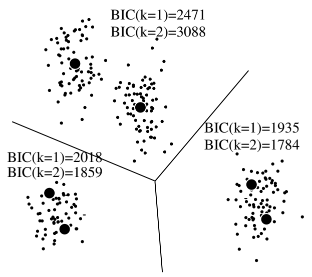

Figure 2.6: The surviving centroids after all the local model scoring tests.

and it determines which one to explore by improving the BIC locally in each region. Compared with ideas 1 and 2 above, this allows an automatic choice of whether to increase the number of centroids by very few (in case the current number is very close to the true number) or very many (when the current model severely underestimates K). Empirically, I have also found that regional K-means runs with just 2 centers tend to be less sensitive to local minima.

We continue oscillating between **Improve-Params** and **Improve-Structure** until the upper bound for K is attained. The implementation uses the following rule to handle the case of a worsening score with increasing K. If no centroids seem worse than their children, the difference between BIC score of parent and their respective children centroids is calculated. The parents are then ranked by this value, and the top 50% are forcibly split.

It remains to discuss the cost of running K-means together with BIC evaluation. We return to this issue after a short digression to statistical scoring.

2.3.2 BIC Scoring

Assume we are given the data D and a family of alternative models M_j, where in our case different models correspond to solutions with different values of K. How do we choose the best? Intuitively we would like to balance goodness of fit (which can be improved by enriching the model with more parameters) and model simplicity (which implies few parameters).

More precisely, we will use the posterior probabilities $\Pr[M_j|D]$ to score the models. In our case the models are all of the type assumed by K-means (that is, spherical Gaussians). To approximate the posteriors, up to normalization, we use the following formula from Kass and Wasserman (1995):

$$BIC(M_j) = \hat{l}_j(D) - \frac{p_j}{2} \cdot \log R$$

where $\hat{l}_j(D)$ is the log-likelihood of the data according to the j-th model and taken at the maximum-likelihood point, and p_j is the number of parameters in M_j. This is also known as the Schwarz criterion (Wasserman, 1997).

The maximum likelihood estimate (MLE) for the variance, under the identical spherical Gaussian assumption, is:

$$\hat{\sigma}^2 = \frac{1}{R-K} \sum_i (x_i - \mu_{(i)})^2 .$$

The point probabilities are:

$$\begin{aligned}\hat{P}(x_i) &= \frac{R_{(i)}}{R} \cdot \frac{1}{\sqrt{2\pi}||\hat{\Sigma}||^{1/2}} \exp\left(-\frac{1}{2\hat{\sigma}^2}||x_i - \mu_{(i)}||^2\right) \\ &= \frac{R_{(i)}}{R} \cdot \frac{1}{\sqrt{2\pi}\hat{\sigma}^M} \exp\left(-\frac{1}{2\hat{\sigma}^2}||x_i - \mu_{(i)}||^2\right) .\end{aligned}$$

The log-likelihood of the data is:

$$\begin{aligned}&l(D) = \log \textstyle\prod_i P(x_i) = \\ &\textstyle\sum_i \left(\log \frac{1}{\sqrt{2\pi}\sigma^M} - \frac{1}{2\sigma^2}||x_i - \mu_{(i)}||^2 + \log \frac{R_{(i)}}{R}\right) .\end{aligned}$$

Fix $1 \leq n \leq K$. Focusing just on the set D_n of points which belong to centroid n and plugging in the maximum likelihood estimates yields:

$$\begin{aligned}\hat{l}(D_n) &= -\frac{R_n}{2}\log(2\pi) - \frac{R_n \cdot M}{2}\log(\hat{\sigma}^2) - \frac{R_n - K}{2} \\ &\quad + R_n \log R_n - R_n \log R .\end{aligned}$$

The number of free parameters p_j is simply the sum:

- $K - 1$ class probabilities (the last one is redundant since they sum to one).
- $M \cdot K$ centroid coordinates.
- One variance estimate.

To extend this formula for all centroids instead of one, we use the fact that the log-likelihood of the points that belong to all centroids in question is the sum of the log-likelihoods of the individual centroids, and replace R above with the total number of points which belong to the centroids under consideration.

We use the BIC formula in two places: globally when X-means finally chooses the best model it encountered, and also locally in all the centroid split tests.

2.3.3 Anderson-Darling Scoring

Recently, Hamerly and Elkan analyzed the BIC criteria as used in X-means and found cases where it can over-estimate k. For the full treatment see Hamerly and Elkan (2003). I provide a short summary here for completeness.

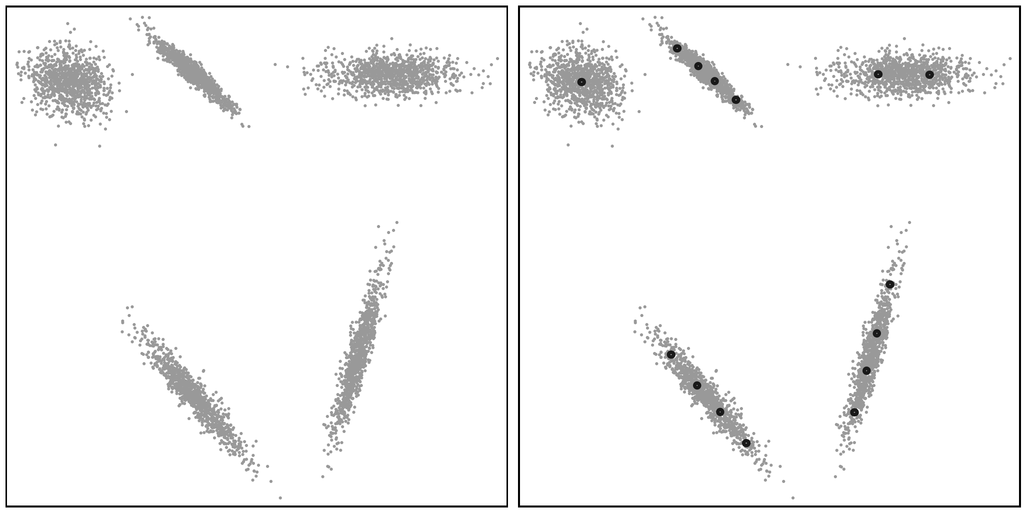

(a) (b)

Figure 2.7: A 2-D set of 5000 points, drawn from a mixture of 5 Gaussians (a). The X-means fit to it when using BIC scoring (b).

The likelihood measure in BIC is using the PDF from the model. For K-means, the model is composed of spherical Gaussians. Therefore we can expect it to perform poorly on non-spherical clusters. Anecdotal evidence shows that it unnecessarily splits centers which fully own elongated clusters. The data in Figure 2.7(a) was generated following a similar example in Hamerly and Elkan (2003). The BIC-guided fit to it with X-means is shown in Figure 2.7(b). We see that elongated clusters contain many more centers than needed.[2]

The proposed remedy is to use a different split test. The one used is the Anderson-Darling test for Gaussianity. It is applied at the local regions after splitting into children and running 2-means. The null hypothesis is that the data is generated from a single Gaussian. If the test rejects it (at a given significance level), the split into two children is accepted.

The Anderson-Darling test works on univariate data. The following transformation is used for multivariate data. Connect the two child centers with a line, and project each point onto the line. Now normalize the univariate data to have zero mean and unit variance. Compute the AD statistic, and apply the Stephens (1974) correction. Compare the value with a critical value for the chosen significance level

[2]It is possible to label all of the centers with the same cluster label to achieve good modeling. This is the "separator variable" approach advocated by Seeger (2000). The discussion here disregards this approach in an attempt to first get a good basic fit.

and accept or reject the null hypothesis. Tables for critical values can be found in Hamerly (2003).

Since published, the AD test has been incorporated into the X-means implementation. The user can choose to use it in the local decision step instead of the BIC test. The global test used is still BIC. Optionally, the run can be terminated as soon as no centers are split (instead of forcibly splitting some centers so as to reach $K_{\max}$).

2.3.4 Acceleration

The X-means algorithm described so far can be implemented as-is for small datasets. But so far we neglected its most important feature. It was invented subject to the design constraint that it should be possible to use cached statistics to scale it up to datasets with massive numbers of records. Much of the material here appears in more detail in Chapter 1. Those familiar with that material can safely skip ahead. Others will probably need the context given here to appreciate the X-means specific additions described later.

Accelerating K-means

We begin by concentrating on a single K-means iteration. The task is to determine, for every data point, which centroid owns it. Then, we can compute the center-of-mass of all points which belong to a given centroid and that defines the new location for that centroid. Immediately we observe that showing that a *subset* of points all belong to a given centroid is just as informative as doing this for a single point, given that we have sufficient statistics for the subset (in our case the sufficient statistics are the number of points and their vector sum). Clearly it may save a lot of computation, provided that doing this is not significantly more expensive than demonstrating the ownership over a single point. Since the *kd*-tree imposes a hierarchical structure on the data set, and we can easily compute sufficient statistics for its nodes at construction time, it makes a natural selection for the partition of the points. Each *kd*-node represents a subset of the data set. It also has a bounding box, which is a minimal axis-parallel hyper-rectangle that includes all points in the subset. In addition it contains pointers to two children nodes, which represent a bisection of the points their parent owns.

Consider a set of counters, one for each centroid, which store a running total of the number of points that belong to each, as well as their vector sum. We now show how to update all the counters by scanning the *kd*-tree just once. The **Update** procedure is a recursive one, and accepts as parameters a node and a list of centroids that may own the points in it. Its task is to update the counters of the nodes in question with the appropriate values of the points in the node. The initial invocation is with the root node and the list of all centroids. After it returns, the new locations may be calculated from the counters. The procedure considers the geometry of the bounding box and the current centroid locations to *eliminate* centroids from the list by proving they cannot possibly own any point in the current node. Hence the name "blacklisting". The point to remember here is that after shrinking the list, the procedure recurses on the children of the current node. The halting condition is met when the list contains just one centroid; then, the centroid's counters are incremented using the statistics stored in the *kd*-node. Frequently this happens in a shallow level of the *kd*-tree, and eliminates the work needed to traverse all of its descendants.

Accelerating Improve-Structure

The procedure described above works well to update the centroid locations of a global K-means iteration. We will now apply the same procedure to carry forward an **Improve-Structure** step. Recall that during **Improve-Structure** we perform 2-means in each Voronoi region of the current structure. We carry this out by first making a list of the parent centroids, and use that as input to the Update procedure. The difference from the global iteration is in the action taken when the list reduces to a single centroid. This event signifies the fact that all points in the current node belong to the single centroid (equivalently, that it is fully contained in a Voronoi region). We now know for certain that the points in the node can only affect a local 2-means step. To quantify this effect we divide the points between the children according to their location. Recall that this is exactly what Update does, when given the appropriate node and centroid list. Specifically, we create a new centroid list containing just the two children, and recurse on Update using this short list and the current node. The rest of the work is done by the Update procedure. After a full scan of the *kd*-tree has been carried out (possibly pruning away many nodes), the counters of the child centroids have their final values and their new locations can be computed. Now a new iteration can take place, and so on until the last of the centroid pairs has settled down. To emphasize, in a single traversal of the *kd*-tree we handle all of the parents and all of their children.

Additional Acceleration

An interesting outcome of the local decision-making is that some regions of the space tend to become active (i.e., a lot of splitting and re-arrangement takes place) while other regions, where the centroids seem to have found the true classes, appear dormant. We can translate this pattern into further acceleration by using caching of statistics from previous iterations. Consider a *kd*-node that contains a boundary between two centroids (that is, either of the two centroids may own any of the node's points). Although we must recurse down the tree in order to update the counters for the centers, there is no reason to do this again in the next iteration, provided that the centroids did not move, and that no other centroid has moved into a position such that it can own any of the node's points. We therefore cache the contribution of this node to each of the centroids' counters in the node, and subsequent iterations do not need to traverse the tree any further than the current node if the list of competing centroids matches.

To enable fast comparison of centroid locations against their position in previous iterations we once again employ a write-once data structure which does not permit alteration of centroid coordinates after the initial insertion. In case a centroid location changes, a new element has to be inserted and it is given a unique identifier. This way only a $O(1)$ comparison of identifiers (per centroid) is needed. Clearly "old" centroids would never be accessed so there is no need to keep storing them in the data-structure. This allows for a fast and memory-efficient implementation using the original $M \cdot K$ memory plus a hash-table for identifier lookup.

A further extension of this idea can also cache the children of a centroid in a regional iteration. Consider the following scenario. Some centroid is rejecting a split into children. Suppose it does not move, and at the next iteration we try to split it again. We want to reuse the information on children nodes (which have no reason to change this time) and save computation. To achieve this, we do not kill children node and instead move them to a "zombie" state. The next regional iteration will resurrect them. Owing to the fact that their identifiers did not change, the caching mechanism immediately recalls the outcome of their last local iteration (which may have been reached after several re-positioning steps). We finally remove children from the data structure when their parent is killed (in our write-once data scheme, this happens when the parent moves).

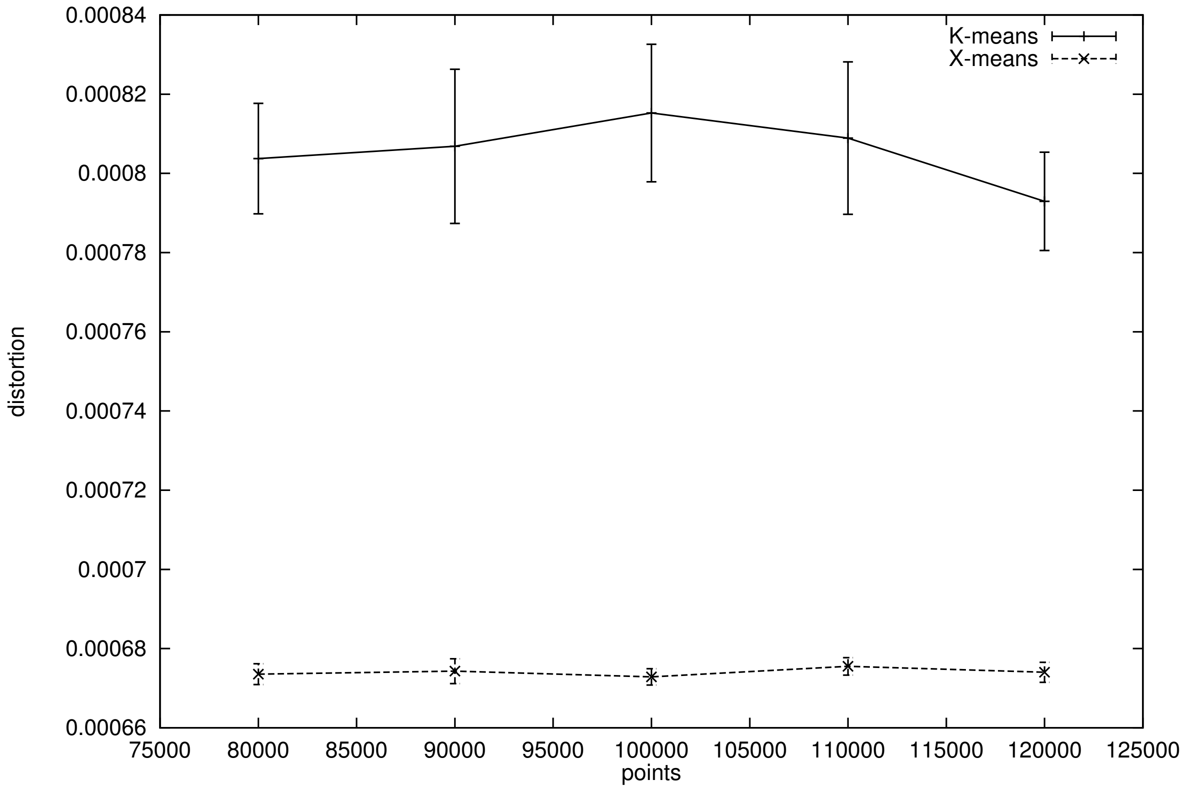

Figure 2.8: Distortion of X-means and K-means. Average distortion per point shown. Results are the average of 30 runs on 3-D data with 250 classes.

2.4 Experimental Results

In my first experiment I tested the quality of the X-means solution against that of K-means. To define quality as the BIC value of the solution would be unfair to the K-means algorithm since it only tries to optimize the distortion (i.e., average squared distance from points to their centroids). I therefore compared both algorithms by the distortion of their output. Gaussian datasets were generated as in Chapter 1, then both algorithms were used. While K-means was given the true number of classes K, the X-means variant had to search for it in the range $[2 \ldots K]$ (see Figure 2.8). Interestingly, the distortion values for the X-means solutions are lower (meaning higher quality solutions). We may attribute this to the gradual way in which X-means adds new centroids in areas where they are needed. This contrasts with the once-only placement of initial centroids used by K-means.

Another interesting question is how good X-means is at revealing the true number of classes. For comparison I used a variant of K-means which simply tries different

Table 2.1: The mean absolute error vs. the number of classes output by the two algorithms, using 2-D data with 4000 to 36000 points.

classes	error	
	K-means	X-means
50	3.53 ± 0.37	$\mathbf{3.00 \pm 0.89}$
100	$\mathbf{5.77 \pm 0.58}$	9.06 ± 1.00
150	$\mathbf{9.65 \pm 4.28}$	21.43 ± 2.26

values of K and reports the configuration which resulted in the best BIC. This differs from X-means in that for each K a new search is started. In contrast, X-means add new centers in very particular locations, based on the outcome of the preceding K-means run.

The permissible range for X-means was $[2 \dots 2K]$, and for K-means I used the 20 equally-distant values up to $2K$. Averaged results are in Table 2.1 and detailed results for the 100-class case are in Figure 2.9. They show that X-means outputs a configuration which is within 15% from the true number of classes. We also see that K-means does better in this respect (about 6% average deviation). The results also show that K-means tends to over-estimate the number of classes, and also to output more classes as the number of records, R, increases, while X-means usually under-estimates the true K, and is in general insensitive to R.

I also show an updated version of Table 1.2 in Table 2.2. It again shows that X-means under-estimates K. Note that in this experiment K-means was now allowed to search over K.

A slightly different picture arises when we examine the BIC score of the output configurations. Note that my K-means variant chooses the best configuration by its BIC score, so this is a fair comparison now. In Figure 2.10 we see that X-means scores not only better than K-means in this respect, but also outperforms the underlying distribution which was used to generate the data. This may be explained by random deviations in the data that cause it to be better modeled by fewer classes than there actually are. For example, two (or more) class centers, which are chosen at random, may fall extremely close to one another so they approximate a single class.

As far as speed is concerned, X-means scales much better than iterated K-means. As shown in Figure 2.11, X-means runs twice as fast for large problems. Note this

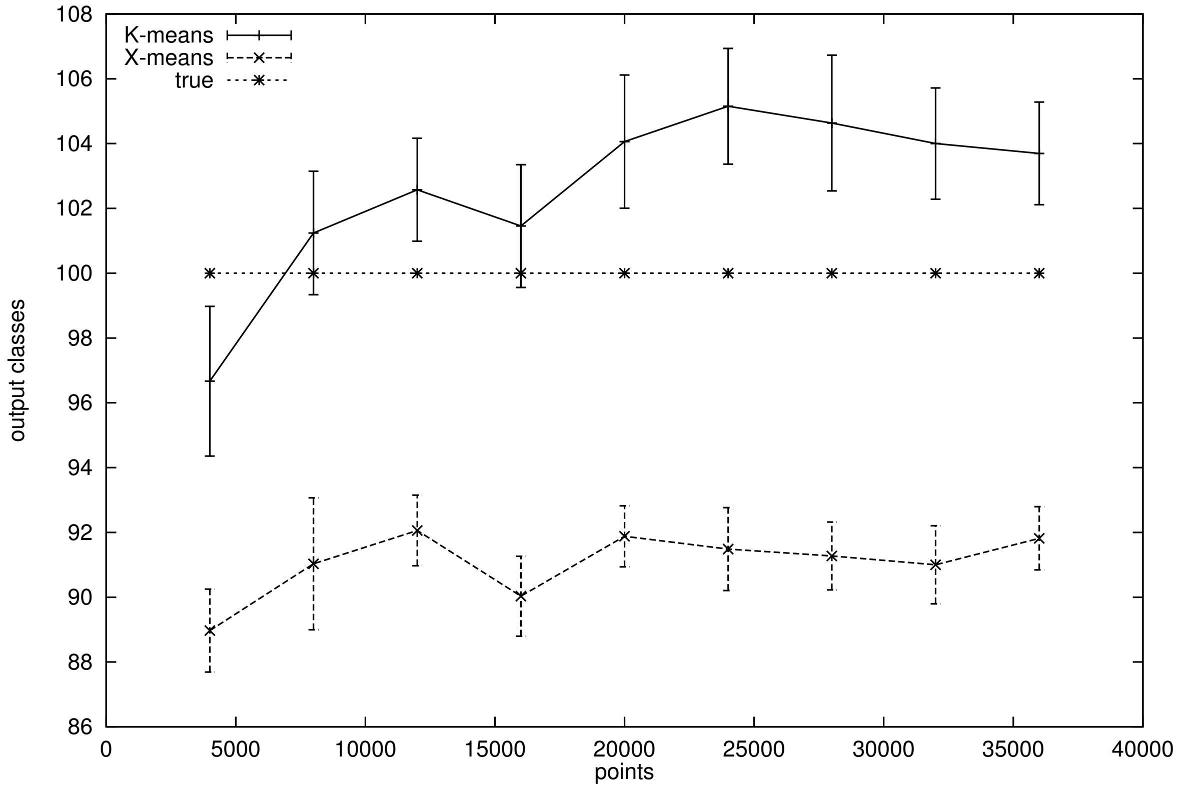

Figure 2.9: The number of output classes as a function of input size for 2-D data with 100 true classes, averaged over 30 randomly generated data sets.

set	form	points	K	blacklisting distortion	BIRCH distortion	BIC distortion	AD distortion	BIC K	AD K
1	grid	100000	100	1.85	1.76	**1.84**	1.84	100	100
2	sine	100000	100	2.44	**1.99**	2.18	2.18	100	100
3	random	100000	100	6.98	8.98	**6.33**	6.43	100	100
4	real	100000	1000	3.59e-2	**3.17e-2**	1.38e-1	1.67e-1	185	96
5	real	200000	1000	**3.40e-2**	3.51e-2	1.22e-1	8.35e-2	279	191
6	real	300000	1000	**3.73e-2**	4.19e-2	1.37e-1	8.20e-2	204	194
7	real	433208	1000	**3.37e-2**	4.08e-2	1.84e-1	8.02e-2	117	196

Table 2.2: Comparison of K-means, BIRCH, and X-means using two scoring functions. The distortion for the K-means and BIRCH algorithms, given equal run-time, is shown. Also shown are results for X-means using the BIC and AD scores. For X-means, the run time is unlimited, and it was allowed to split the centroid set 20 times, up to a limit of 100 (sets 1–3) or 1000 (sets 4–7). Both distortion and the number of centroids associated with the best configuration are shown for each scoring function. The data is the same as in Table 1.2.

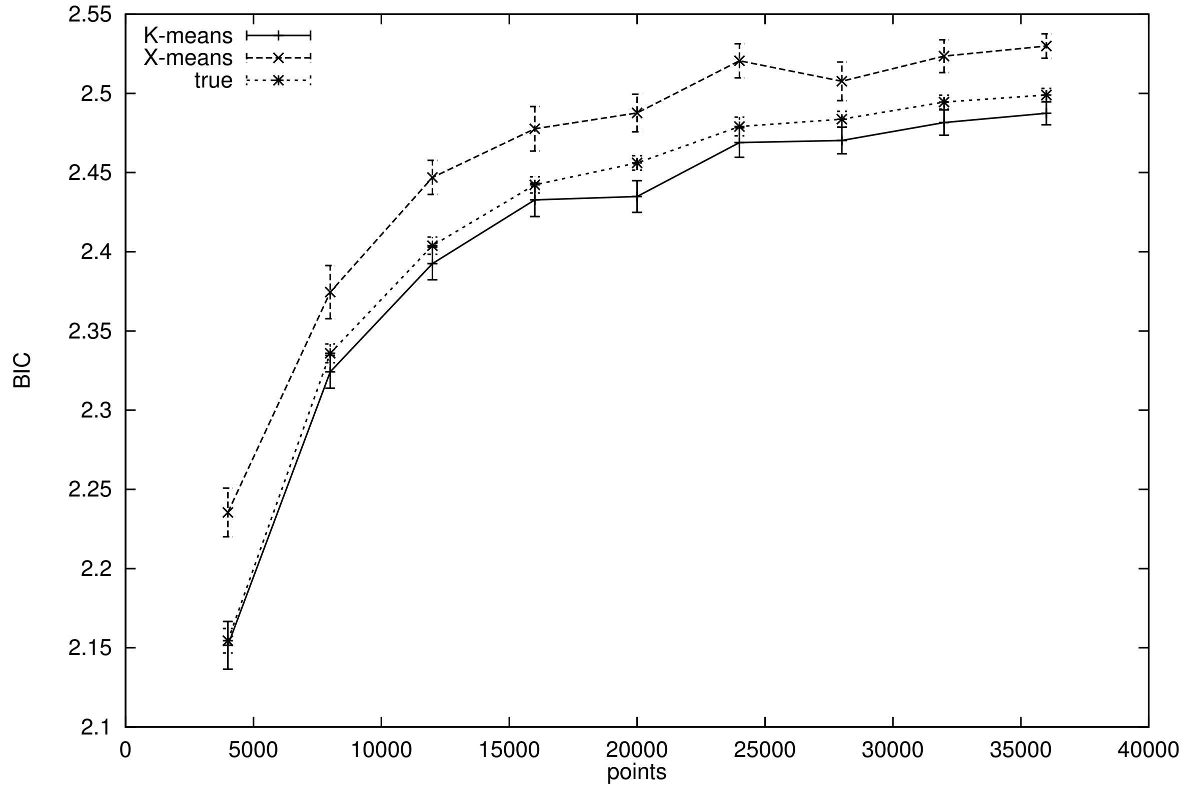

Figure 2.10: BIC of X-means and K-means. Average BIC per point is shown. Results are the average of multiple runs on 2-D data with 100 classes. The label "true" stands for the BIC score of the centroids used to generate the data.

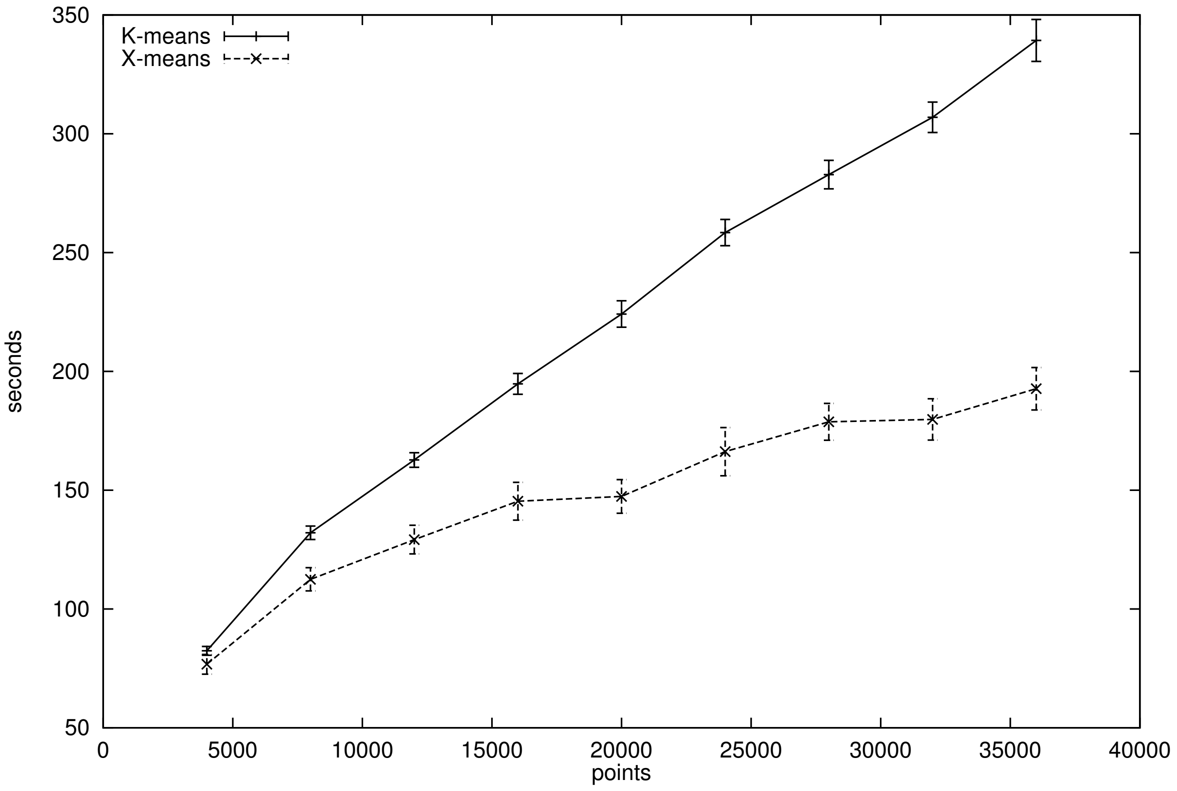

Figure 2.11: Run times of X-means and K-means. Average run-times are shown for 3 dimensions and 250 classes on a 233-MHz Pentium-2.

is a competition against an already accelerated version of K-means as described in Chapter 1. When compared against naive K-means (that is, compute distances from every point to all centroids and pick the minimal), X-means fares much better. On a dataset of over $330,000$ galaxies, X-means completed in 238 seconds where traditional K-means choosing among 10 values of K took 7793 seconds. Both algorithms were set up to perform just one iteration in the **Improve-Params** stage (and X-means is programmed to iterate once more in the **Improve-Structure** stage, and to augment the split by another global iteration). The quality of the X-means solution was superior in terms of either BIC or distortion.

An interesting application of X-means arises in the astrophysics domain. Given a dataset composed of galaxies and their (x, y) coordinates, one would like to ask what is a typical size of a cluster of galaxies. I selected the brightest galaxies in a preliminary version of the SDSS (1998) data. This input set of approximately $800,000$ sky objects[3] was divided by an 18×3 grid (the ranges of the data are not proportional

[3]Since this experiment was performed, the size of the survey grew significantly.

in both axis). The cells had approximately the same number of objects. On each cell with R objects I ran K-means iterated over the 10 values in the range $[R/1000, R/100]$ and X-means searching for K in the same range, and recorded the resulting number of clusters (equivalently, the average cluster size).

The average cluster size according to X-means was 473 ± 25.5, and 572 ± 40.8 according to K-means. While it is hard to validate these manually, I tend to believe X-means since it is free to choose the number of clusters from a wide range where K-means can only validate a small number of specified K. This fact is well reflected in the smaller variance of the X-means output. In early experiments, where the range for K was large and the number of sample points small, this effect was more noticeable (see Figure 2.12).

In terms of run-time, X-means is not only faster, but increases its advantage as the number of points increases, similarly to the way it does so for synthetic datasets. An X-means run over the full data set of some $800,000$ points and $4,000$ resulting centroids takes about 4.5 hours on a 600-MHz DEC Alpha. A similar K-means invocation ran into a hard-coded limit after running for twice as long.

In a similar experiment on the important task of clustering galaxies in the LCRS (1998) data I compared X-means against a highly optimized but traditional (i.e, no *kd*-tree) implementation of K-means. Traditional K-means tried 10 different values of K between 50 and 500. Both algorithms found solutions with almost identical BIC scores, though X-means chose a larger value of K. X-means completed its search eight times faster than K-means.

2.5 Conclusion

I have presented a new K-means based algorithm that incorporates model selection. By adopting and extending algorithmic improvements to K-means, it is efficient to the extent that running it once is cheaper than looping over K with the fixed-model algorithm. It uses statistically-based criteria to make local decisions that maximize the model's posterior probabilities. Experimental results on both synthetic and real-life data show it is performing faster and better than K-means.

My implementation for X-means and K-means is available for researchers[4] and was downloaded by over 200 users as of March 2004. It was used for the following applications:

[4]See `http://www.pelleg.org/kmeans`.

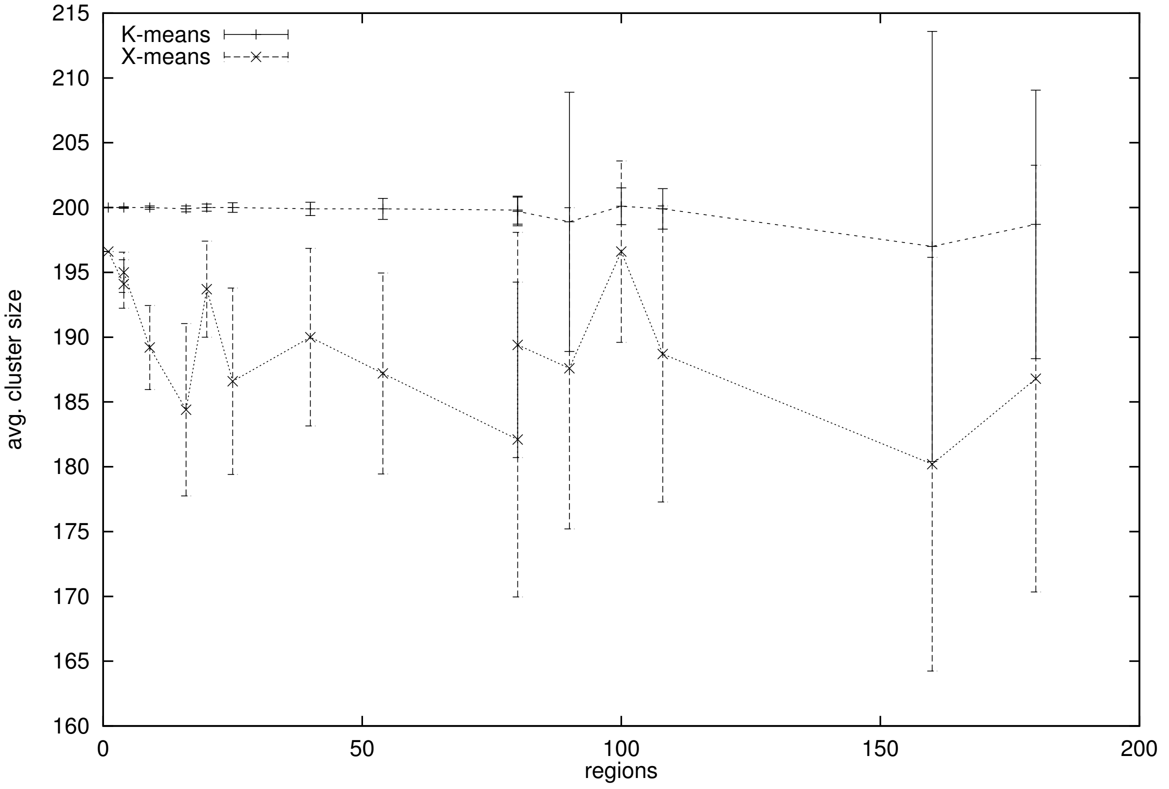

Figure 2.12: Galaxy cluster sizes, averaged over different regions of the space. Averages and standard deviations of the cluster sizes are shown. A finer grid means a higher number of regions.

- Music information retrieval (Logan & Salomon, 2001). Multiple features vectors are extracted for each one of 8500 songs. A specialized inter-cluster distance metric is used to determine a distance matrix for song similarity.
- Computer program analysis in the Daikon package (Ernst et al., 2001). Likely invariants for a program are detected dynamically. To determine conditional properties of the program, clustering is performed on the invariants.
- Natural language processing (Kruengkrai, 2004).
- Computer architecture (Sherwood et al., 2002). A large trace (several billion instructions) of a computer program is taken. Instructions are grouped into basic blocks. Time intervals of a program's execution are represented by a vector of counts of the times each basic block was executed. The vectors are clustered to determine phases in the program's execution.
- Speaker identification.
- Image segmentation (Kruengkrai, 2004).

In addition, after its publication, the algorithm was independently implemented in the popular Weka package (Witten & Frank, 2000). The BIC scoring measure was analyzed and refined by Hamerly and Elkan (2003).

The choice of BIC as the splitting criterion is not the only possible one. While I have found BIC to perform well for my test-sets and applications, using other criteria, such as AIC or the Anderson-Darling test may make sense in other areas. Incorporating such measures into my algorithm is straightforward: AIC is trivial since all the sub-expressions for it are needed in the BIC formula. The Anderson-Darling measure was retrofitted following the publication of Hamerly and Elkan (2003) and required only minor code changes. Therefore, we may classify this work as a whole new family of algorithms that differ only in their local optimization criteria.

Another direct extension is the application of BIC (or similar criteria) to direct a model search in an unrestricted-Gaussian EM algorithm (since blacklisting is assuming hard membership, this is non-trivial). One can also think of other ways to conduct the search for a model, even under the K-means assumption (e.g., removing centroids, as well as adding them).

Using my algorithms, statistical analysis of millions of data points and thousands of classes is performed in a matter of hours. Consequently, we are able to test astrophysical theories using observations that are much larger in scale than were ever available in the past. As hinted above, this work opens up an opportunity for a large class of algorithms to aid in such endeavors.

Finally, we need to consider the question of the dimensionality of the data. This paper has only empirically demonstrated X-means on up to four-dimensional data, although simpler algorithms (e.g., fast K-means) still give significant accelerations up to seven dimensions. But are even seven dimensions enough to be interesting? I say yes for three reasons.

First, many big-science disciplines need to cluster data sets with between millions and billions of low-dimensional records very quickly. Spatial galaxy, color-space sky objects, and protein gel clustering are just three such examples on which I am collaborating with natural scientists.

Second, for high-dimensional data sets it is frequently preferable to model the PDF by a factored representation (Meila, 1999b) such as a Bayesian network in which node distributions can be represented by lower-dimensional clusters. X-means is a step towards a fast inner-loop for these expensive algorithms.

Finally, it is possible to implement the regional splitting steps efficiently in high dimensions using ball trees (Moore, 2000), similarly to the way it is done with the fast version of K-means.

Chapter 3

Mixtures of Rectangles

Imagine an end-user of a clustering tool, seeking help with important decisions such as credit approval. A popular and general tool for clustering is the mixtures-of-Gaussians model. This is a powerful tool which allows for a wide variety of cluster shapes. It can be fitted accurately and quickly with the EM method. On the surface it looks appropriate for clustering the applicants into credit-worthy and others.

So far, our user has no trouble in taking the output of a Gaussian mixture learner and using it for decision making. But if he or she would also like to know *why* a particular applicant is rejected, the only way they have to do that is to examine the PDF, namely a mixture of Gaussians. In arithmetic terms, this boils down to subtractions and multiplications of record attributes, most probably represented in different, often incomparable, units. This kind of obscure manipulation does not inspire confidence in the outcome of the operation.

What I suggest is choosing a model that is aesthetically pleasing, even if the price is reduced expressiveness. This way, the cluster definitions themselves can be used directly in the application domain both for classification and for reasoning. Specifically, I fit the data to a mixture model in which each component is a hyper-rectangle in M-dimensional space. Hyper-rectangles may overlap, meaning some points can have "soft" membership in several components. Each component is simply described by, for each attribute, lower and upper bounds of points in the cluster.

The computational problem of finding a locally maximum-likelihood collection of k rectangles is made practical by allowing the rectangles to have soft "tails" in the early stages of an EM-like optimization scheme. My method requires no user-supplied parameters except for the desired number of clusters. These advantages make it highly attractive for "turn-key" data-mining applications. I demonstrate the usefulness of the method in subspace clustering for synthetic data, and in real-life datasets. I also show its effectiveness in a classification setting.

3.1 Introduction

My model is a mixture of uniform density M-dimensional hyper-rectangles, supplemented with Gaussian "tails". The tails mean that (as is the case with conventional Gaussians), the probability of a data point decreases with the distance from the "centroid". But, in contrast to conventional Gaussians, there is a difference in the way we measure distances. We consider the distance from the point to the closest point to it that is still included in the rectangular kernel. Note that under this definition all points contained in the kernel are equally (and maximally) likely. We fit the model by means of an EM procedure. Finally, we report the rectangular kernels. These are just lists of intervals (one interval per dimension, per cluster) the intersection of which defines the dense regions. This model has just $O(M)$ parameters, as opposed to $O(M^2)$ for mixtures of Gaussians. However, it is likely to require more components than the more general Gaussian-based model.

The difference between soft and hard membership is important to understand. With hard membership, each element belongs to exactly one class. This is intuitive to understand and makes sense in the original data domain. I also showed how this very property enables acceleration of K-means and related algorithms, by eliminating from the computation the elements which can be proven not to own a point. The problem with hard membership models is that they are harder to optimize directly. They have lower resilience to bad initial configuration and may ignore better configurations that are "nearby" (Zhang et al., 2000; Hamerly & Elkan, 2002). In contrast, soft membership models have smooth objective functions that are easy to manipulate and optimize. The downside is the loss of direct interpretation of the model in simple terms. Often, the consumer of the model now needs to reconcile statements of the form "this element is 67% in class A and 30% in class B". What I propose below offers the simplicity of hard membership with the amenability of soft models.

Much of the related work in the area of clustering is concerned with scaling of the algorithms to support huge datasets. CLARANS (Ng & Han, 1994) performs a search over the space of centroids for a k-means model (Duda & Hart, 1973; Bishop, 1995). BIRCH (Zhang et al., 1995) aims to scale this to massive datasets by concentrating on heuristic clustering of the data into spherical clusters while minimizing running time and memory usage. In Chapter 1 I showed how to use a kd-tree to make this calculation exact, and extended this result to automatic estimation of the number of clusters in Chapter 2.

Liu et al. (2000) show how to use decision-trees, traditionally used in supervised learning, in clustering. While the generated cluster description is human-readable for simple problems, one can easily construct an example where the cutoff points chosen by the decision tree are not very meaningful. This approach also assumes hard membership. CLIQUE (Agrawal et al., 1998) is specifically designed to generate interpretable output in the form of a DNF formula. The creation of these formulas, however, is done as a post-processing step and may miss the goal of presenting the clusters succinctly. Another problem is that they support only a single notion of membership (whether the data point is in a dense region or not). This precludes multiple class memberships. It also requires two user-supplied parameters (the resolution of the grid and a density threshold) which are unlikely to be specified correctly for all but expert users and simple densities. Nagesh et al. (1999) try to fix this, but the hard-membership assumption still holds in their work.

Learning axis-parallel boxes and their unions has been discussed in Maass and Warmuth (1995). Note, however, that my algorithm is unsupervised whereas the learning-theory work is mainly concerned with supervised learning. Another example of a machine learning approach that searches rectangles is Friedman and Fisher (1999), which addresses the supervised learning problem of finding a hyper-rectangle in input space that contains points with relatively high mean output value.

3.2 The Probabilistic Model and Derivation of the EM Step

3.2.1 Tailed Rectangular Distributions

We begin by defining M to be the number of dimensions. A hyper-rectangle R will be represented by a pair of M-length vectors, which define the upper (R^h) and lower (R^l) boundaries for each dimension. Let x_d denote the d-th element of the vector x. Define the function closest(x_d, l, h) as the closest point to x_d on the interval $[l, h]$:

$$\text{closest}(x_d, l, h) = \begin{cases} l & \text{if } x_d < l \\ x_d & \text{if } l \leq x_d \leq h \\ h & \text{if } h < x_d \end{cases} \tag{3.1}$$

with the natural multi-dimensional extension of closest(x, R) being the point in

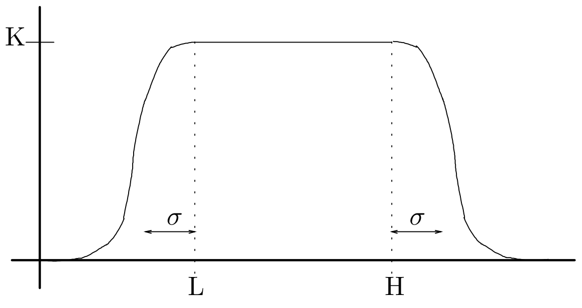

Figure 3.1: The 1-dimensional form of a rectangle (in this case a line-segment) with tails. An M-dimensional tailed rectangle is simply a product of these.

R which is closest to x. Consider the following single-rectangle PDF:

$$P(x) = K \exp -\frac{1}{2} \sum_{d=1}^{M} \left(\frac{x_d - \text{closest}(x_d, R_d^l, R_d^h)}{\sigma_d} \right)^2 \tag{3.2}$$

$P(x)$ can be thought of as a generalization of the Gaussian distribution with a diagonal covariance matrix. What makes it different from Gaussian is the way it measures distances to the distribution mean; instead of being the distance between two fixed points, we measure how far away x is from the boundary of the rectangle R.[1]

Another important property of this distribution is that it can be factored into independent components, thus:

$$\begin{aligned} & K \exp -\frac{1}{2} \left[\sum_{d=1}^{M} \left(\frac{x_d - \text{closest}(x_d, R_d^l, R_d^h)}{\sigma_d} \right)^2 \right] \\ = & \prod_{d=1}^{M} K_d \exp -\frac{1}{2} \left(\frac{x_d - \text{closest}(x_d, R_d^l, R_d^h)}{\sigma_d} \right)^2 , \end{aligned}$$

for suitable factors K_d (see below). Examples of such components are shown in Figures 3.1 and 3.2.

Consequently, when we proceed to integrate Formula 3.2 we only need to consider the single-dimensional case:

$$\int_{-\infty}^{\infty} \exp -\frac{1}{2} \left(\frac{x - \text{closest}(x, R)}{\sigma} \right)^2 dx$$

[1]Strictly speaking, the definition is how far x is from any point in R. This is implied since $\text{closest}(x, R) = x$ for $x \in R$.

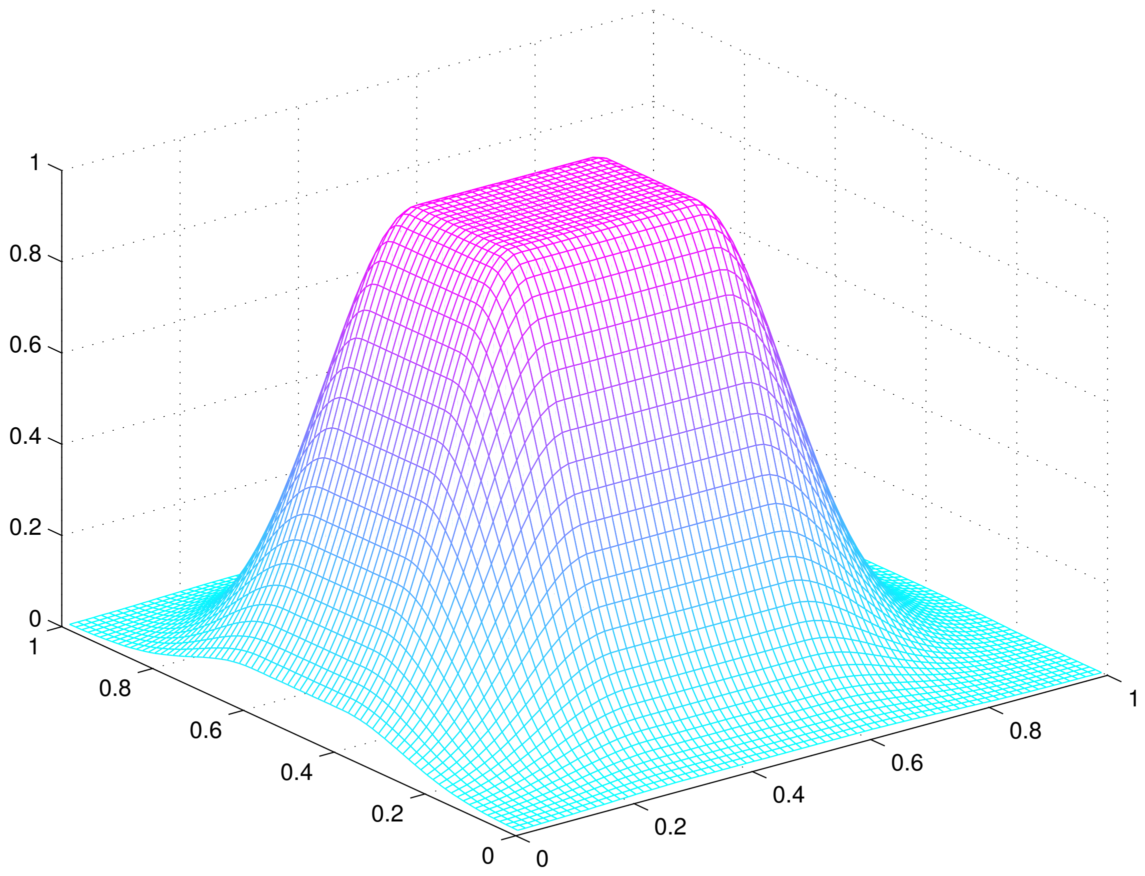

Figure 3.2: The 2-dimensional form of a rectangle with tails.

where x and σ are now real numbers and R is an interval $[l, h]$. We get an integral similar to the one derived from the univariate Normal distribution, except for the fact that the mean point is stretched into an interval:

$$\begin{aligned} & \int_{-\infty}^{l} \exp -\frac{1}{2}\left(\frac{x-l}{\sigma}\right)^2 dx \\ + & \int_{l}^{h} \exp(0) dx \\ + & \int_{h}^{\infty} \exp -\frac{1}{2}\left(\frac{x-h}{\sigma}\right)^2 dx \\ = & \sqrt{2\pi}\sigma + (h-l) \ . \end{aligned}$$

Thus the normalizing constant in Equation 3.2 is simply the product of the following per-dimension constants:

$$K^{-1} = \prod_{d=1}^{M} \left[\sqrt{2\pi}\sigma_d + (R_d^h - R_d^l) \right] \ .$$

Note the penalty imposed on high-volume rectangles. This will later prevent them from expanding infinitely to try and capture all possible points.

3.2.2 Maximum Likelihood Estimation of a Single Tailed Rectangular Distribution

Suppose we have a dataset $X = \{x^1, x^2, \ldots x^R\}$ and, given σ, we wish to find the Maximum Likelihood (MLE) set of $2M$ parameters defining the rectangle. The log-likelihood function is

$$\begin{aligned} LL(X) \ &= \qquad (3.3) \\ &\sum_d \Big(-R\log(\sqrt{2\pi}\sigma_d + R_d^h - R_d^l) \\ &+ \ \sum_i -\frac{1}{2}\left[\frac{x_d^i - \mathrm{closest}(x_d^i, R_d^l, R_d^h))}{\sigma_d}\right]^2 \Bigg) \ . \end{aligned}$$

From this equation it is immediately clear that we can perform the MLE for each dimension independently. For each dimension d in turn find the values l and h that maximize

$$\Big(-R\log(\sqrt{2\pi}\sigma + h - l)\Big) + \sum_i -\frac{1}{2}\left[\frac{x_d^i - \mathrm{closest}(x_d^i, l, h)}{\sigma_d}\right]^2 \ .$$

We do this by first guessing an initial value of (l, h). Then we fix the low-point at l, and find a good candidate for the new high boundary h'. Then we find a good candidate for the low boundary l' based on the existing h. Figure 3.3 shows an example of a single fitting step for a single one-dimensional component. For each of the boundaries, we want to maximize the likelihood which is a function of the new value. To achieve this we use the golden-ratio one-dimensional optimizer (Press et al., 1992). Under the assumption that the function is unimodal in the given range, this optimizer will find a maximum point of it, up to the specified tolerance value. The number of function evaluations is logarithmic in the width of the range. Although I have not yet proved that the likelihood function is indeed unimodal, empirical evidence suggests this is indeed the case.

3.2.3 EM Search for a Mixture of Tailed Rectangles

EM for mixture model clustering generally takes the following form:

1. Begin with a guess of the the mixture parameters $\{p_1, \theta_1, p_2, \theta_2, \dots p_k, \theta_k\}$ where p_j is the probability of the mixture generating a data point from component j and θ_j are the parameters for the j-th component. In our example θ_j consists of $2M$ parameters: the upper and lower bounds of the j-th rectangle. Note that we are holding σ fixed during the iterations—we are not estimating it by EM.

2. For each data point x^i and each mixture component j let w_{ij} be:

$$P(\text{generated by } j\text{-th component} \,|\, \text{located at } x_i)$$

   or, more succinctly,

$$w_{ij} = P(\text{class} = j \,|\, x_i) \; .$$

   This, by Bayes' rule, is

$$w_{ij} = \frac{P(x_i \,|\, \text{class} = j) \cdot p_j}{\sum_l P(x_i \,|\, \text{class} = l) \cdot p_l} \; .$$

3. For each component j, re-fit the parameters θ_j to a "weighted" version of the dataset in which the i -th data point is given weight w_{ij}. Each data point thus only counts as a fraction of a full data point in its contribution to the likelihood.

   In our case this means we need to reestimate the coordinates of rectangle $R = R_j$ to maximize

$$\begin{aligned} & LL(X) = \\ & \sum_d \Bigg(-(\sum_i w_{ij}) \log(\sqrt{2\pi}\sigma_d + R_d^h - R_d^l) \\ + \quad & \sum_i -\frac{w_{ij}}{2} \left[\frac{x_d^i - \text{closest}(x_d^i, R_d^l, R_d^h)}{\sigma_d} \right]^2 \Bigg) \; . \end{aligned}$$

   This can again be achieved one dimension at a time with two golden-ratio searches per dimension: one for the lower and one for the upper bound.

3.2.4 The Full Algorithm

The full algorithm follows. Initialize the mixture components by taking, e.g. initial points as used in the anchors hierarchy (Moore, 2000). Initialize σ (I currently use some constant fraction of the range of the data in each dimension). For each dimension and component, compute a new upper boundary based on the existing lower one, and a new lower boundary, based on the current upper one. Change the boundaries and iterate. Once stability is obtained, decrease σ (I multiply it by a constant factor smaller than one) and continue iterating. Terminate if the components are all stable immediately after decreasing σ.

3.2.5 Example

For illustration, Figures 3.4, 3.5, 3.6, 3.7 show runs on synthetic two-dimensional datasets made by drawing points from component-wise rectangular distributions. Initially, the boundaries are quite arbitrary and σ is large. This allows the rectangles to freely move to better locations. In following iterations, as σ decreases, the rectangles try to reposition the boundaries to capture as many points as possible (since now the penalty for excluding them is high). After a few more iterations, the distribution is modeled accurately.

3.2.6 Intuition

Ultimately we are interested in obtaining a final mixture of hard rectangles (i.e., with infinitely steeply declining tails). But the key to the whole algorithm is the use of relatively wider tails in the early stages. Without them, it is impossible for rectangles to move because they would pay an infinite penalty for missing a single data point with weight $w_{ij} > 0$. Thus, without the tails, the initial EM iterations see all rectangles jump to the bounding box of the whole data, where they remain. It is only with the tails that the rectangles are guided in directions to grow or shrink, and are able to negotiate ownership of points with the other rectangles.

3.3 Experimental Results

Our first test is as follows. Fix two parameters r and M. As usual, M is the dimensionality of the data. Additionally, choose a set $R \subseteq \{1 \dots M\}$ of r relevant

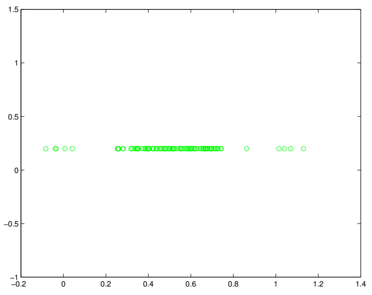

(a)

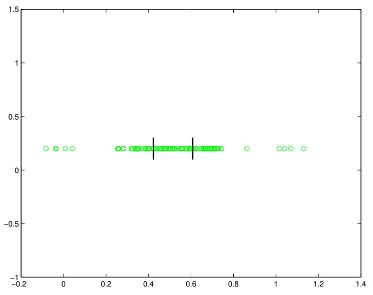

(b)

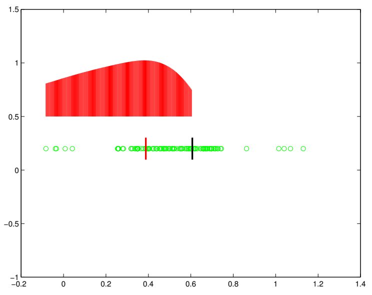

(c)

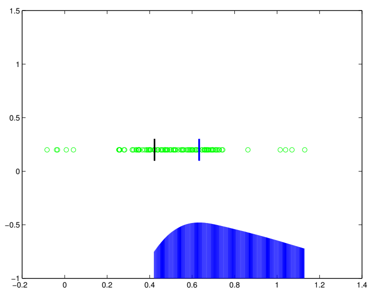

(d)

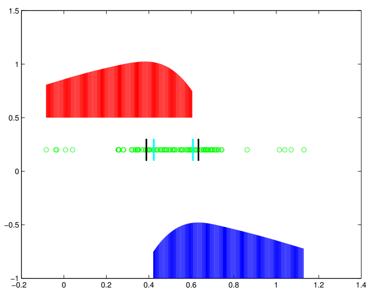

(e)

Figure 3.3: Fitting an interval with tails in one dimension. The input data (a). The current estimate for the interval (b). Fixing the upper boundary, the likelihood function is represented by the height of the red line, as the lower boundary is varied (c). Fixing the lower boundary, the likelihood function is shown by the blue line as the upper boundary is varied (d). Both boundaries are moved to maximize likelihood (e).

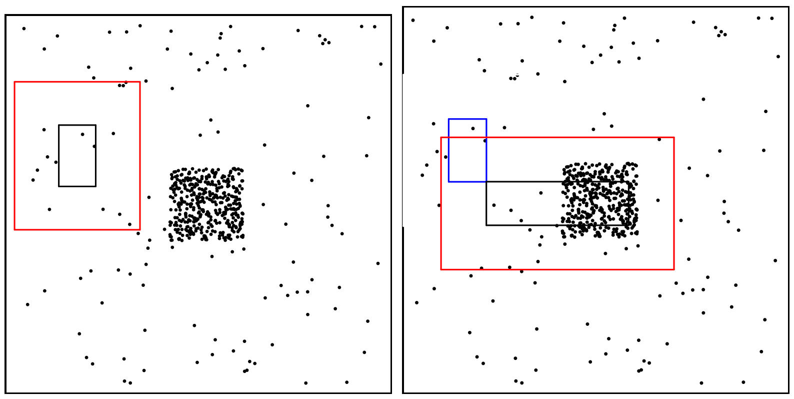
(a) (b)

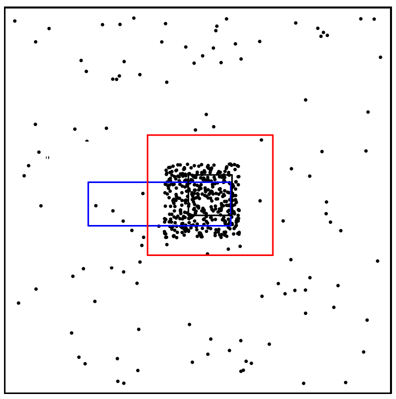
(c)

Figure 3.4: Fitting a two-dimensional rectangle. The inner rectangles mark the kernel boundary, while the outer ones are σ away from them. The data and the initial rectangle (a). The new configuration after one fitting step (b). For reference, the initial configuration is show in blue. Configuration after a second fitting step (c), with the previous fit in blue for reference. Subsequent iterations move the rectangle boundaries to closely match the dense region.

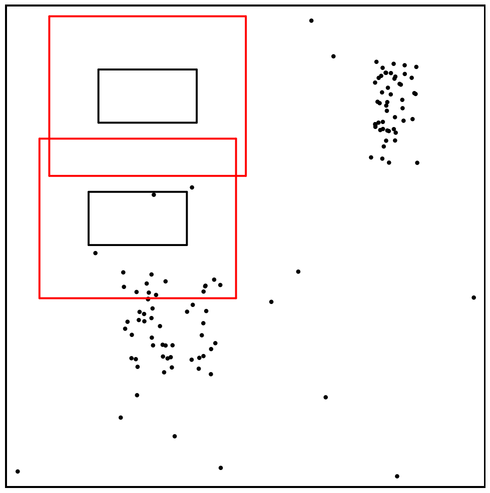

(a)

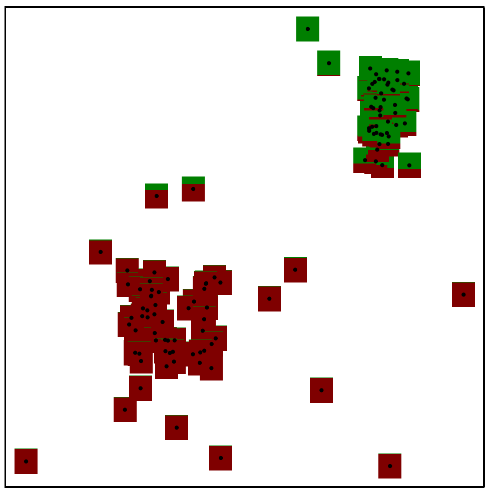

(b)

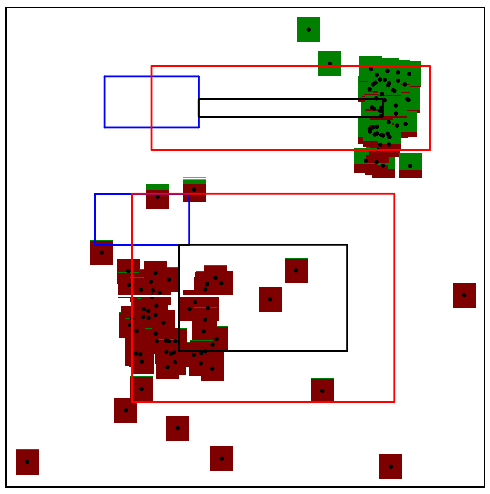

(c)

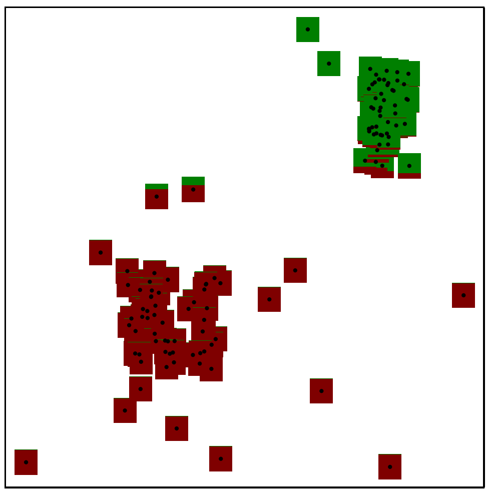

(d)

Figure 3.5: Fitting a two-dimensional mixture. The input data and initial placement for two rectangles (a). The inner rectangles mark the kernel boundary, while the outer ones are σ away from them. Each data point is weighed by its level of ownership by either rectangle (b). The rectangles move according to weighted re-estimation step (c). The previous location for each rectangle is shown for reference. Each point is weight according to the new location (d).

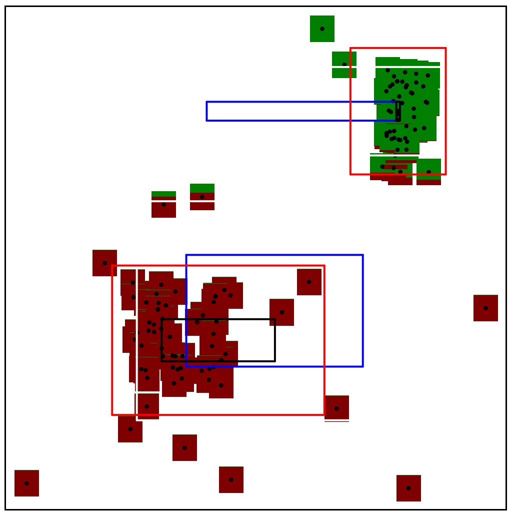

(a)

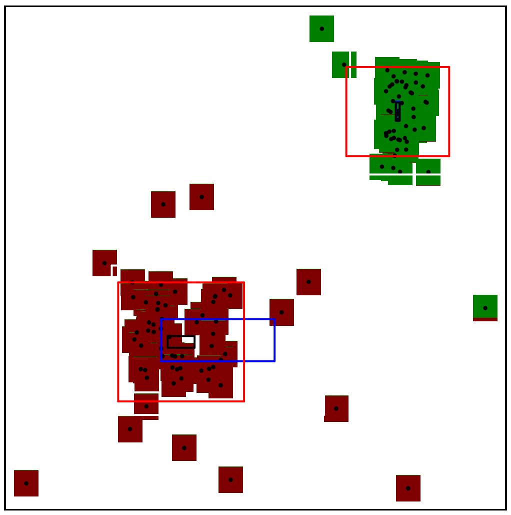

(b)

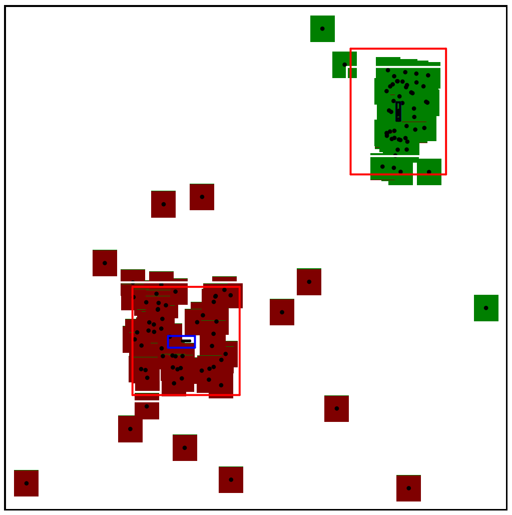

(c)

Figure 3.6: Fitting a two-dimensional mixture (cont'd). The rectangles are fitted again (a). Subsequent weighing and estimation steps (b,c).

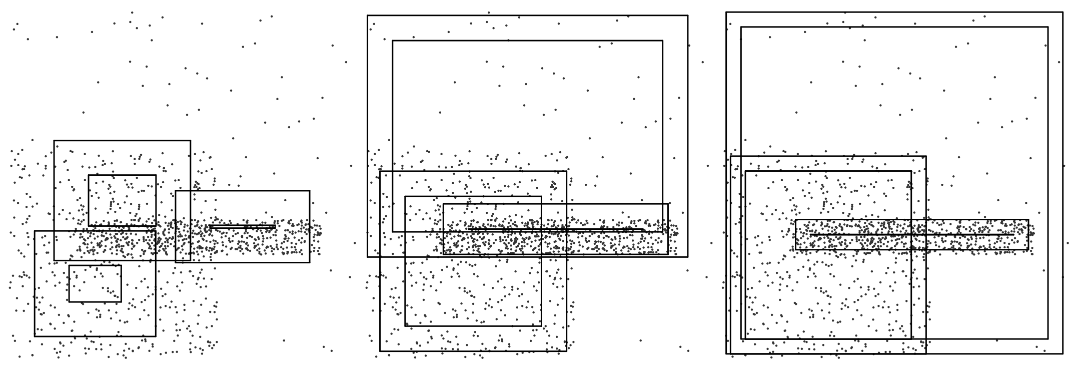

(a) (b) (c)

Figure 3.7: A three-component example. Shown from left to right, the components after the first, 20-th, and 40-th iteration. The inner rectangles mark the kernel boundary, while the outer ones are σ away from them.

dimensions. Now generate points, choosing one of two classes for each point x, and then setting the i-th coordinate to be:

$$\begin{cases} \text{uniform}(0,1) \text{ if } i \notin R \\ \text{uniform}(0,0.5) \text{ if } i \in R \text{ and } x \text{ is in class 1} \\ \text{uniform}(0.5,1) \text{ if } i \in R \text{ and } x \text{ is in class 2} \end{cases}$$

For $M = r = 2$, this distribution looks like a 2×2 checkerboard. This set is interesting because it clearly contains clusters, yet when the data is projected onto any single dimension, the distribution is indistinguishable from uniform. The parameter r adds another source of noise (greater with decreasing r).

After estimating the rectangles, I evaluated the result by rounding the boundaries to $0, 0.5$, or 1 if they lie within less than 2σ away from these values, and keeping them unchanged otherwise (σ was never more than 0.075 in any dimension). I then declare the run a "success" if the rounded boundaries match the generating rectangles exactly — that is, they always have 0 and 1 in the irrelevant dimensions, and $0, 0.5$, or 1, as the case may be, in the relevant ones. Results are shown in Figure 3.8. In general, it was possible to identify the relevant $r = 5$ dimensions from data with dimensionality up to $M = 30$.

Another experiment involves a similar setup, this time in three dimensions. Consider the a 3^3 grid placed on the unit cube. We will use nine of the resulting grid cells to generate data points from. See Figure 3.9. Now, projection along any *two* dimensions is indistinguishable from the joint two-dimensional uniform distribution.

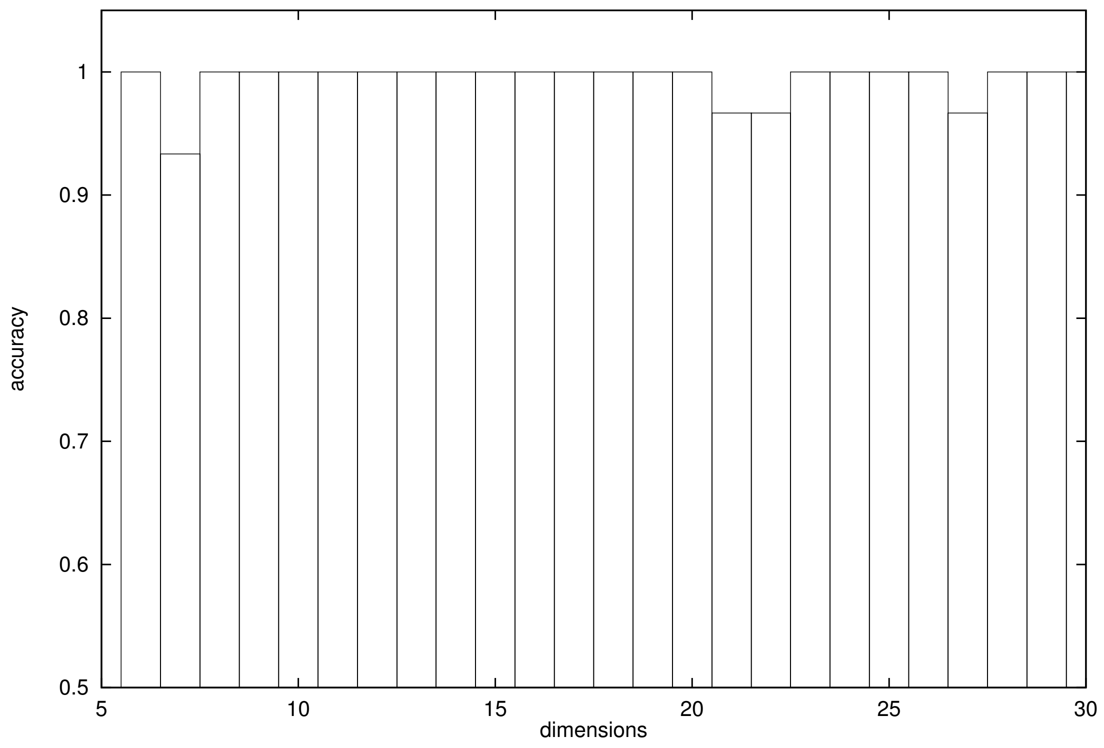

Figure 3.8: Estimated boundaries for the "checkerboard" data with 5 relevant dimensions. The y axis is the fraction of the experiments in which exactly the relevant dimensions were identified (out of 30 trials). The x axis is the dimensionality of the data (M). Similar experiments were held for 2 and 10 relevant dimensions (not shown).

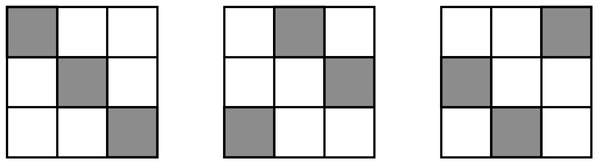

Figure 3.9: Grid cells used for generation of data. Shown, from left to right, "slices" along the third dimension, each of width 1/3.

Again, the estimated mixture is very close to the original one, as seen in Figure 3.10.

In another experiment, data points were generated from a mixture as follows. In each dimension, a random interval with expected width 0.4 was drawn from $[0, 1]$. The intersection of these intervals defines a hyper-rectangle, and data points were generated from the union of several such components. The estimated distribution was evaluated as follows. Fix a mapping from the true distribution to the estimated one. Each estimated rectangle is compared to the matching true rectangle by taking the M-th root of the ratio between the volumes of the intersection of the two rectangles to their union. The *similarity* of the two distributions is just the average of these values, taken over all rectangle pairs. The values reported here are the maximum similarity values taken over all possible mappings (i.e., all permutations over $[1, \ldots k]$, where k is the number of components). See Figure 3.11. The results show that generally similarity of in the 90% range.

I have also performed sporadic experiments to test the sensitivity of the algorithm to the different parameters. Figure 3.12 shows how supplying the wrong number of rectangles might affect the run. Another parameter is the initial value for σ. I currently use a rather simplistic estimate of 1/10 of the range of the input. It does work for my datasets. A more sophisticated approach would be to first try and estimate σ (say, using a model with spherical Gaussians) and use the estimate to set the rectangle tails.

Experiments on real-life data were done on the "mpg" and "census" datasets from the UCI repository (Blake & Merz, 1998). The "mpg" data has about 400 records with 7 continuous[2] attributes. Running on this data with the number of components set to three, we get the results shown in Table 3.1. Interpreting this data, we see that cars with at most four cylinders are the most economical, and that eight-cylinder cars

[2]We treat discrete attributes as continuous if the values can be linearly ordered (e.g., number of cylinders and model year).

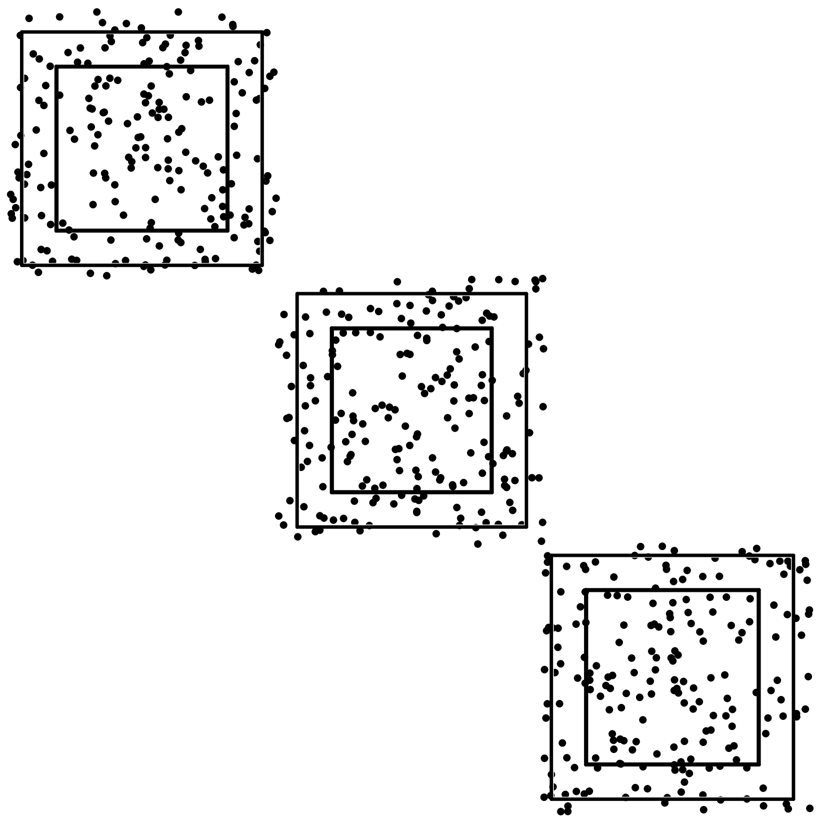

Figure 3.10: Estimated distribution along the first two dimensions for the dataset. Only data points in the first “slice” are shown. The inner rectangles mark the kernel boundary, while the outer ones are σ away from them.

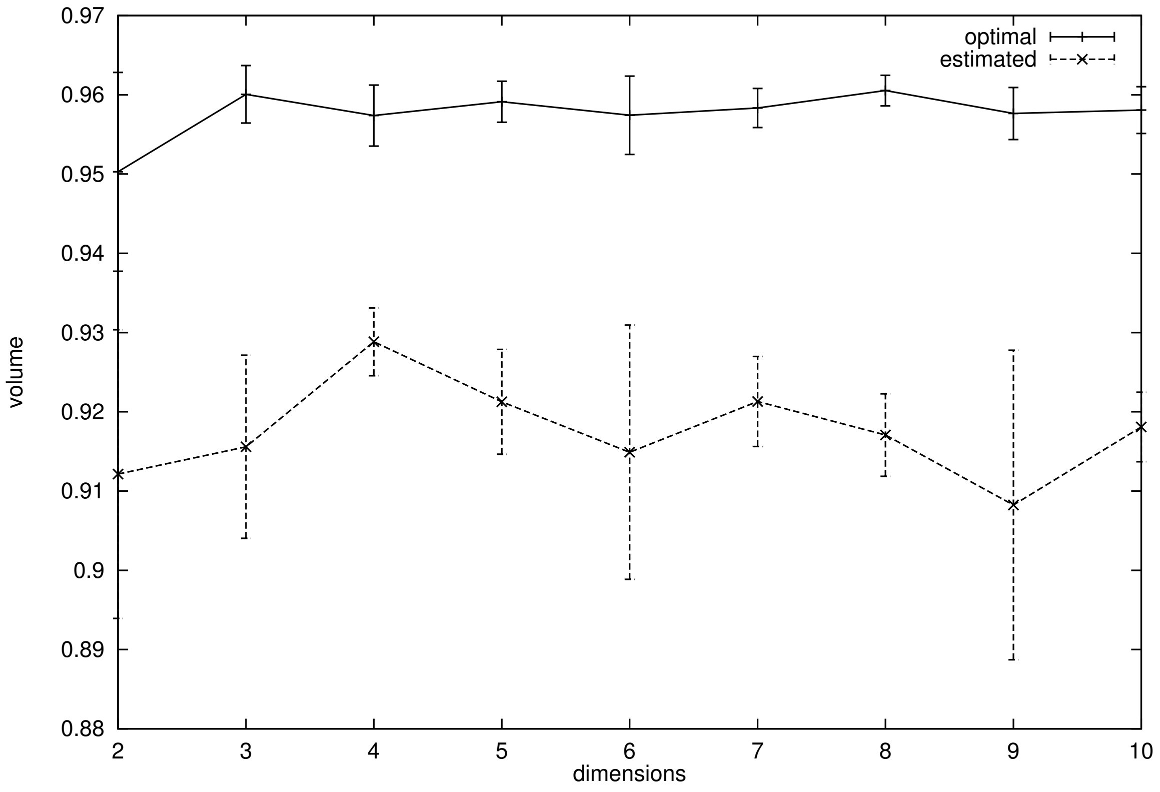

Figure 3.11: Similarity, by relative volume of intersection, of the estimated distribution to the true one. There were 4 rectangles in the distribution. The "estimated" line shows the performance of the proposed algorithm. The "optimal" line is for a version that initializes the distribution with the true one, therefore providing a theoretical upper bound for the similarity.

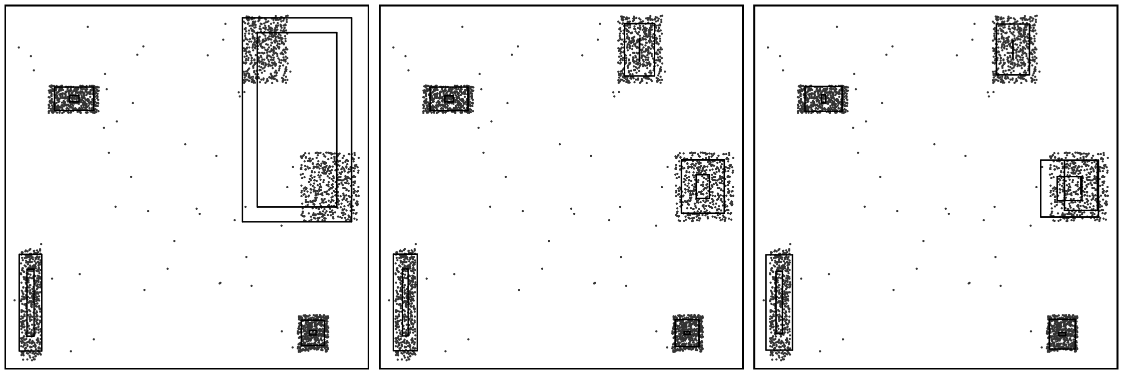

Figure 3.12: Results when the reported number of rectangles k differs from the true number (which is 5). From left to right, the reported number was 4, 5, and 6. In (a), one of the estimated rectangles takes over two clusters. In (c), two estimated rectangles "fight" over the points in a single cluster.

Table 3.1: Clusters for the "mpg" data. "Prob." is the mixture probability for the cluster; the remaining attributes are from the input (MPG, cylinders, displacement, horsepower, weight, acceleration, model-year). Numbers are rounded to the nearest integer.

PROB.	MPG	CYLS	DISP.	HP	WEIGHT	ACCEL	YEAR
52%	$[18, 46]$	$[3, 4]$	$[75, 150]$	$[49, 112]$	$[1700, 3205]$	$[12, 25]$	$[70, 82]$
23%	$[10, 18]$	$[8, 8]$	$[303, 453]$	$[130, 227]$	$[3134, 5092]$	$[8, 18]$	$[70, 79]$
25%	$[15, 37]$	$[5, 8]$	$[126, 347]$	$[70, 162]$	$[2539, 3993]$	$[11, 22]$	$[70, 82]$

weighing more than 3000 pounds are the most environmentally-harmful. While these facts should come as no surprise, it is important to note that the "mpg" attribute was not flagged as special in the input. It was found useful in defining clusters because it has inherent correlation with other attributes. Had we been asked to classify the model year, for example, we would run the program in the exact same way. From the results we would conclude that this attribute is not informative (because all clusters have the same boundaries for it, approximately). Another interesting feature of this output is the fact that eight-cylinder cars are included in both the second and third cluster. So these clusters are overlapping, and further distinction can be made on other attributes (such as displacement, or weight). This effect is due to the "soft" membership that is inherent in the model.

Table 3.2: Clusters for the "census" data. "Prob." is the mixture probability for the cluster; the remaining attributes are from the input (age, taxweight, edunum, capitalgain, capitalloss, hours, income). Numbers are rounded to the nearest integer.

PROB.	AGE	TAXWEIGHT	EDU	GAIN	LOSS	HOURS	INCOME
14%	$[28, 65]$	$[65863, 319616]$	$[7, 15]$	$[748, 767]$	$[3, 2391]$	$[28, 70]$	$[1, 1]$
11%	$[18, 88]$	$[44770, 998117]$	$[1, 16]$	$[45, 805]$	$[2, 33]$	$[4, 98]$	$[0, 1]$
8%	$[26, 70]$	$[63389, 395858]$	$[9, 16]$	$[73, 99452]$	$[32, 33]$	$[20, 71]$	$[1, 1]$
67%	$[19, 65]$	$[62643, 342083]$	$[4, 14]$	$[45, 787]$	$[4, 1898]$	$[15, 59]$	$[0, 0]$

The "census" set is significantly bigger (about $32,000$ records in the training set). It has a binary "income" attribute (indicating whether the annual income is over $\$50K$) which is to be predicted, based on other values. Again, I did not specify this to the algorithm directly, but rather let it cluster the whole data. On termination, I inspect to see if the resulting clusters have a very narrow range for this attribute, indicating that they represent records that are mostly in the same income class.[3] This was observed clearly when the number of clusters was set to four. Results are in Table 3.2. Three of the clusters predict the "income" attribute to be either zero or one. I built a simple classifier based on these clusters. If a data point is contained in one of the regions defined by the kernel boundaries, plus or minus the vector σ, it predicts the label zero or one according to the value in the corresponding estimated cluster. It also predicts one or zero if the point belongs in more than one cluster, but all said clusters have the same label. If we treat all other cases as wrong classification, we get accuracy of 78% on the test-set. But, if we classify as "zero" (the more frequent label in the training-set) the 3537 records that belong in no component, the accuracy increases to 97%. Note that the UCI repository contains a survey of the performance of classical techniques, such as C4.5, Naive Bayes, and nearest-neighbor, on this data. The reported accuracies for about 16 algorithms range from 79% to 86%. This experiment shows the usefulness of clustering (and, in particular, of my technique) in a supervised-learning task, when the label attribute is informative.

[3]The interval width is typically not zero, due to both numerical and statistical reasons, such as the inclusion of outliers.

3.4 Conclusion

I have demonstrated a method that benefits from the usefulness of soft membership and the expressiveness and clean analysis of mixture models. At the same time, the produced clusters have a compact representation which people can find comprehensible. As an added bonus, expanding the Gaussian means into a rectangular form seems to help avoid the inherent statistical problems that come with high-dimensional distance computations. The resulting clusters are highly readable and allow for the construction of very simple, yet very effective, classifiers. The proposed model was also shown to be effective in dimension-reduction tasks.

My implementation has been used to visualize highway traffic data (Raz et al., 2004). Truck weigh-in-motion data collected by the Minnesota department of transportation was analyzed with a variety of methods and presented to a domain expert. The mixture of rectangles was reported to produce crisp models and made it easy to point out the anomalies. For example, a common misclassification failure was detected where the low-level software would determine some trucks had one axle. Another observation made clear was a system-wide change around November 1999. Later it was discovered that a vendor of one of the software components made unreported configuration changes at that date.

I believe it would be straightforward to extend this method to data involving discrete attributes. For a given mixture component, each discrete attribute would be modeled independently by a multinomial distribution. The parameters needed for an n-ary attribute would simply be the n multinomial probabilities (which must sum to one). In the case of all-discrete (i.e., no real-valued) attributes, this would degenerate to the well-known mixtures of products of multinomials distribution (e.g. Meila and Heckerman (1998)).

A natural extension would be to get rid of the single parameter that the user needs to supply — the desired number of clusters. Ideally the algorithm would estimate this by itself.

I argue that the representation of clusters as intersection of intervals is succinct. However, there is room for improvement, especially if the data dimensionality is very large. I believe that a post-processing step that identifies the irrelevant dimensions and removes them from the output can be easily implemented. Another useful operation would be to sort the dimensions by their "importance" (or contribution to the log-likelihood) before presenting the intervals.

Chapter 4

Fast Dependency Tree Construction

We continue our quest to find useful models. Bayesian networks are a popular class of very general models. They are also appealing from the cognitive aspect as their structure — if not too complex — can often be visualized and easily understood. However, they are hard to fit from data because of their richness.

I am interested in restricting the search space by considering only a simpler sub-class of graphical models, namely trees. For trees, a well-known algorithm can find optimal solutions in polynomial time. As an added feature, the trees can be described more simply to human users. I show how to accelerate the known algorithm to run in sub-linear time. Empirical evidence shows run time which is linear in the number of attributes, and constant regardless in the input size. The constant depends only on intrinsic properties of the data. This allows processing of very large data sets.

4.1 Introduction

Bayes nets are widely used for data modeling. However, the problem of constructing Bayes nets from data remains a hard one, requiring search in a super-exponential space of possible graph structures. Despite recent advances (Friedman et al., 1999), learning network structure from big data sets demands huge computational resources. We therefore turn to a simpler model, which is easier to compute while still being expressive enough to be useful. Namely, we look at dependency trees, which are belief networks that satisfy the additional constraint that each node has at most one parent. In this simple case it has been shown (Chow & Liu, 1968) that finding the tree that maximizes the data likelihood can be reduced to a much simpler problem. First, construct a full graph where each node corresponds to an attribute in the input data. Next, assign edge weights; these are are derived from the mutual information values of the corresponding attribute pairs. Finally, run a minimum[1] spanning tree algorithm on the weighted graph. The output tree is the desired one.

Dependency trees are interesting in their own right. They form a complete representation. Additionally they can act as initializers for search, as mixture components (Meila, 1999b), or as components in classifiers (Friedman et al., 1998). It is my intent to eventually apply the technology introduced here to the full problem of Bayes Net structure search.

Once the weight matrix is constructed, executing a minimum spanning tree (MST) algorithm is fast. The time-consuming part is the population of the weight matrix, which takes time $O(RM^2)$. This becomes expensive when considering datasets with hundreds of thousands of records (R) and hundreds of attributes (M).

To overcome this problem, I propose a new way of interleaving the spanning tree construction with the operations needed to compute the mutual information coefficients. I develop a new spanning-tree algorithm, based solely on Tarjan's (1983) red-edge rule. This algorithm is capable of using partial knowledge about edge weights and of signaling the need for more accurate information regarding a particular edge. The partial information we maintain is in the form of probabilistic confidence intervals on the edge weights; an interval is derived by looking at a sub-sample of the data for a particular attribute pair. Whenever the algorithm signals that a currently-known interval is too wide, we inspect more data records in order to shrink it. Once the interval is small enough, we may be able to prove that the corresponding edge is *not* a part of the tree. Whenever such an edge can be eliminated without looking at the full data set, the work associated with the remainder of the data is saved. This is where performance is gained.

I have implemented the algorithm for numeric and categorical data and tested it on real and synthetic data sets containing hundreds of attributes and millions of records. I show experimental results of up to 5,000-fold speed improvements over the traditional algorithm. The resulting trees are, in most cases, of near-identical quality to the ones grown by the naive algorithm.

Use of probabilistic bounds to direct structure-search appears in Maron and Moore

[1]To be precise, we will use it as a *maximum* spanning tree algorithm. The two are interchangeable, requiring just a reversal of the edge weight comparison operator. Historically, minimum has been far more popular a name.

(1994) for classification and in Moore and Lee (1994) for model selection. In a sequence of papers, Domingos et al. have demonstrated the usefulness of this technique for decision trees (Domingos & Hulten, 2000), K-means clustering (Domingos & Hulten, 2001a), and mixtures-of-Gaussians EM (Domingos & Hulten, 2001b). In the context of dependency trees, Meila (1999a) discusses the discrete case that frequently comes up in text-mining applications, where the attributes are sparse in the sense that only a small fraction of them are true for any record. In this case it is possible to exploit the sparseness and accelerate the Chow-Liu algorithm.

Throughout the chapter we use the following notation. The number of data records is R, the number of attributes M. When x is an attribute, x_i is the value it takes for the i-th record. We denote by ρ_{xy} the correlation coefficient between attributes x and y, and omit the subscript when it is clear from the context. H_x is the entropy of an attribute or an attribute set x.

4.2 A Slow Minimum-Spanning Tree Algorithm

We begin by describing our MST algorithm. Although in its given form it can be applied to any graph, it is asymptotically slower than established algorithms (as predicted in Tarjan (1983) for all algorithms in its class). We then proceed to describe its use in the case where some edge weights are known not exactly, but rather only to lie within a given interval. In Section 4.4 we will show how this property of the algorithm interacts with the data-scanning step to produce an efficient dependency-tree algorithm.

In the following discussion we assume we are given a complete graph with n nodes, and the task is to find a tree connecting all of its nodes such that the total tree weight (defined to be the sum of the weights of its edges) is minimized. This problem has been extremely well studied and numerous efficient algorithms for it exist.

We start with a rule to *eliminate* edges from consideration for the output tree. Following Tarjan (1983), we state the so-called “red-edge” rule:

Theorem 7: The heaviest edge in any cycle in the graph is not part of the minimum spanning tree.

Traditionally, MST algorithms use this rule in conjunction with a greedy “blue-edge” rule, which chooses edges for *inclusion* in the tree. In contrast, we will repeatedly use the red-edge rule until all but $n-1$ edges have been eliminated. The proof this results in a minimum-spanning tree follows from Tarjan (1983).

Let E be the original set of edges. Denote by L the set of edges that have already been eliminated, and let $\bar{L} = E \setminus L$. As a way to guide our search for edges to eliminate we maintain the following invariant:

Invariant 8: At any point there is a spanning tree T, which is composed of edges in $\bar{L}$.

In each step, we arbitrarily choose some edge e in $\bar{L} \setminus T$ and try to eliminate it using the red-edge rule. Recall that the rule needs a cycle to act on. Let P be the path in T between e's endpoints. The cycle we will apply the red-edge rule to will be composed of e and P. It is clear we only need to compare e with the heaviest edge in P. If e is heavier, we can eliminate it by the red-edge rule. However, if it is lighter, then we can eliminate the tree edge by the same rule. If this is indeed the case, we do so and add e to the tree to preserve Invariant 8. The algorithm, which we call Minimum Incremental Spanning Tree (MIST), is listed in Figure 4.1. Figures 4.2,4.3,4.4 and 4.5 illustrate how it may run on an example graph.

The MIST algorithm can be applied directly to a graph where the edge weights are known exactly. And like many other MST algorithms, it can also be used in the case where just the relative order of the edge weights is given. Now imagine a different setting, where edge weights are not given, and instead an oracle exists, who knows the exact values of the edge weights. When asked about the relative order of two edges, it may either respond with the correct answer, or it may give an inconclusive answer. Furthermore, a constant fee is charged for each query. In this setup, MIST is still suited for finding a spanning tree while minimizing the number of queries issued. In step 2, we go to the oracle to determine the order. If the answer is conclusive, the algorithm proceeds as described. Otherwise, it just ignores the "if" clause altogether and iterates (possibly with a different edge e).

For the moment, this setting may seem contrived, but in Section 4.4, we go back to the MIST algorithm and put it in a context very similar to the one described here.

4.3 Probabilistic Bounds on Mutual Information

We now concentrate once again on the specific problem of determining the mutual information between a pair of attributes. We show how to compute it given the complete data, and how to derive probabilistic confidence intervals for it, given just a sample of the data.

```
1. $T \leftarrow$ an arbitrary spanning set of $n-1$ edges.

   $L \leftarrow$ empty set.

2. While $|\bar{L}| > n-1$ do:

        Pick an arbitrary edge $e \in \bar{L} \setminus T$.
        Let $e'$ be the heaviest edge on the path in $T$ between the
        endpoints of $e$.
        If $e$ is heavier than $e'$:
            $L \leftarrow L \cup \{e\}$
        otherwise:
            $T \leftarrow T \cup \{e\} \setminus \{e'\}$
            $L \leftarrow L \cup \{e'\}$

3. Output $T$.
```

Figure 4.1: The MIST algorithm. At each step of the iteration, T contains the current "draft" tree. L contains the set of edges that have been proven to *not* be in the MST and so $\bar{L}$ contains the set of edges that still have some chance of being in the MST. T never contains an edge in L.

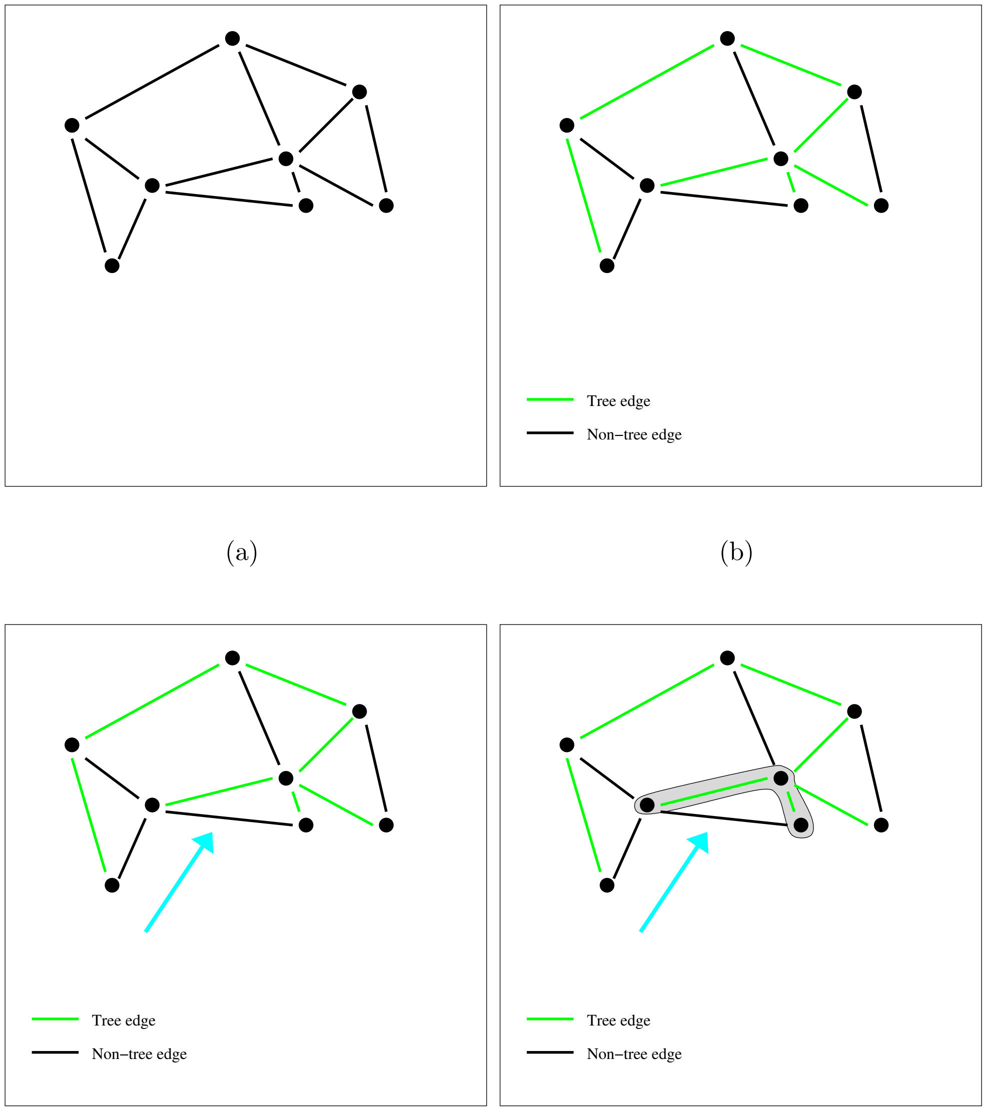

Figure 4.2: Walkthrough of the MIST algorithm. The original graph (a). An arbitrary spanning tree is chosen (b). An arbitrary edge is chosen for elimination (c). The tree path completes the edge to a cycle (d). (Continued)

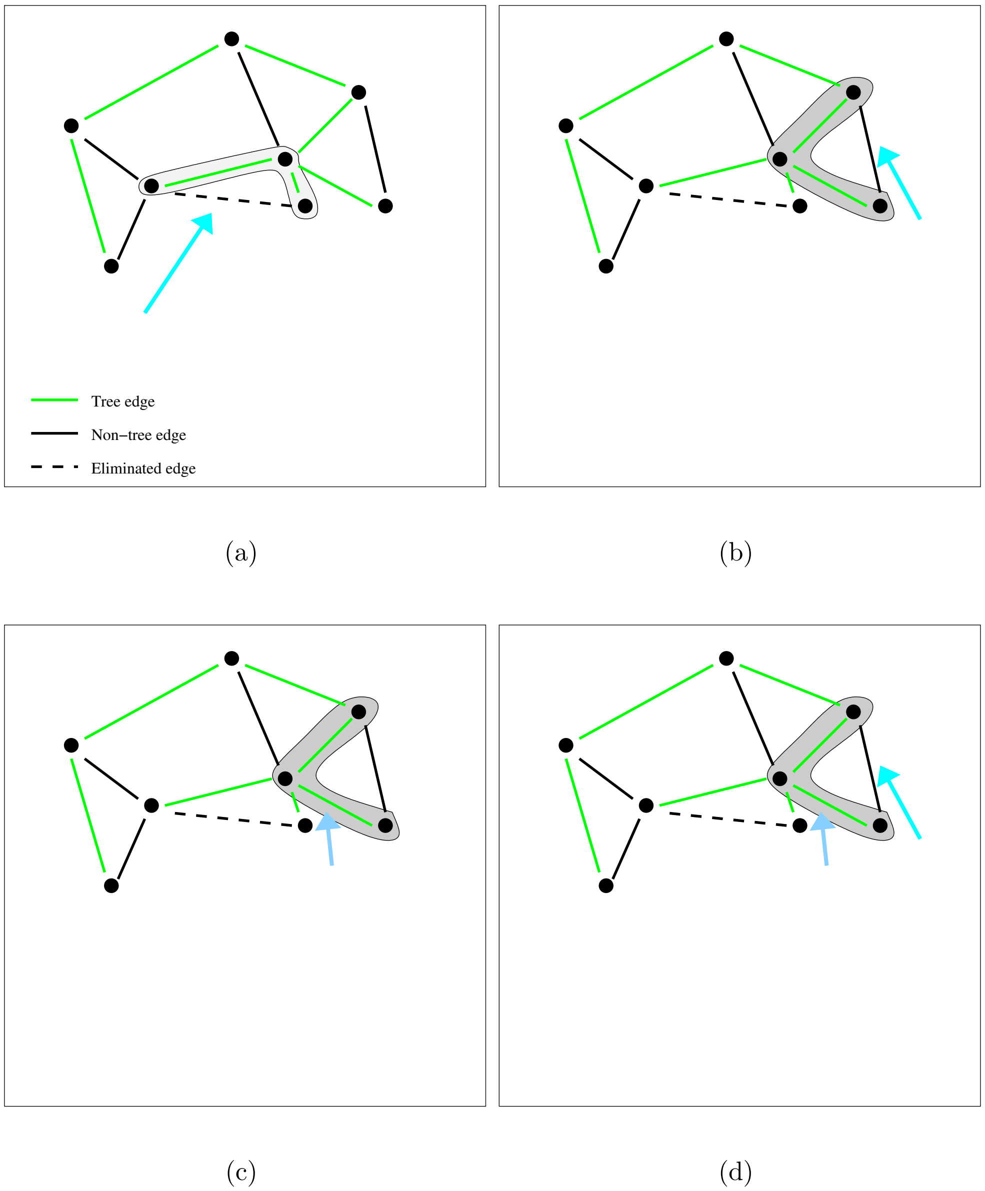

Figure 4.3: Walkthrough of the MIST algorithm (cont'd). The edge is discovered to be the heaviest on the cycle and eliminated (a). Another edge is chosen (b). On completing the cycle, some other edge in it is discovered to be heaviest (c). The tree edge is eliminated, and the non-tree edge swapped in (d). (Continued)

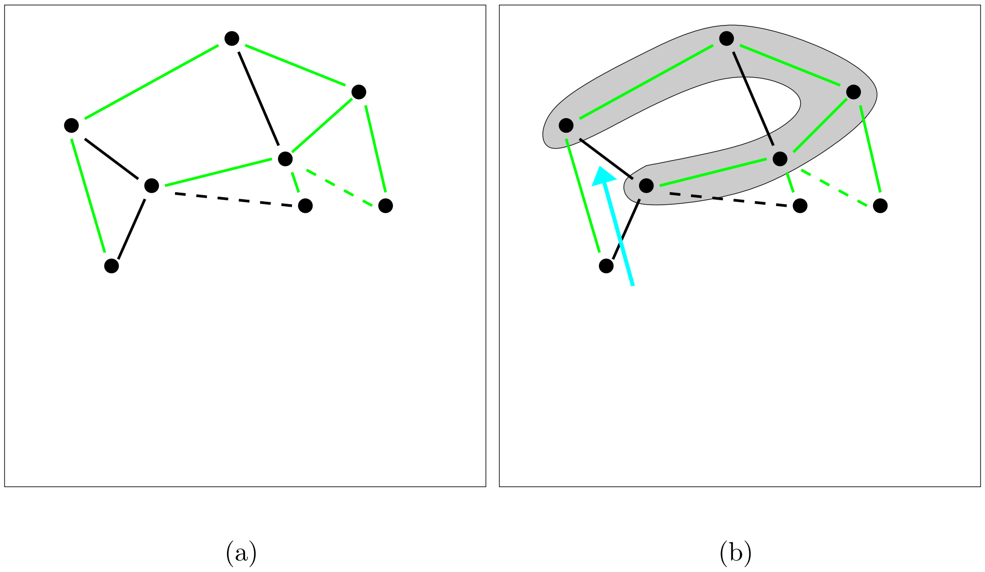

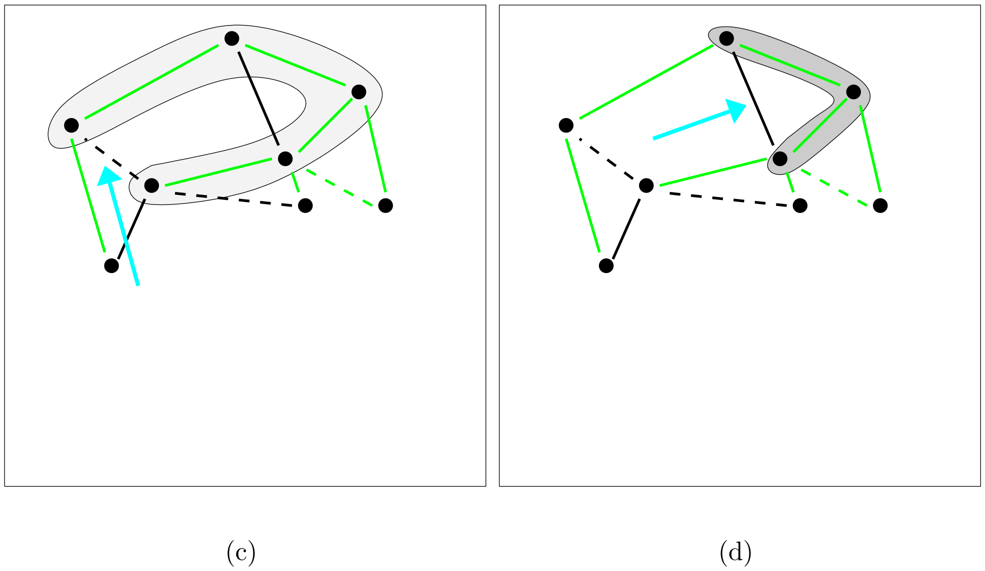

Figure 4.4: Walkthrough of the MIST algorithm (cont'd). The updated tree (a). Another edge is chosen (b). The tree cycle is completed and the non-tree edge eliminated (c). The next edge is chosen (d). (Continued)

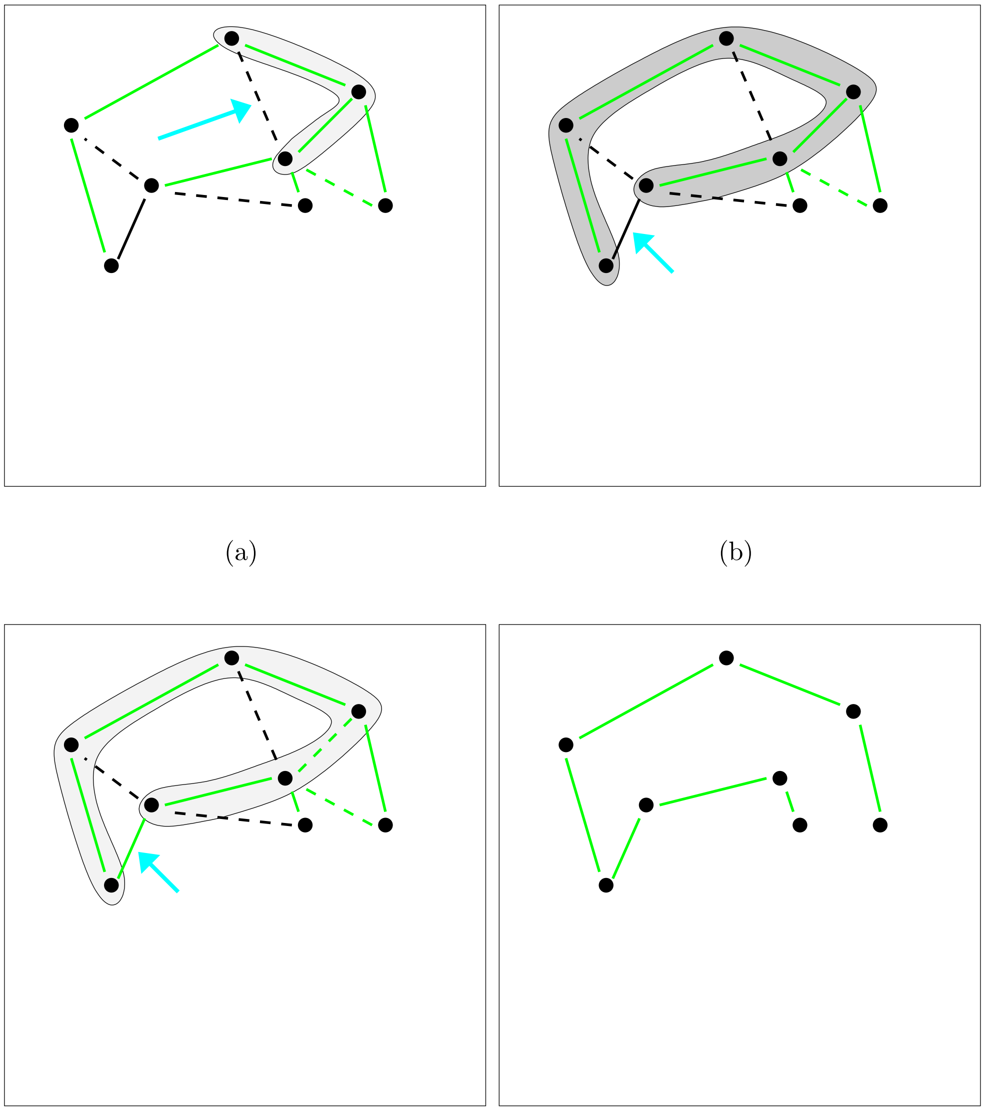
(a) (b) (c) (d)

Figure 4.5: Walkthrough of the MIST algorithm (cont'd). The edge is eliminated (a). The last remaining non-tree edge is chosen (b) and swapped in (c). The output tree (d).

As shown in (Reza, 1994), the mutual information for two jointly Gaussian numeric attributes X and Y is:

$$I(X;Y) = -\frac{1}{2}\ln(1-\rho^2)$$

where the correlation coefficient $\rho = \rho_{XY} =$

$$\frac{\sum_{i=1}^{R}\left((x_i - \bar{x})(y_i - \bar{y})\right)}{\hat{\sigma}_X^2 \hat{\sigma}_Y^2}$$

with $\bar{x}, \bar{y}, \hat{\sigma}_X^2$ and $\hat{\sigma}_Y^2$ being the sample means and variances for attributes X and Y. In practice, we standardize the data in a pre-processing step to have zero mean and unit variance. This leaves $x_i \cdot y_i$ as the only unknown.

Since the log function is monotonic, $I(X;Y)$ is also monotonic in $|\rho|$. This is a sufficient condition for the use of $|\rho|$ as the edge weight in a MST algorithm. Consequently, the sample correlation can be used in a straightforward manner when the complete data is available. Now consider the case where just a sample of the data has been observed.

Let x and y be two data attributes. We are trying to estimate $\sum_{i=1}^{R} x_i \cdot y_i$ given the partial sum $\sum_{i=1}^{r} x_i \cdot y_i$ for some $r < R$. To derive a confidence interval, we use the Central Limit Theorem.[2] It states that given samples of the random variable Z (where for our purposes $Z_i = x_i \cdot y_i$), the sum $\sum_i Z_i$ can be approximated by a Normal distribution with mean and variance closely related to the distribution mean and variance. Furthermore, for large samples, the sample mean and variance can be substituted for the unknown distribution parameters. Note in particular that the central limit theorem *does not require us to make any assumption about the Gaussianity of Z.* We thus can derive a two-sided confidence interval for $\sum_i Z_i = \sum_i x_i \cdot y_i$ with probability $1-\delta$ for some user-specified δ, typically 1%. Given this interval, computing an interval for ρ is straightforward.

[2]One can use the weaker Hoeffding bound instead, and my implementation supports it as well, although it is generally much less powerful.

In the case of binary categorical data, we follow Meila (1999b) and write:

$$\begin{aligned}
I(X;Y) &= H_X + H_Y - H_{XY} \\
&= \frac{1}{R}[-\text{zlogz}(N_X) - \text{zlogz}(N - N_X) \\
&- \text{zlogz}(N_Y) - \text{zlogz}(N - N_Y) \\
&+ \text{zlogz}(N_{XY}) + \text{zlogz}(N_X - N_{XY}) \\
&+ \text{zlogz}(N_Y - N_{XY}) \\
&+ \text{zlogz}(R - N_X - N_Y + N_{XY}) \\
&+ \text{zlogz}(R)] \qquad (4.1)
\end{aligned}$$

where zlogz(z) is shorthand for $z \log z$ and N_z denotes the number of times an attribute or a set of attributes are observed all true. As before, N_{XY} is the quantity we are deriving a probabilistic estimate for, which we do from the counts in a sample and application of the CLT.

Now, observe that:

$$\begin{aligned}
d(zlogz(y))/dx &= dy \log y/dx \\
&= dy/dx \log y + y \cdot \frac{1}{y} \cdot dy/dx \\
&= (1 + \log y)dy/dx \ .
\end{aligned}$$

We take a derivative of $I(X;Y)$ with respect to measured quantity N_{XY}. The only terms in 4.1 which do not zero out are the ones containing N_{XY}.

$$\begin{aligned}
d(I(X;Y))/dN_{xy} &= (1 + \log N_{xy}) - (1 + \log(N_x - N_{xy})) \\
&\quad -(1 + \log(N_y - N_{xy})) + (1 + \log(R - N_x - N_y + N_{xy})) \\
&= \log N_{xy} - \log(N_x - N_{xy}) - \log(N_y - N_{xy}) + \log(R - N_x - N_y + N_{xy}) = \\
&= \log \frac{N_{xy}(R - N_x + N_y + N_{xy})}{(N_x - N_{xy})(N_y - N_{xy})} \ . \qquad (4.2)
\end{aligned}$$

Let $N_{\bar{x}\bar{y}}$ be the number of records for which both attributes were false, and similarly for $N_{x\bar{y}}$ and $N_{\bar{x}y}$. Immediately we get:

$$\begin{aligned}
N_{x\bar{y}} &= N_x - N_{xy} \\
N_{\bar{x}y} &= N_y - N_{xy} \\
N_{\bar{x}\bar{y}} &= R - N_x + N_y + N_{xy} \ .
\end{aligned}$$

Then, equality with zero in Equation 4.2 above is obtained when:

$$N_{xy}N_{\bar{x}\bar{y}} = N_{x\bar{y}}N_{\bar{x}y}$$

or:

$$N_{xy} = \frac{N_{x\bar{y}}N_{\bar{x}y}}{N_{\bar{x}\bar{y}}} \tag{4.3}$$

Therefore, to determine minimum and maximum values for $I(X;Y)$ at the interval, we evaluate it at the endpoints. Additionally, we evaluate at the extreme point if it happens to be included in the interval.

4.4 The Full Algorithm

As we argued, the MIST algorithm is capable of using partial information about edge weights. We have also shown how to derive confidence intervals on edge weights. We now combine the two and give an efficient dependency-tree algorithm.

We largely follow the MIST algorithm as listed in Figure 4.1. We initialize the tree T in the following heuristic way: first we take a small sub-sample of the data, and derive point estimates for the edge weights from it. Then feed the point estimates to any MST algorithm and obtain a tree T.

When we come to compare edge weights, we generally need to deal with two intervals. If they do not intersect, then the points in one of them are all smaller in value than any point in the other, in which case we can determine which represents a heavier edge. We apply this logic to all comparisons, where the goal is to determine the heaviest path edge e' and to compare it to the candidate e. If we are lucky enough that all of these comparisons are conclusive, the amount of work we save is related to how much data was used in computing the confidence intervals — the rest of the data for the attribute-pair that is represented by the eliminated edge can be ignored.

However, there is no guarantee that the intervals are separated and allow us to draw meaningful conclusions. If they do not, then we have a situation similar to the inconclusive oracle answers in Section 4.2. The price we need to pay here is looking at more data to shrink the confidence intervals. We do this by choosing one edge — either a tree-path edge or the candidate edge — for “promotion”, and doubling the sample size used to compute the sufficient statistics for it. After doing so we try to eliminate again (since we can do this at no additional cost). If we fail to eliminate we iterate, possibly choosing a different candidate edge (and the corresponding tree path) this time.

The choice of which edge to promote is heuristic, and depends on the expected success of resolution once the interval has shrunk. This is estimated by first defining a cost measure for a set of tree edges and a candidate edge. It is the sum of the sizes of intersections of the tree edges with the candidate edge, plus the size of intersections between the worst tree edge (as defined by the mid-points of the intervals) and the other tree edges. We now go over the tree edges, in turn, and for each one estimate the size of its interval, if given more data. This estimate depends on the measured variance in the observed data. We record the cost for each of these speculative edges. The one associated with the lowest cost is chosen, unless the expected difference from the current cost is below a threshold. If this holds, we pick an edge at random from the set of edges that define the boundary of the union of the tree edges which intersects with the candidate edge. If this is impossible (for example, all of these edges are already saturated), we choose some tree-path edge at random.

Another heuristic we employ goes as follows. Consider the comparison of the path-heaviest edge to an estimate of a candidate edge. The interval for the candidate edge may be very small, and yet still intersect the interval that is the heavy edge's weight (this would happen if, for example, both attribute-pairs have the same distribution). We may be able to reduce the amount of work by pretending the interval is narrower than it really is. We therefore trim the interval by a constant, parameterized by the user as ϵ, before performing the comparison. This use of δ and ϵ is analogous to their use in "Probably Approximately Correct" analysis: on each decision, with high probability $(1 - \delta)$ we will make at worst a small mistake (ϵ).

4.4.1 Algorithm Complexity

We now discuss the theoretical complexity of the proposed algorithm. Refer to Figure 4.1. In theory, the first step can be done by choosing edges at random. In practice, it is built by sampling some number S of records from the input, and running a Chow-Liu algorithm on the sample. The complexity of obtaining the sample is $O(SM^2)$. If M is very large then this can dominate the run time. A possible countermeasure is to choose S proportional to M^{-2}. However this is not always possible: if M^2 is in the order of R or greater, this will result in a sample size smaller than one. Therefore the worst case time here is $O(M^2)$. Finding the actual minimum spanning tree on the sample can be done in time $O(M^2 + M \log M)$ by Prim's algorithm using Fibonacci heaps (Cormen et al., 1989).

Step 2 in Figure 4.1 requires $O(M^2)$ successful elimination steps. Each step requires, aside from the work required to read more data, finding a tree path between two nodes. In the worst case, this can take $O(M)$ work since the current tree contains $M-1$ edges. Therefore the cost for this step is $O(M^3)$. It is possible that the cost of finding and updating tree paths can be amortized (Tarjan, 1983). But more importantly, elimination of tree edges is a rare occurrence, so the tree structure is generally static. Therefore tree paths can be recorded and re-used instead of discovered. This is done in the current implementation.

Below, I present empirical results showing that the worst case is an overestimate for the data sets in question. In particular Figure 4.7 shows that for synthetic sets with $M < 160$, performance is still comfortably in the linear range.

4.5 Experimental Results

In the following description of experiments, we vary different parameters for the data and the algorithm. Unless otherwise specified, here are the default values for the parameters. We set δ to 1% and ϵ to 0.05 (on either side of the interval, totaling 0.1). The initial sample size is fifty records. There are $100,000$ records and 100 attributes. The data is real-valued. The data-generation process first generates a random tree, then draws points for each node from a normal distribution with the node's parent's value as the mean. In addition, any data value is set to random noise with probability 0.15.

To construct the correlation matrix from the full data, each of the R records needs to be considered for each of the $\binom{M}{2}$ attribute pairs. We evaluate the performance of our algorithm by adding the number of records that were actually scanned for all the attribute-pairs, and dividing the total by $R\binom{M}{2}$. We call this number the "data usage" of our algorithm. The closer it is to zero, the more efficient our sampling is, while a value of one means the same amount of work as for the full-data algorithm (possibly more, when considering the overhead).

We first demonstrate the speed of our algorithm as compared with the full $O(RM^2)$ scan. Figure 4.6 shows that the amount of data the algorithm examines is a constant that does not depend on the size of the data set. This translates to relative runtimes of 0.7% (for the $37,500$-record set) to 0.02% (for the $1,200,000$-record set) as compared with the full-data algorithm. The latter number translates to a $5,000$-fold speedup. Note that the reported usage is an average over the number of attributes. However this does not mean that the same amount of data was inspected for every attribute-pair — the algorithm determines how much effort to invest in each edge

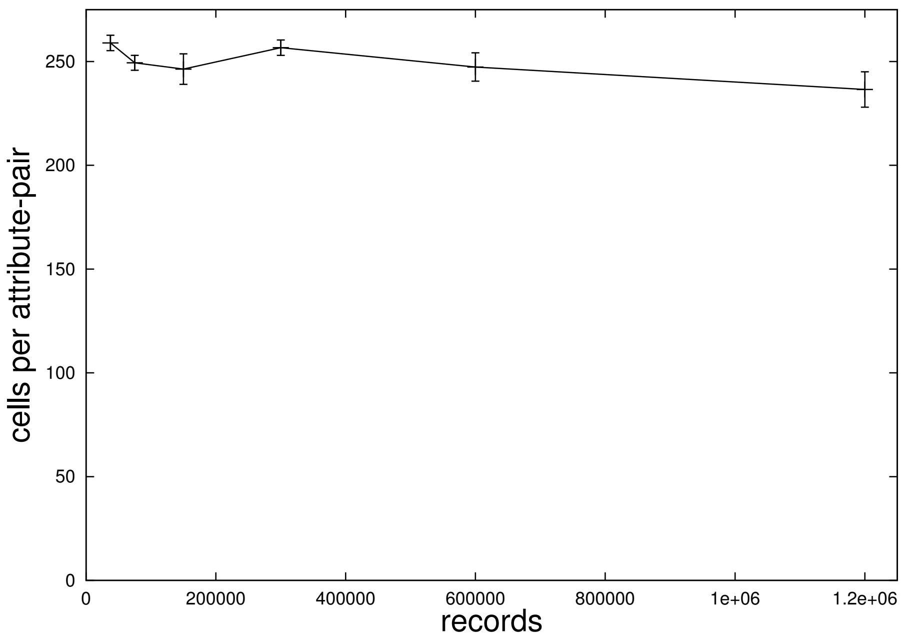

Figure 4.6: Amount of data read (indicative of absolute running time), in attribute-pair units per attribute.

separately. We return to this point below.

The running time is plotted against the number of data attributes in Figure 4.7. A linear relation is clearly seen, meaning that (at least for this particular data generation scheme) the algorithm is successful in doing work that is proportional to the number of tree edges.

Clearly speed has to be traded off. For our algorithm the risk is making the wrong decision about which edges to include in the resulting tree. For many applications this is an acceptable risk. However, there might be a simpler way to grow estimate-based dependency trees, one that does not involve complex red-edge rules. In particular, we can just run the original algorithm on a small sample of the data, and use the generated tree. It would certainly be fast, and the only question is how well it performs.

To examine this effect I have generated data as above, then ran a 30-fold cross-validation test for the trees my algorithm generated. I also ran a sample-based algorithm on each of the folds. This variant behaves just like the full-data algorithm, but instead examines just the fraction of it that adds up to the total amount of data used by our algorithm. Results for multiple data sets are in Figure 4.8. We see that my algorithm outperforms the sample-based algorithm, even though they are both using

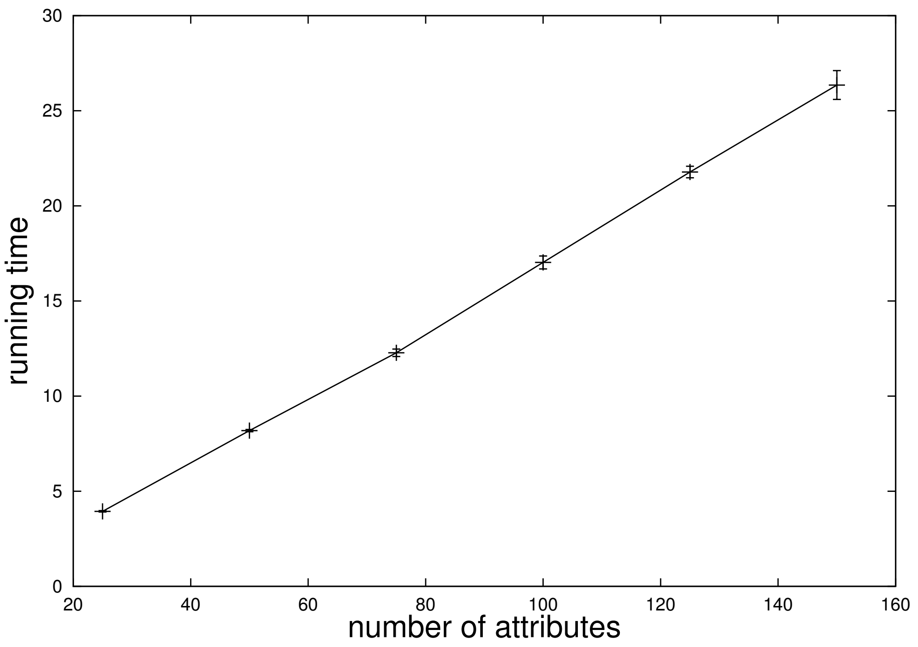

Figure 4.7: Running time as a function of the number of attributes.

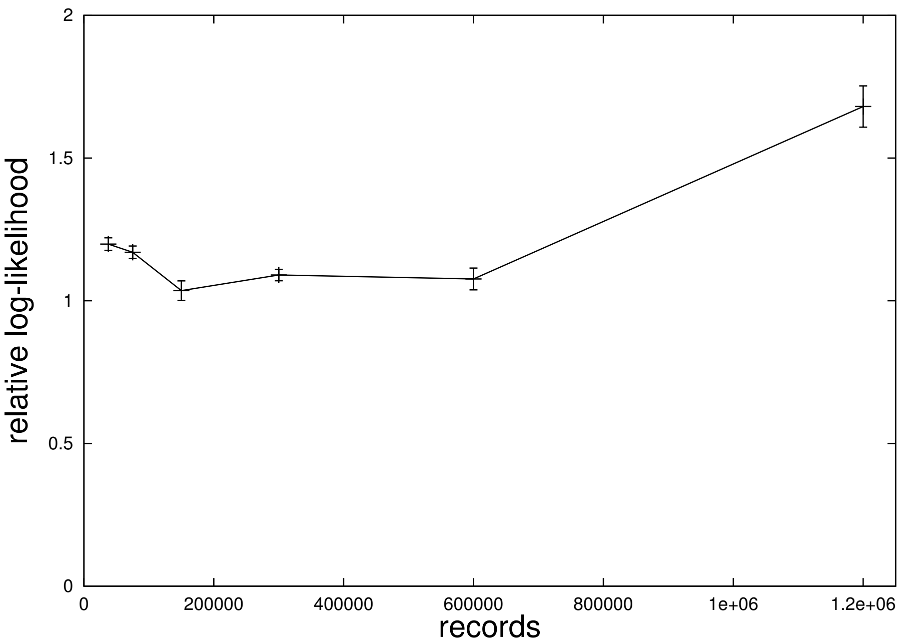

Figure 4.8: Relative log-likelihood vs. the sample-based algorithm. The log-likelihood difference is divided by the number of records.

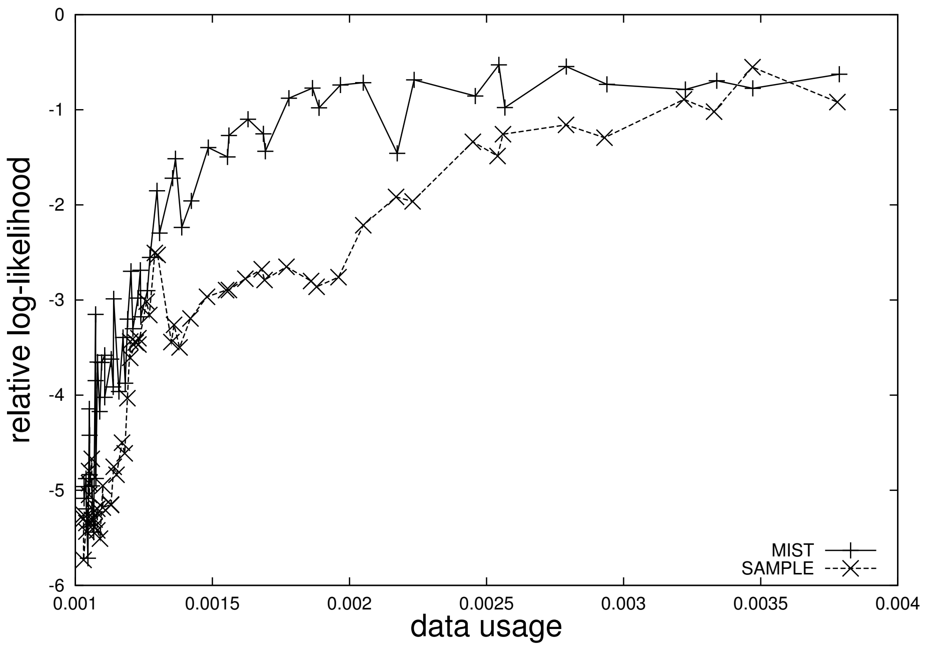

Figure 4.9: Relative log-likelihood vs. the sample-based algorithm, drawn against the fraction of data scanned.

the same total amount of data. The reason is that using the same amount of data for all edges assumes all attribute-pairs have the same variance. This is in contrast to my algorithm, which determines the amount of data for each edge independently. Apparently for some edges this decision is very easy, requiring just a small sample. These "savings" can be used to look at more data for high-variance edges. The sample-based algorithm would not put more effort into those high-variance edges, eventually making the wrong decision. In Figure 4.9 I show the log-likelihood difference for a particular (randomly generated) set. Here, multiple runs with different δ and ϵ values were performed, and the result is plotted against the fraction of data used. The baseline (0) is the log-likelihood of the tree grown by the original algorithm using the full data. Again we see that MIST is better over a wide range of data utilization ratios.

Keep in mind that the sample-based algorithm has been given an unfair advantage, compared with MIST: it knows how much data it needs to look at. This parameter is implicitly passed to it from my algorithm, and represents an important piece of information about the data. Without it, there would need to be a preliminary stage to determine the sample size. The alternative is to use a fixed amount (specified either as a fraction or as an absolute count), which is likely to be too much or too little. Another option is to iterate over increasing data sizes (for example, double the sample size in each iteration). The problem with this approach is that it still leaves

Output: A data-record as a vector $\{X(0) \ldots X(n-1)\}$ of attributes.

- $X(0)$ is a value drawn from $N(0,1)$.
- $X(10i)$ is a value drawn from $N(X(10(i-1)),1)$.
- $X(10k+j)$ for $j \neq 0$ is drawn from $N(X(10k+j-1), j)$.

Figure 4.10: The data-generation algorithm

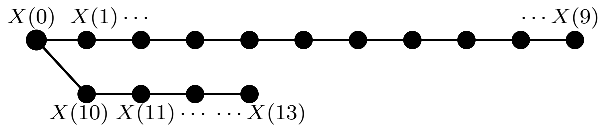

Figure 4.11: Structure of the generated data for 14 attributes.

open the question of how to determine if the size is big enough.

4.5.1 Sensitivity Analysis

We now examine the effect the user-supplied parameters ϵ and δ have on performance. Unless otherwise specified, these are the default values for the parameters. We set δ to 1% and ϵ to 0. The initial sample size is 5000 records. There are 100,000 records and 100 attributes. The data is numeric. The data-generation process for the synthetic sets is as in Figure 4.10. The correct dependency-tree for this process is shown in Figure 4.11. In the categorical case, the network is identical, but parent-child relationships are as follows. The root is true with probability 0.5. For the other nodes, the probability of them being true given that their parent is true is $0.5 + c$ for some constant c, and the probability of them being true given that their parent is false is $0.5 - c$. By setting the "coupling" parameter c to 0 we get a completely random data, while a value of 0.5 generates a highly-structured, noiseless data set.

Our next experiment examines the sensitivity of our algorithm to noisy data. Data was generated in the usual way, except that some fraction of the records had completely random values in all attributes. As shown in Figure 4.12, when ϵ is 0, data-usage is kept below 15% of maximum, similar to the performance with noiseless data, as long as the noise level is below 30%. With ϵ set to 0.01, this is true for all

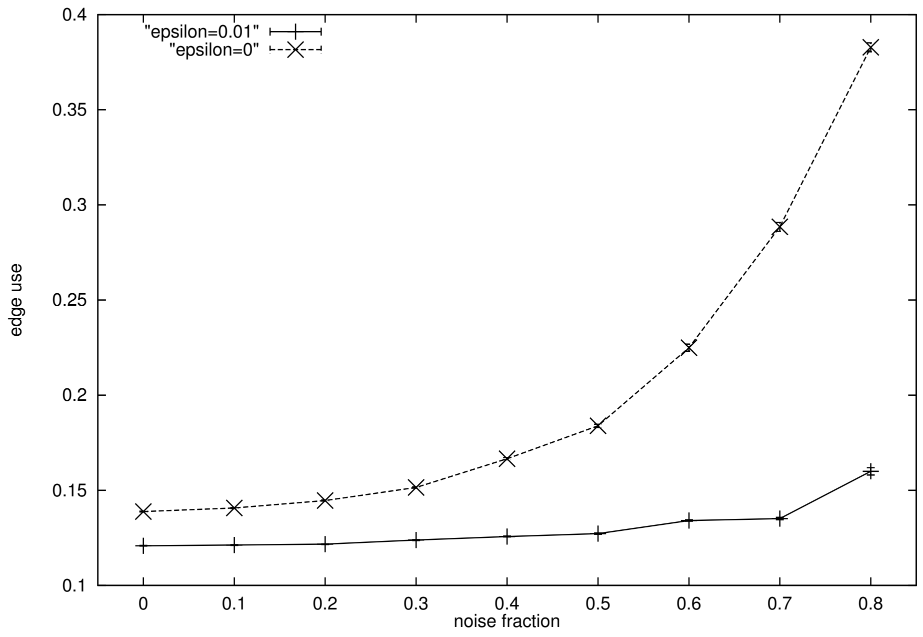

Figure 4.12: Edge usage as a function of noise.

noise levels up to 80%.

Recall that the δ parameter controls how loose the confidence intervals are. The bigger it is, the higher the chance that a wrong decision about a tree-edge inclusion or exclusion will be made. Figure 4.13 shows the effect of δ on the running time. When ϵ is 0, it appears that higher values of δ do not improve the running time significantly, while increasing the chance of deviation from the output of the full algorithm. However, when ϵ was set to 0.05, an improvement in running-time can be traded for some decrease in the quality of the output (Figure 4.14). For this case none of the 30 runs in any of the 10 values for δ resulted in the same identical tree as with the full algorithm.

We continue to examine the effect the ϵ parameter has on performance. Recall that it controls a heuristic that may decrease the edge usage, but may also lead to the wrong edges being included in the tree. See Figure 4.15 for the effect on running time (or, equivalently, on the the number of data-cells scanned). We see that changes in ϵ can dramatically improve performance, down from 70% to about 10% on this data-set, with a sharp drop in the 0.002 — 0.004 range. The interesting question is, how badly is the output quality affected by this heuristic. To answer this I have plotted the data from the same experiments, but now with the X (not Y) axis being the relative log-likelihood of the output (Figure 4.16). The worst log-likelihood ratio

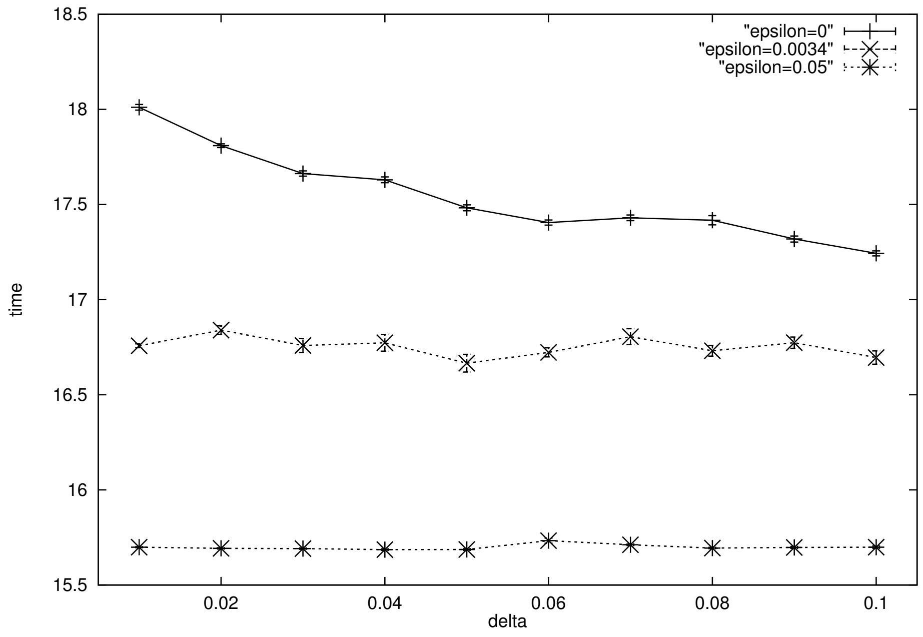

Figure 4.13: Running time, in seconds, as a function of δ and ϵ.

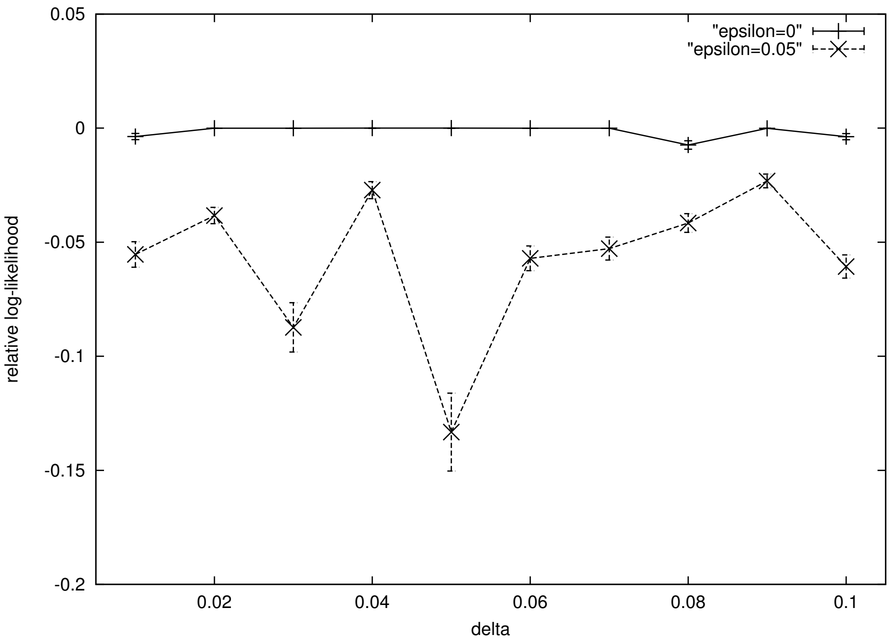

Figure 4.14: Difference in log-likelihood (divided by the number of records) of the generated trees, as a function of δ and ϵ. Baseline log-likelihoods were in the order of 3.5×10^6.

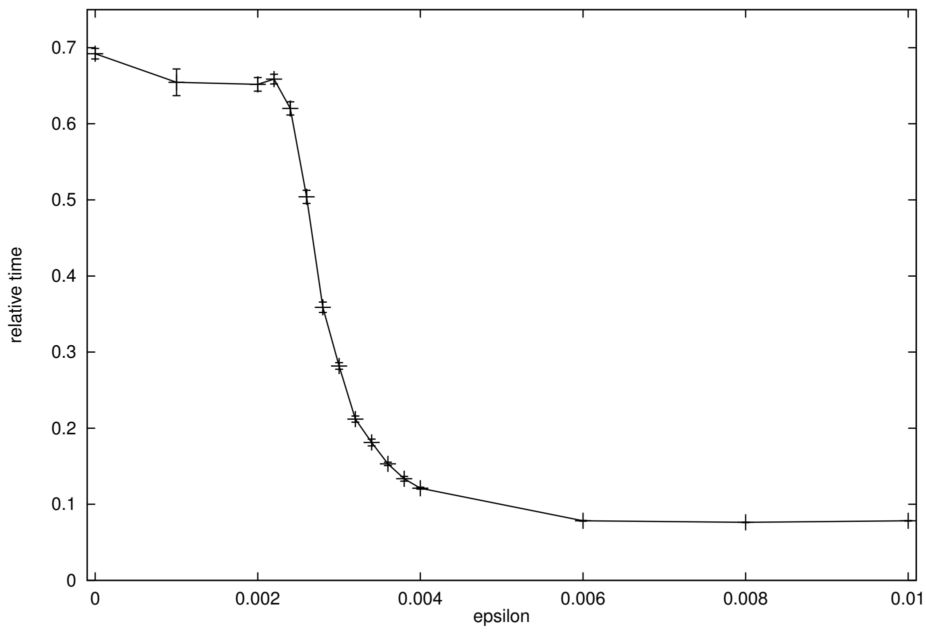

Figure 4.15: Edge-usage as a function of ϵ. The data is categorical, with the "coupling" parameter c set to 0.04.

is about 0.05, and it seems that with careful selection of ϵ it is possible to enjoy most of the time savings while sacrificing very little accuracy. For this particular data set this "sweet-spot" approximately corresponds to $\epsilon = 0.0028$.

4.5.2 Real Data

To test my algorithm on real-life data, I used data sets from various public repositories (Blake & Merz, 1998; Hettich & Bay, 1999), as well as analyzed data derived from astronomical observations taken in the Sloan Digital Sky Survey. On each data set I ran a 30-fold cross-validation test as described above. For each training fold, I ran our algorithm, followed by a sample-based algorithm that uses as much data as my algorithm did. Then the log-likelihoods of both trees were computed for the test fold. Table 4.1 shows whether the 99% confidence interval for the log-likelihood difference indicates that either of the algorithms outperforms the other. In seven cases the MIST-based algorithm was better, while the sample-based version won in four, and there was one tie. Remember that the sample-based algorithm takes advantage of the "data usage" quantity computed by our algorithm. Without it, it would be weaker or slower, depending on how conservative the sample size was.

I then turned this data into a *second-order* data set to provide an example of data

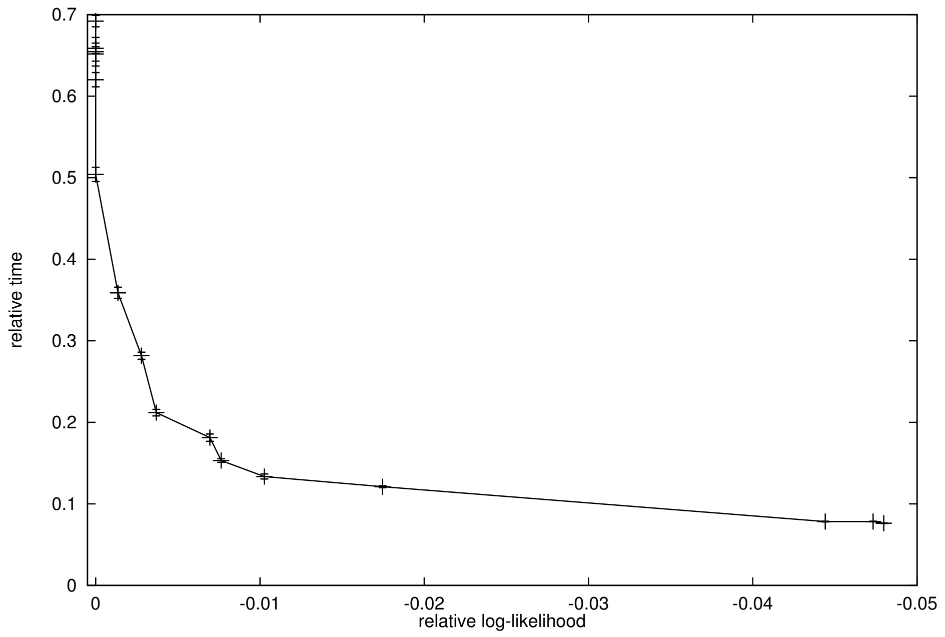

Figure 4.16: Relative log-likelihood vs. relative time, as a function of ϵ. This is data from the same experiments as plotted in Figure 4.15.

with many attributes and many records. I first discretized all of the attributes. Then I added all pairwise conjunctions of these attributes. There were 23 original attributes $X_1 \dots X_{23}$ to which were added $\binom{23}{2}$ additional attributes $A_{i,j}$ where $A_{i,j} = X_i \wedge X_j$.

After doing that for all attributes and removing attributes which take on constant values I was left with 148 attributes and the original 2.4 million records. The naive algorithm constructs a tree for this set in 6.6 hours, while the fast algorithm (with default settings) takes about 21 minutes, meaning a speedup of 19. The tree generated by the fast algorithm weights 99.89% of the naive tree, and the difference in log-likelihoods is 1.26×10^5, or about 0.05 per record.

4.6 Red vs. Blue Rule

My algorithm is based on the "red edge" rule. As mentioned above, it is also possible to base MST algorithms on the "blue edge" rule. A natural question to ask is: will the blue edge rule be beneficial in a framework that utilizes probabilistic intervals on edge weights?

Before attempting to answer, I review the difference between the rules. The red

Table 4.1: Results, relative to the sample-based algorithm, on real data. "Type" means numerical or categorical data.

NAME	ATTR.	RECORDS	TYPE	DATA USAGE	MIST BETTER?	SAMPLE BETTER?
CENSUS-HOUSE	129	22784	N	1.0%	×	√
COLORHISTOGRAM	32	68040	N	0.5%	√	×
COOCTEXTURE	16	68040	N	4.6%	×	√
ABALONE	8	4177	N	21.0%	×	×
COLORMOMENTS	10	68040	N	0.6%	×	√
CENSUS-INCOME	678	99762	C	0.05%	√	×
COIL2000	624	5822	C	0.9%	√	×
IPUMS	439	88443	C	0.06%	√	×
KDDCUP99	214	303039	C	0.02%	√	×
LETTER	16	20000	N	1.5%	√	×
COVTYPE	151	581012	C	0.009%	×	√
PHOTOZ	23	2381112	N	0.008%	√	×

rule operates on a *cycle* in the graph; the heaviest edge on the cycle can be eliminated.[3] See Figure 4.17. In contrast, the blue rule operates on a *cut* in the graph. A cut is defined by a subset of the nodes, and consists of the edges that have exactly one endpoint in the set. The lightest edge in a cut can be proven to be in the MST.[4] Therefore it is an inclusion rule. See Figure 4.18. The blue rule is used exclusively in the popular Prim and Kruskal algorithms. There are also algorithms that combine both rules.

Returning to the question of using the blue rule in a Chow-Liu framework, I believe it will not be beneficial, for the following reason. The number of edges in a cut can be much larger than in a cycle: up to $O(M^2)$. To calculate the expected number of edges in a random cut, denote the number of nodes on one side of the cut by i. We assume the probability of a cut is uniform over i. All cuts of this size have the same

[3]The cycle must not contain any red edges.

[4]The cut can not contain any blue edges.

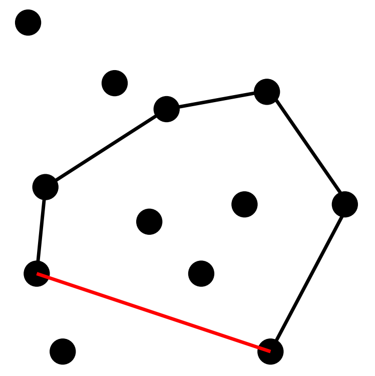
Figure 4.17: The Red Edge rule.

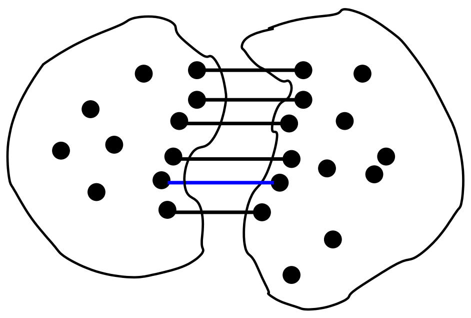
Figure 4.18: The Blue Edge rule.

number of edges $i \cdot (M-i)$, therefore the expected value is:

$$\begin{aligned}
\frac{1}{M-1}\sum_{i=1}^{M-1} i\cdot(M-i) &= \frac{1}{M-1}\left[M\sum_{i=1}^{M-1} i - \sum_{i=1}^{M-1} i^2\right] \\
&= \frac{1}{M-1}\left[M\frac{M(M-1)}{2} - \frac{M(M-1)(2M-2+1)}{6}\right] \\
&= \left[\frac{M^2}{2} - \frac{M(2M-1)}{6}\right] \\
&= \frac{M^2+M}{6}
\end{aligned}$$

That is, $O(M^2)$. Consider that for a cycle, the *maximal* number of edges $M-1$. Therefore cuts require knowledge of more edge weights, which in our case usually translates to reading of more data. This is exactly what we are trying to avoid.

4.7 Error Analysis

The use of probabilistic bounds means that there is a risk of making a wrong decision. We now quantify this risk. For the purpose of the analysis, we treat the tree built by the Chow-Liu algorithm, when given exact edge weights, as optimal. We consider every deviation from this tree as an error.[5] For simplicity we assume that the edge weights are all unique and so is the optimal weight. We call the edges that form the optimal tree "optimal edges". We also ignore the δ optimization (i.e., assume it is set to zero). The event that we are interested in is that the tree output by the modified MIST algorithm is identical to the optimal tree.

Consider a MIST run which ends in the optimal tree. It starts with an arbitrary tree, and eliminates and swaps edges as in Section 4.4. We make two observations. One, it is sufficient to consider just steps in which an edge is eliminated. This is true because there is no risk of making a mistake by deferring the decision due to insufficient data. Two, in all the elimination steps, edges that are not in the optimal tree are eliminated.

Follow the sequence of execution; each elimination step corresponds to one of the following scenarios:

1. Eliminate a non-optimal and non-tree edge because it is heavier than a tree edge.
2. Swap an optimal and a non-optimal edge because the optimal edge is lighter. The non-optimal edge swapped out from the current tree is then eliminated.

In both cases, a non-optimal edge is eliminated because a weight comparison determines it is heavier than an optimal edge. We calculate the probability of arriving at the opposite decision erroneously. Let A be the true weight of the optimal edge (meaning the value used by the original Chow-Liu algorithm), and let a be the corresponding confidence interval. Similarly, let B be the true value for the non-optimal edge and b its interval. See Figure 4.19.

In our case $B > A$. A mistake happens by having a and b such that the edge associated with a is eliminated. Since the algorithm defers all decisions based on overlapping intervals, the only configuration allowing this is where $\min(a) > \max(b)$ (see Figure 4.19(d)). Given that $B > A$, this cannot hold if both a and b contain their

[5]A less strict error analysis would consider the expected weight difference between the generated and optimal trees. Conceivably one could make some assumptions on edge weight distribution to perform this kind of analysis.

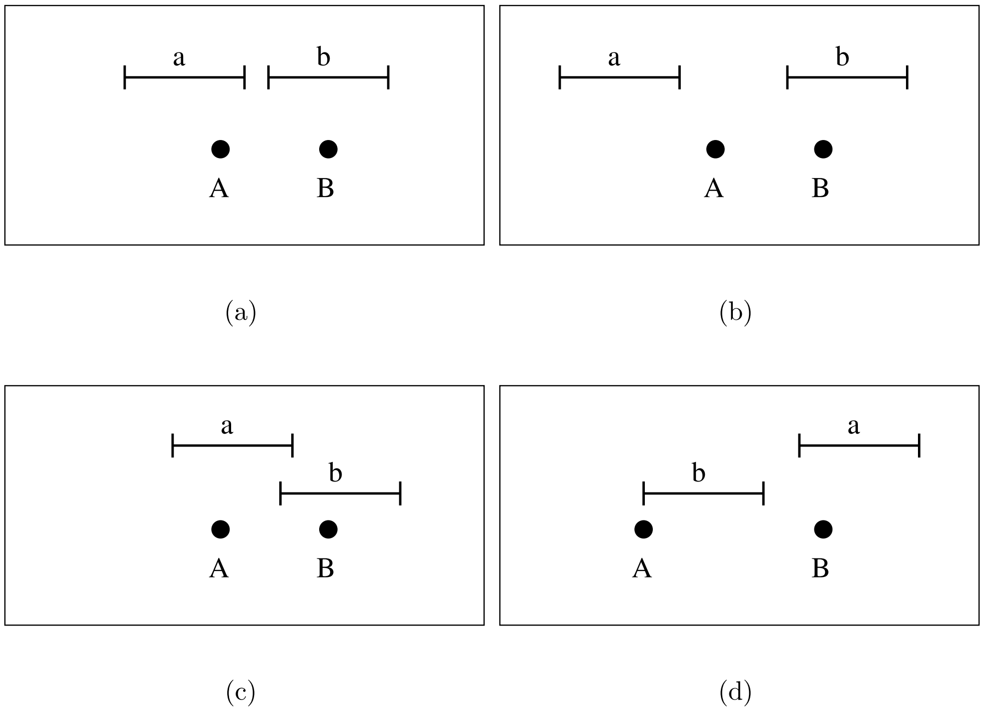

Figure 4.19: Several possibilities for two estimated intervals a and b and their respective exact values A and B.

respective true values. The probability of each interval not containing the true value is at most ϵ, and the probability of not making either mistake is at most $(1-\epsilon)^2$. Therefore the probability of making the wrong decision is at most $1-(1-\epsilon)^2 = \epsilon(2-\epsilon)$. Note that this bound is loose, since not every failure to include the exact value in the intervals results in full inversion of the intervals.

As explained above, this kind of decision is made exactly once per eliminated edge. Their number is just the total number of edges which are not tree edges, or $\binom{M}{2} - (M-1) = (M-1)^2$. We now have a bound on the probability of failure in a single test, and we know the number of tests. We can hence derive a lower bound on the probability of making no mistakes: $[\epsilon(2-\epsilon)^2]^{(M-1)^2} = [\epsilon(2-\epsilon)]^{2\cdot(M-1)^2}$. $\square$

4.8 Conclusion

I have presented an algorithm that applies a "probably approximately correct" approach to dependency-tree construction for numeric and categorical data. Experiments in sets with up to millions of records and hundreds of attributes show it is capable of processing massive data sets in time that is constant in the number of records, with just a minor loss in output quality.

Future work includes embedding my algorithm in a framework for fast Bayes Net structure search.

A additional issue I would like to tackle is disk access. One advantage the full-data algorithm has is that it is easily executed with a single sequential scan of the data file. I will explore the ways in which this behavior can be attained or approximated by my algorithm.

While I derived formulas for both numeric and categorical data, I currently do not allow both types of attributes to be present in a single network.

Chapter 5

Active Learning for Anomaly Detection

Consider an astronomer who needs to sift through a large set of sky survey images, each of which comes with many real-valued parameters. Most of the objects (say 99.9%) are well explained by current theories and models. For the remainder of this chapter we consider them not interesting, since our goal is to find the extraordinary objects which are worthy of further research. For example, the astronomer might want to cross-check such objects in various databases and allocate telescope time to observe them in greater detail.

The remaining data are anomalies, but 99% of these anomalies are uninteresting. These are records which are strange for mundane reasons such as sensor faults or problems in the image processing software. Only 1% of the remainder (0.001% of the full data set) are useful. The goal of my work in this chapter is finding this set of rare and useful anomalies.

5.1 Introduction

The following example concerns astrophysics, but the same scenario can arise wherever there is a very large amount of scientific, medical, business or intelligence data. In this example, a domain expert wants to find truly exotic rare events while not becoming swamped with uninteresting anomalies.

The "rare events" are distinguished from the traditional statistical definition of anomalies as outliers or merely ill-modeled points. My distinction is that the useful-

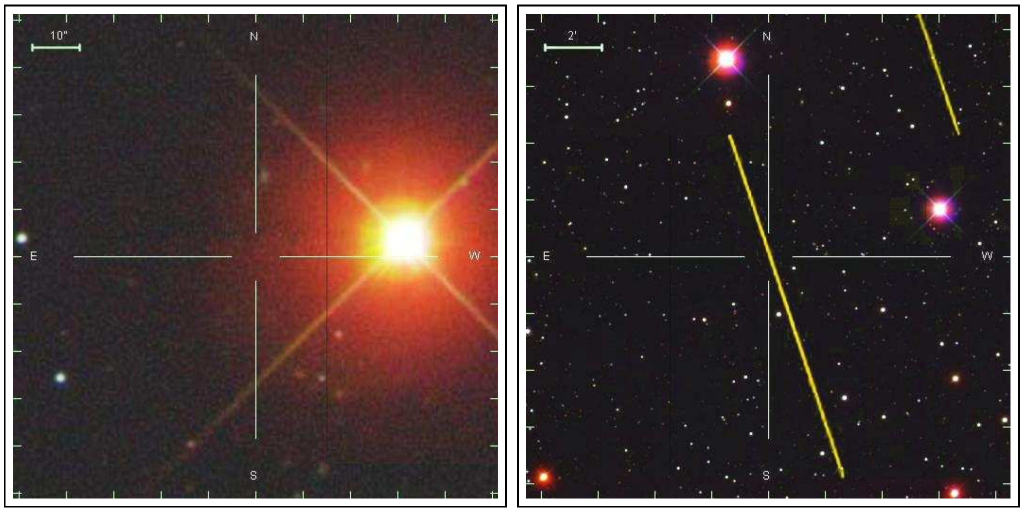

(a) Diffraction spikes. (b) Satellite trails.

Figure 5.1: Anomalies (Sloan data).

ness of anomalies is categorized by the user's subjective classification.

Two rare categories of anomalies in my test astrophysics data are shown in Figure 5.1. The first, a well-known optical artifact, is the phenomenon of diffraction spikes (see Figure 5.1(a)). The second (Figure 5.1(b)) consists of satellites that happened to be flying overhead as the photo was taken. For both of them, we have statistical justification to flag them as anomalies, but they have very little scientific value. Therefore we would like our tool to generally ignore them.

Admittedly, it is possible to build special-purpose filters to eliminate known classes of objects (and in the cases above, such filters have been built by astrophysicists). But if the data is rich enough, new classes of anomalies (both useful and useless) will emerge. At that point new classifiers would need to be built, only to lead to an "arms race" where the statistical model of the data is being continuously refined. Moreover, this does not address the need to build a filter that corresponds to a specific user's subjective judgment of the anomalies. What we would ultimately like is for the user to see the boring anomalies once, and be able to say "do not show me any more items like these". Figure 5.14 shows examples of anomalies found with this kind of process using real data.

More precisely, I make two assumptions. First, there are extremely few useful anomalies to be hunted down within a massive data set. Second, both useful and useless anomalies may sometimes exist within tiny classes of similar anomalies. The

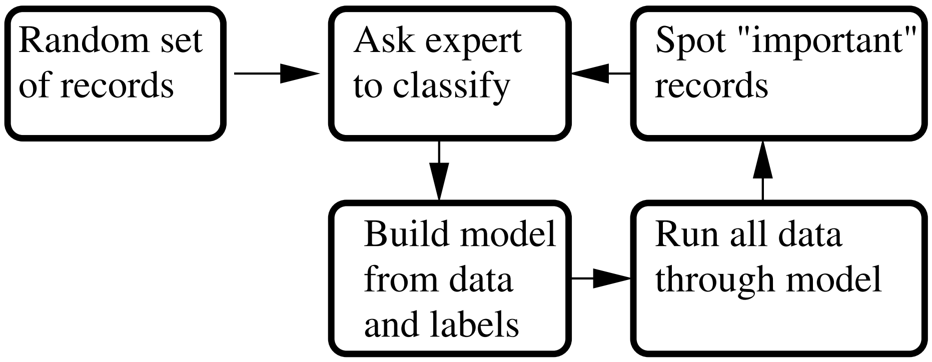

Figure 5.2: The active learning loop.

challenge, therefore, is to identify “rare category” records in an unlabeled noisy set with help, in the form of class labels, from a human expert who has a small budget of data points that they are prepared to categorize.

The computational and statistical question is then how to use feedback from the human user to iteratively reorder the queue of anomalies to be shown to the user in order to increase the chance that the user will soon see an anomaly of a whole new category.

I do this in the familiar pool-based active learning framework.[1] In our setting, learning proceeds in rounds. Each round starts with the teacher labeling a small number of examples. Then the learner models the data, taking into account the labeled examples as well as the remainder of the data, which we assume to be much larger in volume. The learner then identifies a small number of input records (“hints”) which are important in the sense that obtaining labels for them would help it improve the model. These are shown to the teacher (in our scenario, a human expert) for labeling, and the cycle repeats. The model is shown in Figure 5.2.

It may seem too demanding to ask the human expert to give class labels instead of a simple “interesting” or “boring” flag. But in practice, this is not an issue. In fact it seems easier to place objects into such “mental bins”. For example, in the

[1]More precisely, we allow multiple queries and labels in each learning round — the traditional presentation has just one.

astronomical data we have seen a user place most objects into previously-known categories: point sources, low-surface-brightness galaxies, etc. This also holds for the negative examples: it is frustrating to have to label all anomalies as "bad" without being able to explain why. In fact, the data is better understood as time goes by, and people like to revise some of their old labels in light of new examples. Remember that the statistical model does not care about the names of the labels. For all it cares, the label set can change completely from one round to another. My tools allow exactly that: the labels are unconstrained and the user can add, refine, and delete classes at will. Certainly it is possible to accommodate the simplistic "interesting or not" model in this richer framework.

My work differs from traditional applications of active learning in that I assume the distribution of class sizes to be extremely skewed. Typically, the smallest class may have just a few members whereas the largest may contain a few million. Generally in active learning, it is believed that, right from the start, examples from each class need to be presented to the oracle (Basu et al., 2004; Seeger, 2000; Brinker, 2003). If the class frequencies were balanced, this could be achieved by random sampling. But in data sets with the rare categories property, this no longer holds, and much of my effort is an attempt to remedy the situation.[2]

Previous active-learning work tends to tie intimately to a particular model (Cohn et al., 1995; Brinker, 2003). In contrast, I would like to be able to "plug in" different types of models or components and therefore propose model-independent criteria. The same reasoning also precludes us from directly using distances between data points, as is done in Wiratunga et al. (2003). The only assumption I make is that my model is a mixture, and each component is a probability density estimator.

Another desired property is resilience to noise. Noise can be inherent in the data (e.g., from measurement errors) or be an artifact of a ill-fitting model. In any case, we need to be able to identify query points in the presence of noise. This is a not just a bonus feature: points which the model considers noisy could very well be the key to improvement if presented to the oracle. This is in contrast to the approach taken by Cohn et al. (1994) and Plutowski and White (1993): a pre-assumption that the data is noiseless.

[2]However, it is interesting to note that in some cases, it is useful to add a random sampling expert to an ensemble (Baram et al., 2003).

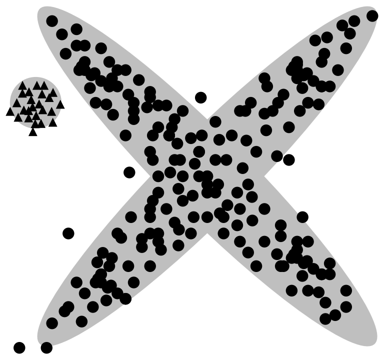

Figure 5.3: Underlying data distribution for the example.

5.2 Overview of Hint Selection Methods

In this section we survey several proposed methods for active learning as they apply to our setting. We give anecdotal evidence of their weaknesses. While the general tone is negative, what follows should not be construed as general dismissal of these methods. Rather, it is meant to highlight specific problems with them when applied to a particular setting.

The data shown (Figure 5.3) is a mixture of two classes. One is an X-shaped distribution, from which 2000 points are drawn. The other is a circle with 100 points. In this example, the classifier is a Gaussian Bayes classifier trained in a semi-supervised manner from labeled and unlabeled data, with one Gaussian per class. The model is learned with a standard EM procedure, with the following straightforward modification (Shahshashani & Landgrebe, 1994; Miller & Uyar, 1997) to enable semi-supervised learning. Before each M step we clamp the class membership values for the hinted records to match the hints (i.e., one for the labeled class for this record, and zero elsewhere).

Given fully labeled data, our learner would perfectly predict class membership for this data[3]: one Gaussian centered on the circle, and another spherical Gaussian with high variance centered on the X. Now, suppose we plan to perform active learning in which we take the following steps:

1. Start with entirely unlabeled data.

2. Perform semi-supervised learning (which, on the first iteration degenerates to

[3]It would, however, be a poor generative model.

unsupervised learning).

3. Ask an expert to classify the 35 strangest records.

4. Go to Step 2.

On the first iteration (when unsupervised) the algorithm will naturally use the two Gaussians to model the data as in Figure 5.4(b), with one Gaussian for each of the arms of the "X", and the points in the circle represented as members of one of them. What happens next all depends on the choice of the data points to show to the human expert.

We now survey the previously published methods for hint selection.

5.2.1 Choosing Points with Low Likelihood

A rather intuitive approach is to select as hints the points which the model performs worst on. This can be viewed as model variance minimization (as in Cohn et al. (1995)) or as selection of points furthest away from any labeled points (Wiratunga et al., 2003). We do this by ranking each point in order of increasing model likelihood, and choosing the top items.

I show what this approach would flag in the given configuration in Figure 5.4. It is derived from a screenshot of a running version of my code, and is hand-drawn for clarity. Each subsequent drawing shows a model which EM converged to in one round, and the hints it chooses under a particular scheme (here it is what we call lowlik). These hints affect the model shown for the next round. The underlying distribution is shown in gray shading. We use this convention for the other methods below.

In the first round, the Mahalanobis distance for the points in the corners is greater than those in the circle, therefore they are flagged. Another effect we see is that one of the arms is over-represented. This is probably due to its lower variance. In any event, none of the points in the circle is flagged. The outcome is that the next round ends up in a similar local minimum. We can also see that another step will not result in the desired model. Only after obtaining labels for all of the "outlier" points (that is, those on the extremes of the distribution) will this approach go far enough down the list to hit a point in the circle. This means that in scenarios where there are more than a few hundred noisy data, classification accuracy is likely to be very low.

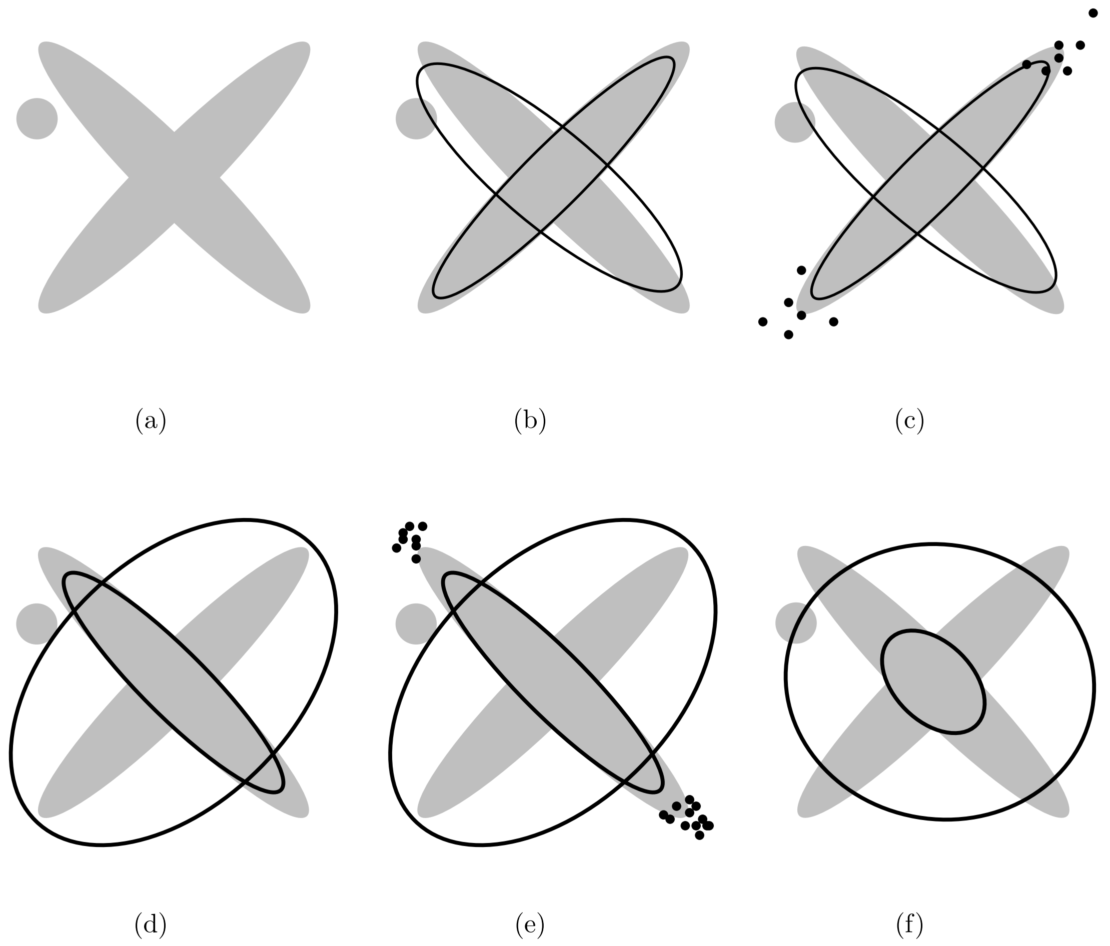

Figure 5.4: Behavior of the lowlik method. The original data distribution is in (a). The unsupervised model fit to it in (b). The anomalous points according to lowlik, given the model in (b), are shown in (c). Given labels for the points in (c), the model in (d) is fitted. Given the new model, anomalous points according to lowlik are flagged (e). Given labels for the points in (c) and (e), this is the new fitted model (f).

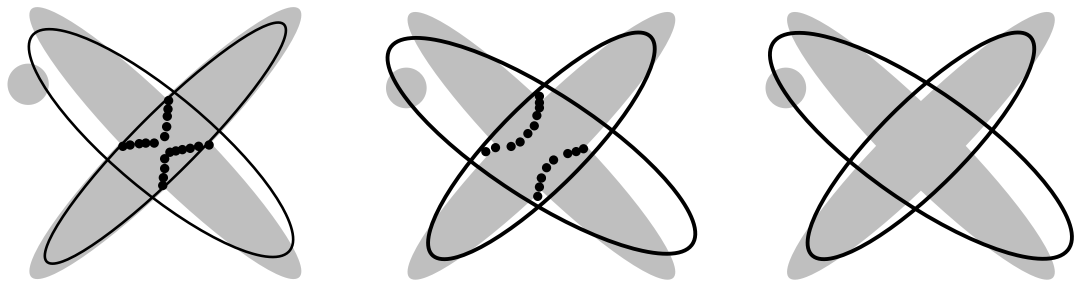
(a) (b) (c)

Figure 5.5: Behavior of the ambig method. The unsupervised model and the points which ambig flags as anomalous, given this model (a). The model learned using labels for these points is (b), along with the points *it* flags. The last refinement, given both sets of labels (c).

5.2.2 Choosing Ambiguous Points

Another popular approach is to choose the points which the learner is least certain about. This is the spirit of "query by committee" (Seung et al., 1992) and "uncertainty sampling" (Lewis & Catlett, 1994). In our setting this is implemented in the following way. For each data point, the EM algorithm maintains an estimate of the probability of its membership in every mixture component. For each point, we compute the entropy of the set of all such probabilities, and rank the points in decreasing order of the entropy. This way, the top of the list will have the objects which are "owned" by multiple components.

For our example, this would choose the points shown in Figure 5.5. As expected, points on the decision boundaries between classes are chosen. Here, the ambiguity sets are useless for the purpose of modeling the entire distribution. One might argue this only holds for this contrived distribution. However, in general this is a fairly common occurrence, in the sense that the ambiguity criterion works to nudge the decision surfaces so they better fit a relatively small set of labeled examples. It may help modeling the points very close to the boundaries, but it does not improve generalization accuracy in the general case. Indeed, we see that if we repeatedly apply this criterion we end up asking for labels for a great number of points in close proximity, to very little effect on the overall model.

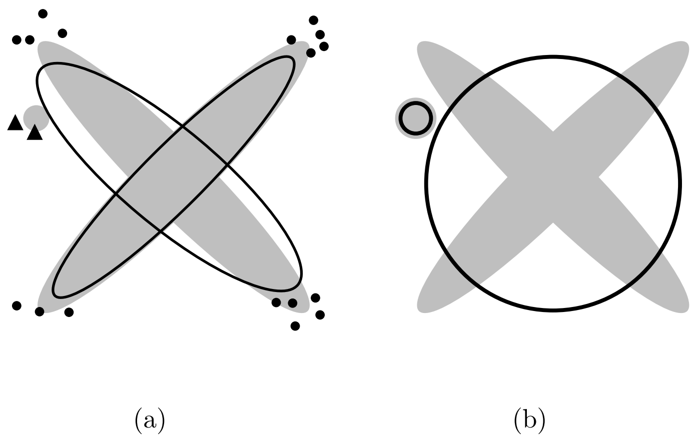
Figure 5.6: Behavior of the interleave method.

5.2.3 Combining Unlikely and Ambiguous Points

Our next candidate is a hybrid method which tries to combine the hints from the two previous methods. Recall they both produce a ranked list of all the points. We merge the lists into another ranked list in the following way: alternate between the lists when picking items. For each list, pick the top item that has not already been placed in the output list. When all elements are taken, the output list is a ranked list as required. We now pick the top items from this list for hints.

As expected we get a good mix of points in both hint sets (not shown). But, since neither method identifies the small cluster, their union fails to find it as well. However, in general it is useful to combine different criteria in this way, as my empirical results below show.

5.2.4 The "interleave" Method

I now present what I consider is the logical conclusion of the observations above. To the best of my knowledge, the approach is novel. The idea is to query each of the mixture components for the points it "believes" should be hints. We do this as follows. Let c be a component and i a data point. The EM algorithm maintains, for every c and i, an estimate z_i^c of the degree of "ownership" that c exerts over i. For each component c we create a list of all the points, ranked by z_i^c.

Having constructed the sorted lists, we merge them in a generalization of the merge method described above. We cycle through the lists in some order. For each list, we pick the top item that has not already been placed in the output list, and place it at the next position in the output list.

The results for this strategy are shown in Figure 5.6. We see it meets the requirement of comprehensive representation for all true components. Most of the points are along the major axes of the two elongated Gaussians, but two of the points are inside the small circle. Correct labels for even just these two points result in perfect classification in the next EM run.

To gain insight for this method we look at the estimates z_i^c. These are measures of the conditional likelihood of point i given that it was generated by component c, normalized by the sum of the same measure over all components c'. To minimize z_i^c the point needs to have a low conditional likelihood for c (this is the numerator) and a high denominator. For a high sum over all components, it is not enough for a point to be nearly uniquely owned by a single component. Rather, it needs to be fairly equally "divided" among the components. Intuitively, this means that for a component c to nominate a point, it needs to be considered unlikely for c, and also not obviously belong to some other component. This means that each component c identifies low-likelihood points that are "orphaned" by all of the other components.

Using separate component lists, we can in fact detect two different kinds of mis-modeled points. See Figure 5.7. The first kind are points which are associated with some component, and are similar in many ways to most of the other points in it. However they are slightly different — for example, they may have an outlying value in just one attribute. These points will be flagged because they are in a low-density region for this components. The other kind are points which are isolated in "empty" regions, and do not naturally belong to a particular component. In some cases these points will be picked up by the closest (in density space) component, and will be flagged in the same way. But it is also possible to introduce a uniform-density "background" component. This component gets to nominate in the usual way. By its nature, it picks up the "orphan" points which do not naturally belong to any other component. This way, isolated points will be ranked highly in the hint list.

Admittedly, the discussion above is merely an illustrative example. Below I present empirical evidence further supporting the same ideas.

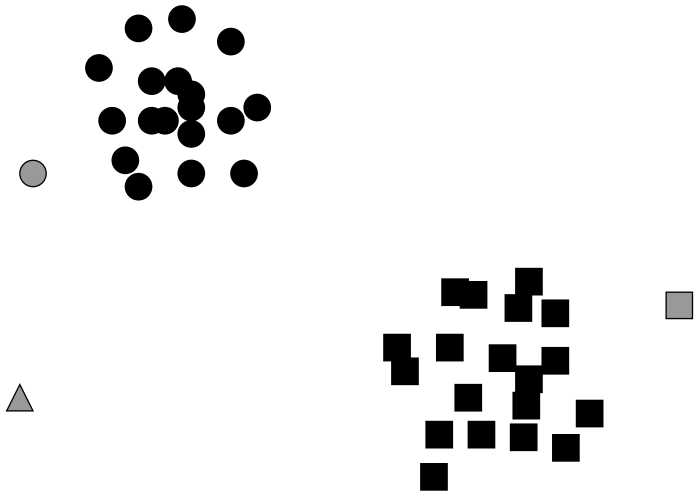

Figure 5.7: Different kinds of detected anomalies. The gray points are anomalies: the square and circle still belong to the respective components, while the triangle is an isolated anomaly.

5.3 Experimental Results

To establish the results hinted by the intuition above, I conducted a series of experiments. The first one uses synthetic data. The data distribution is a mixture of components in $5, 10, 15$ and 20 dimensions. The class size distribution is a geometric series with the largest class owning half of the data and each subsequent class being half as small.

The components are multivariate Gaussians whose covariance structure can be modeled with dependency trees. Each Gaussian component has its covariance generated in the following way. Random attribute pairs are chosen, and added to an undirected dependency tree structure unless they close a cycle. Each edge describes a linear dependency between nodes, with the coefficients drawn at random. Additionally, random noise is added to each value. Each data set contains $10,000$ points. There are ten tree classes and a uniform background component, with size ranging from 50 to 200 points. Only the results for 15 dimensions and 100 noisy points are shown as they are representative of the other experiments. In each round of learning the learner queries the teacher with a list of 50 points for labeling, and has access to all the queries it submitted previously and their replies.

This data generation scheme is still very close to the one which our tested model assumes. Note, however, that I do not require different components to be easily identifiable. The results of this experiment are shown in Figure 5.8.

Our scoring function is driven by our application, and estimates the amount of effort the teacher has to expend before being presented by representatives of every single class. The assumption is that the teacher can generalize from a single example (or a very few examples) to an entire class, and the valuable information is concentrated in the first queried member of each class. More precisely, if there are n classes, then the score under this metric is $1/n$ times the number of classes represented in the query set. In the query set I include all items queried in preceding rounds, as I do for other applicable metrics.

We now list of the names of the algorithms as they appear in the graphs, and a short description for each.

- lowlik This algorithm lists the least likely points first as described in Section 5.2.1.
- ambig This algorithm lists the most ambiguous points first as described in Section 5.2.2.
- mix-ambig-lowlik This algorithm merges the lists of lowlik and abmig as described in Section 5.2.3.
- interleave This algorithm lets each component "nominate" hints as described in Section 5.2.4, with the following modification. The background uniform-density component gets to nominate more often than any other component. In terms of list merging, we take one element from each of the lists of standard components, and then several elements from the list produced for the background component. All of the results shown were obtained using an oversampling ratio of 20.
- random This is a baseline method which chooses hints at random.

The best performer so far is interleave, taking five rounds or less to reveal all of the classes, including the very rare ones. Below I show how it is superior in most of the real-life data sets as well. We can also see that ambig performs worse than random. This can be explained by the fact that ambig only chooses points that already have several existing components "competing" for them. Rarely do these points belong to a new, yet-undiscovered component.

I was concerned that the poor performance of lowlik was just a consequence of my choice of metric. After all, it does not measure the number of noise points found. So it is possible that lowlik is being penalized unfairly for its focusing on the noise points. After examining the fraction of noise points (i.e., points drawn from the

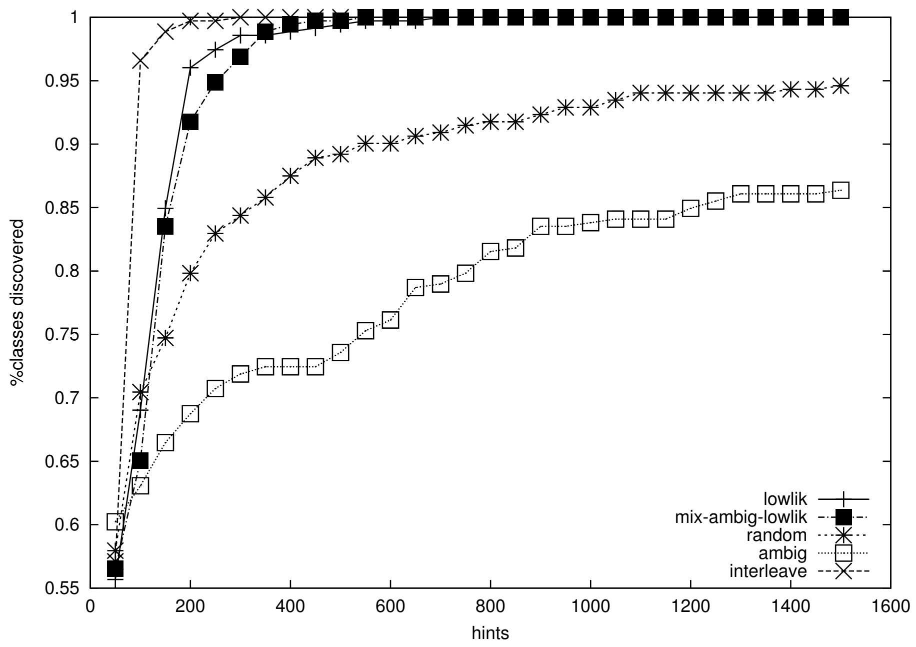

Figure 5.8: Learning curves for simulated data drawn from a mixture of dependency trees. The Y axis shows the fraction of classes represented in queries sent to the teacher.

uniform background component) found by each algorithm, I discovered that lowlik actually scores worse than interleave even on this metric. Additionally, I repeated the experiment, this time generating no points from the background class, and the results were essentially identical to Figure 5.8.

The remaining experiments were run on various standard and real data sets. Table 5.1 has a summary of their properties. The sets ABALONE and KDD are taken from the UCI repository (Blake & Merz, 1998). The SHUTTLE set is from the StatLog project (P.Brazdil & J.Gama, 1991). The EDSGC set was used in (Nichol et al., 2000). The SDSS set is derived from the Sloan Digital Sky Survey's Data Release One (SDSS, 1998).

Results for the ABALONE set appear in Figure 5.9. For this set, I first removed the "sex" attribute, which is not numerical. I used the "rings" attribute (the target for classification) as the class label. I then labeled all members of classes smaller than ten elements to be in the "background" class. We see that it takes the interleave algorithm ten rounds to spot all classes, whereas the next best are random, requiring 32 and lowlik, with 37. Also we see again that ambig can perform more poorly than random selection. This did not repeat in the SHUTTLE set (see Figure 5.10). Here, we

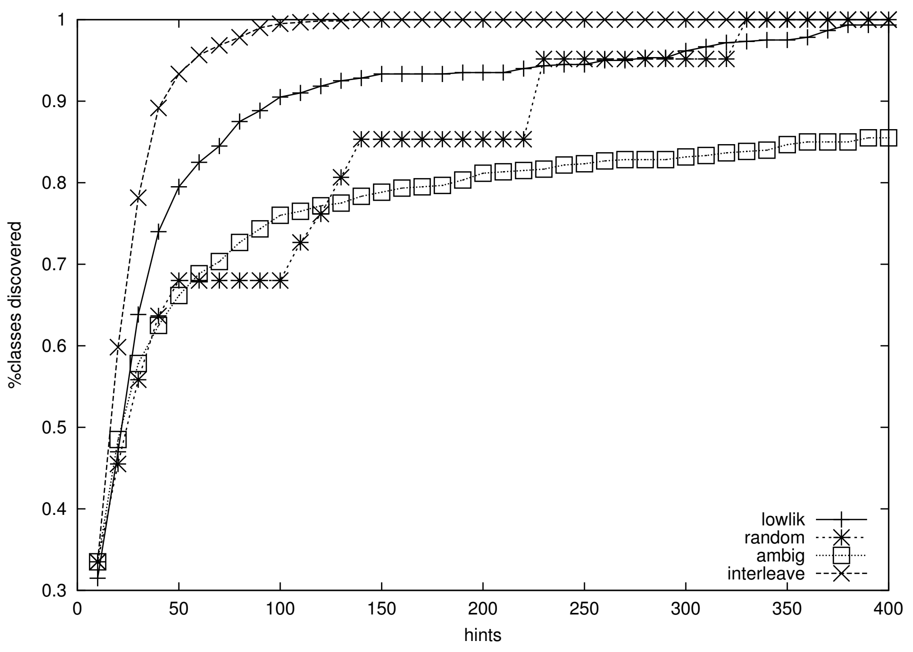

Figure 5.9: Learning curves for the ABALONE set. In each round the learner issues 10 queries.

also observe that unlike previous experiments, lowlik is nearly as good as interleave. However interleave is again the best performer.

Due to resource limitations, results for kdd were obtained on a 50000-record random sub-sample of the original training set (which is roughly ten times bigger). This set has an extremely skewed distribution of class sizes, and a large number of classes. In Figure 5.11 we see that lowlik performs uncharacteristically poorly. Another surprise is that the combination of lowlik and ambig outperforms them both. It also outperforms interleave, and this is the only case where I have seen it do so.

The EDSGC set, as distributed, is unlabeled. I added labels based on shapes derived from two attributes related to the shape and size of the observed sky object (umajax and uminax). The two defining attributes were then removed from the data. The decision boundaries I imposed were linear in the space defined by the two attributes. This created polygonal classes which proved hard for my Gaussian-based tree nodes to model accurately. Nevertheless, we see in Figure 5.12 that for the purpose of class discovery, we can do a good job in a small number of rounds. This statement is also true for the SDSS data (Figure 5.13). Here a human would have had to label just 200 objects before being presented with a member of the smallest class - comprising just 240 records out of a set of half a million.

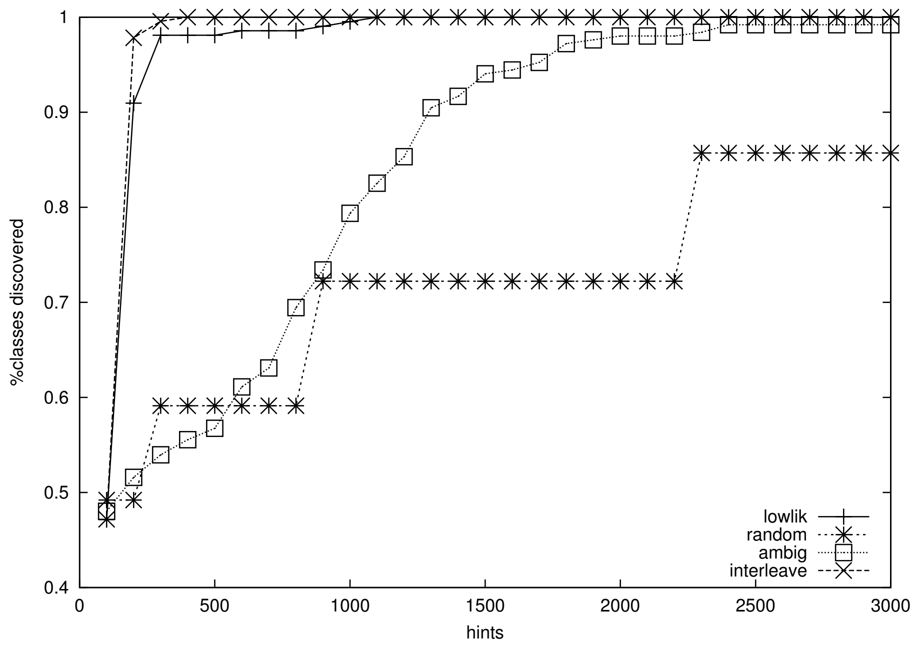

Figure 5.10: Learning curves for the SHUTTLE set. In each round the learner issues 100 queries.

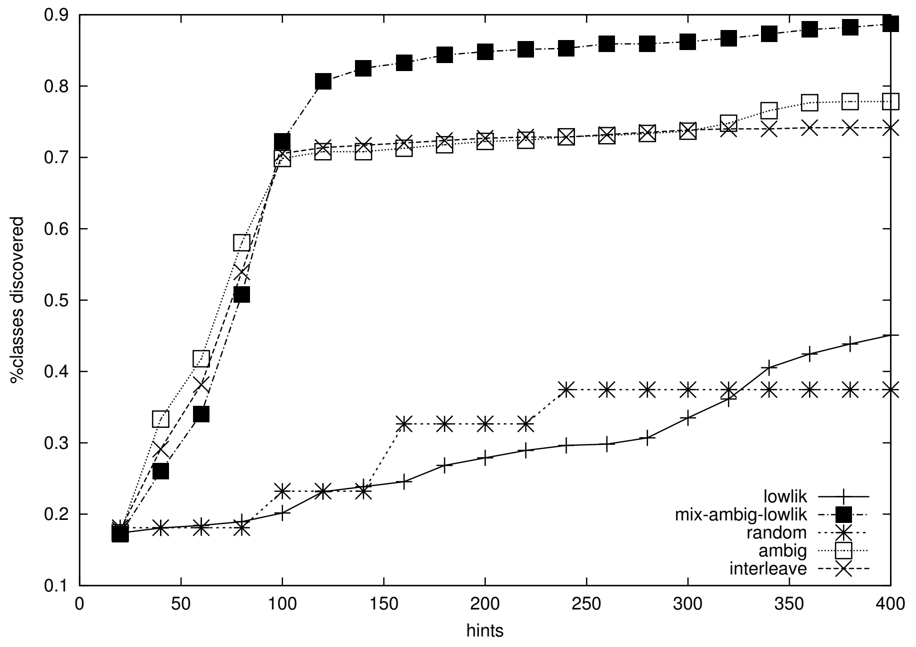

Figure 5.11: Learning curves for the KDD set. In each round the learner issues 20 queries.

Table 5.1: Properties of the data sets used.

NAME	DIMS	RECORDS	CLASSES	SMALLEST CLASS	LARGEST CLASS
ABALONE	7	4177	20	0.34%	16%
SHUTTLE	9	43500	7	0.01%	78.4%
KDD	33	50000	19	0.002%	21.6%
EDSGC	26	1439526	7	0.002%	76%
SDSS	22	517371	3	0.002%	50.6%

I also experimented with a hint-selection scheme which ranks the points solely on z_B^i, where B represents the background class. This can be thought of as changing the oversampling ratio in my version of interleave from 20 to infinity. In the six experiments described above, this scheme outperforms interleave just once.

Other methods I tested include variants of interleave where each component is only allowed to nominate points it owns as hints (i.e., component c can only mark i as a hint if $c = \arg\max_{c'} z_{c'}^i$). This turns out to perform very well, and yet not as well as interleave.

5.4 Scalability

The presentation so far ignored the size of the input set. In practice, this issue cannot be neglected. On the one hand, the very premise is huge data sets. On the other hand, a human interacts with the model and cannot be expected to wait too long for results. To accelerate model learning, I use mixtures of Gaussian dependency trees, and each component is learned with an accelerated Chow-Liu algorithm as in Chapter 4. This method scales very well for high dimensions and large number of records. Note that in two dimensions a dependency tree degenerates to a Gaussian, which is compatible with our example. Having implemented that, I discovered that the actual flagging of anomalies is the bottleneck, as it has to scan the entire data. For interactive sessions, I plan on implementing the hint-chooser in a background process, which will quickly show the user a few hints (chosen from a small sample), and later update the display as it progresses.

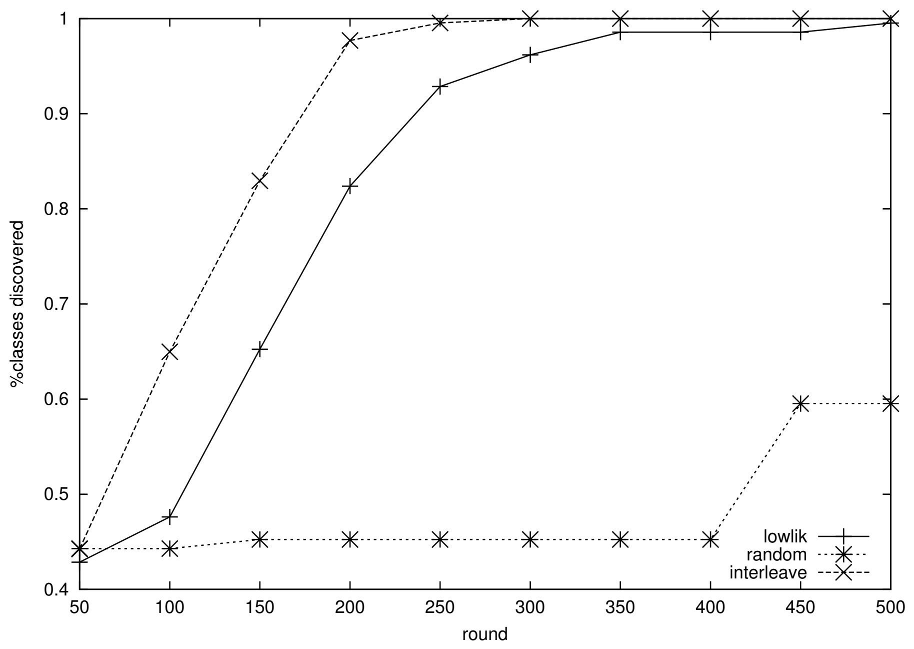

Figure 5.12: Learning curves for the EDSGC set. In each round the learner issues 50 queries.

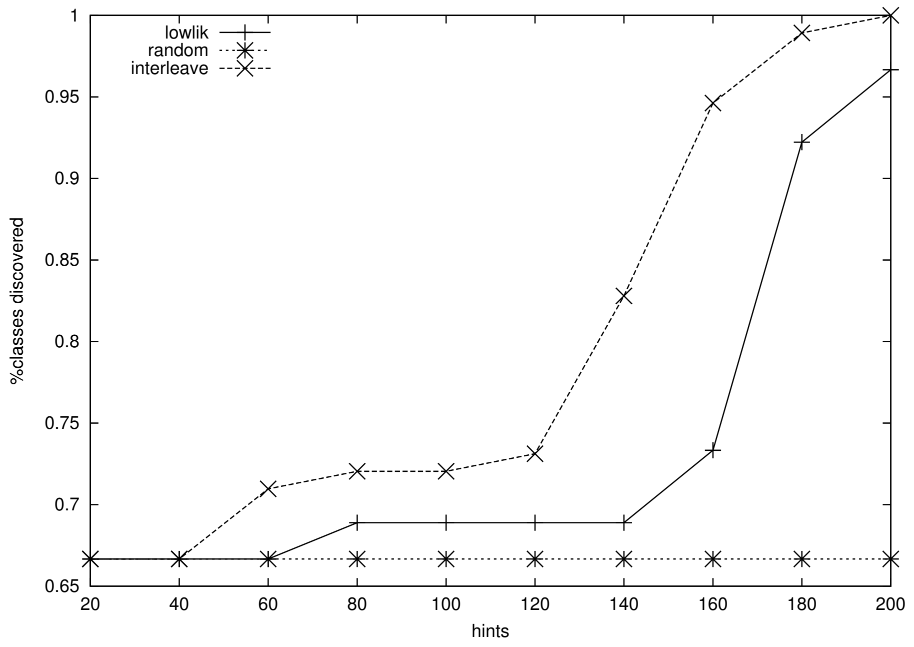

Figure 5.13: Learning curves for the SDSS set. In each round the learner issues 20 queries.

5.5 Conclusion

I have shown that some of the popular methods for active learning perform poorly in realistic active-learning scenarios. Working from the definition of a mixture model I was able to propose methods which let each component "nominate" its favorite queries. These methods work well in the presence of noisy data and extremely rare classes and anomalies. My simulations show that a human user only needs to label one or two hundred examples before being presented with very rare anomalies in huge data sets. This kind of interaction typically takes just an hour or two of combined human and computer time.

Furthermore, I make no assumptions about the particular form a component takes (beside it being a PDE). Consequently, I expect my results to apply to many different kinds of component models, including the case where components are not all from the same distribution.

I am using lessons learned from my empirical comparison in an application for anomaly-hunting in the astrophysics domain. My application presents multiple indicators to help a user spot anomalous data, as well as controls for labeling points and adding classes. Some interesting objects found after a few rounds of interaction with the Sloan data are shown in Figure 5.14. The application will be described in Chapter 6.

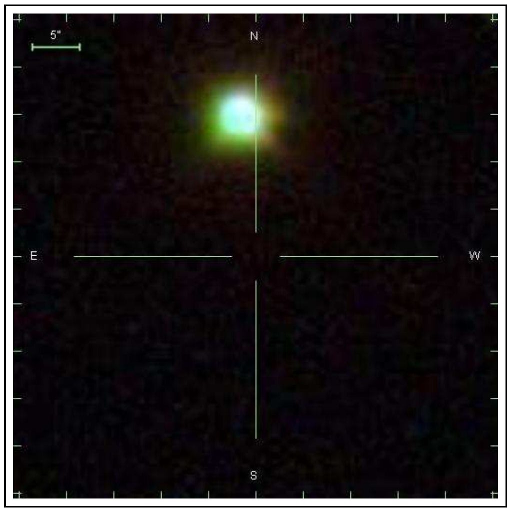

(a) Chromatic aberration

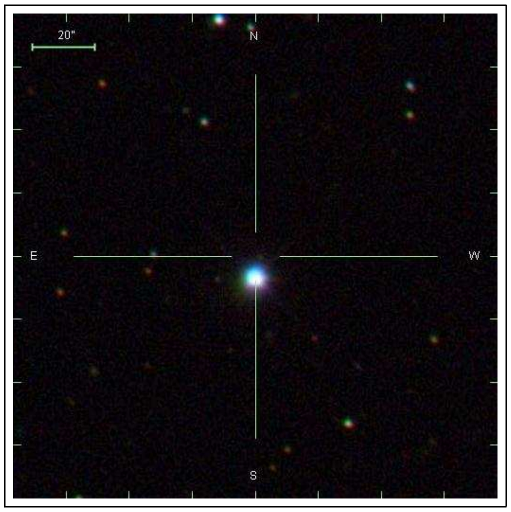

(b) Chromatic aberration

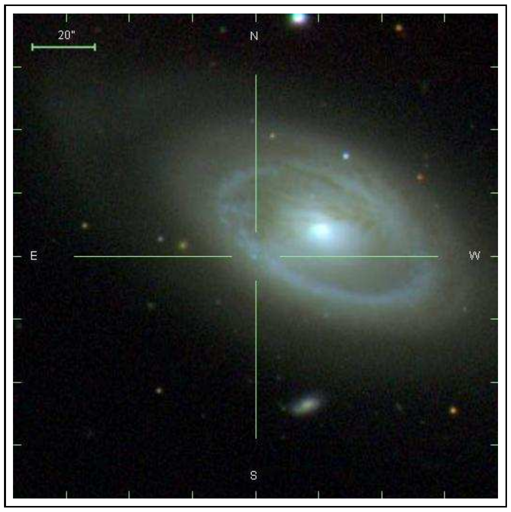

(c) An $H2$ region

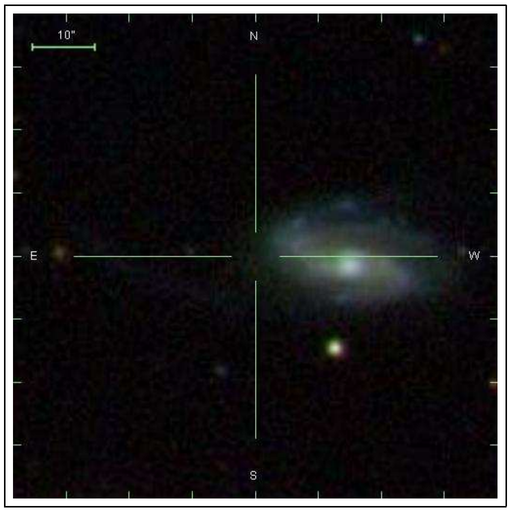

(d) A galaxy

Figure 5.14: Various objects spotted with the anomaly-hunting tool (Sloan data).

Chapter 6

Anomaly Hunting

This chapter describes a data-mining application which builds on the methods outlined in Chapter 5. The task is anomaly hunting in large data sets. The tool is generally geared towards astronomical observations, but can be directly applied to other kinds of data. I outline a new process using a combination of a graphical application, and the algorithmic techniques from the previous chapters. I also conducted a case study with a cosmologist analyzing SDSS data, and report the results.

6.1 Background

Before I start describing the new anomaly hunting process, I outline how similar analyses were carried out at the early stages of my involvement with such work. First, the raw data was not as well-organized as it is now. Mappings from object identifiers to image cutouts had to be done by hand. Once the images were obtained, they were viewed with generic image viewing and manipulation tools. Consequently, any kind of feedback had to also be carried over manually.

The main feedback loop proceeded as follows. After a night of telescope observations the results would be informally analyzed. Common characteristics of the anomalous objects which were boring or produced bad results were defined. Then, a predicate to filter them out of the data set was written manually. The cleaned data was fed to a learner and was fitted by a mixture of dependency trees. This is the same model as currently used. However no individual labels were assigned because of the difficulty of doing so. Instead, the learner itself decided how to split the data among classes. The current learner still has this capability, but it falls back to it only in the absence of specific labels.

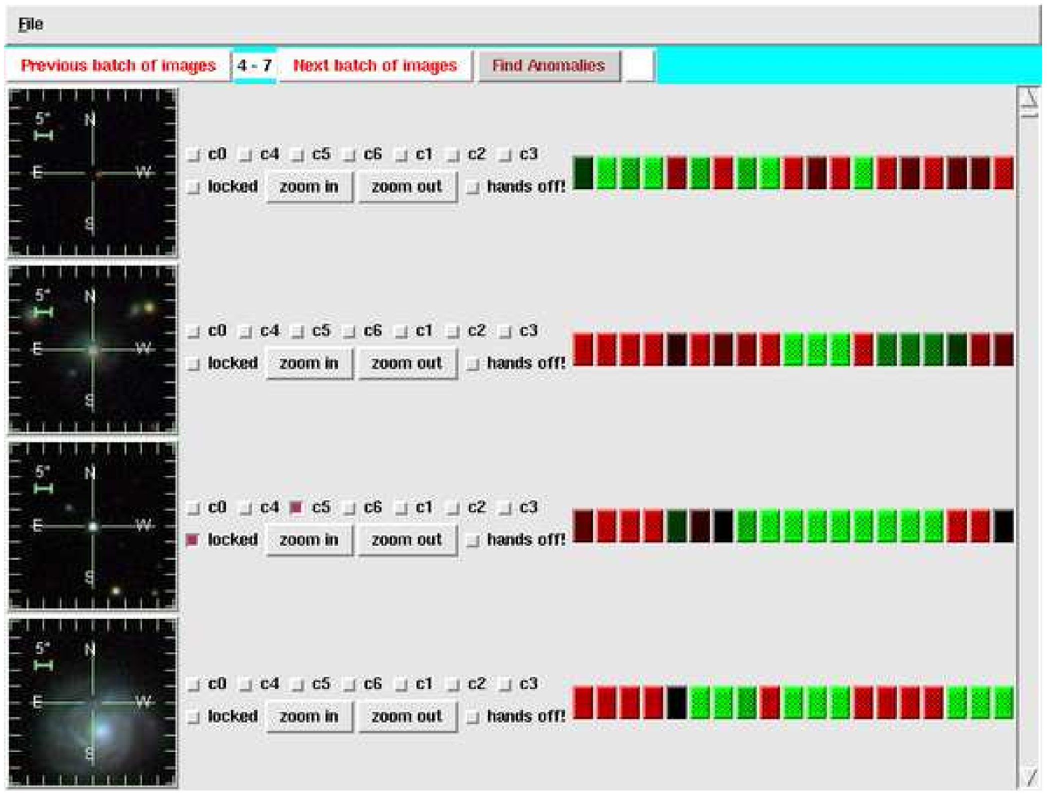

Figure 6.1: The anomaly hunting application.

6.2 Indicators and Controls

The main interaction screen for the current tool is shown in Figure 6.1. On the left we see "postage stamp" photos of several objects. The objects are shown as ordered by the anomaly hunting algorithm. Generally speaking, the least well-explained object is in the top spot, and the objects are "more normal" as one progresses down the list. The user can scroll the list of objects to see other batches of photos.

The colored rectangles on the right indicate the value each object takes on for different attributes. The goal is to provide a quick way of comparing numerical values. Each column of rectangles is for a different attribute. For example, all the leftmost rectangles in the picture stand for the value of "isoAGrad_r" for the respective objects. The values are quantized and color-coded. Black means the value for this object and attribute is close to the median for the attribute, taken over the entire data. Red means above median, and the brighter shade of red is used, the higher quantile the value falls in. Similarly, green means under-median values, with the darkest green standing for the lowest value.

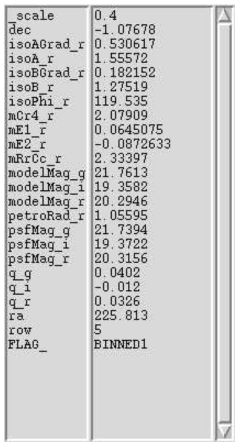

_scale	0.4
dec	-1.07678
isoAGrad_r	0.530617
isoA_r	1.55572
isoBGrad_r	0.182152
isoB_r	1.27519
isoPhi_r	119.535
mCr4_r	2.07909
mE1_r	0.0645075
mE2_r	-0.0872633
mRrCc_r	2.33397
modelMag_g	21.7613
modelMag_i	19.3582
modelMag_r	20.2946
petroRad_r	1.05595
psfMag_g	21.7394
psfMag_i	19.3722
psfMag_r	20.3156
q_g	0.0402
q_i	-0.012
q_r	0.0326
ra	225.813
row	5
FLAG_	BINNED1

Figure 6.2: The object information window.

The class buttons (labeled c0 through c6 in this example) let the user assign labels to objects. Whenever the user believes that an object naturally belongs to a certain class, he or she can check the box next to the appropriate label. The names are arbitrary and selected by the user. Multiple labels are supported, as well as assigning no label. New labels can be created freely.

The "locked" button indicates that the underlying statistical modeling stage may not re-assign this object to a class other than the one specified by the user. By default it is selected. If it is not, the specified label is used to seed the EM process, but can otherwise change if this (locally) improves the fit.

The "zoom" controls let the user zoom the photo in and out. This is supported by an on-line repository which provides arbitrary image cut-outs. The SkyServer (Szalay et al., 2004) is one such repository which we use for the astronomical data.

When selecting an object, a window with detailed information about the object pops up. An example is shown in Figure 6.2. It simply lists the exact values for the object in each of a specified list of attributes. This provides a way to examine an object's parameters exactly.

The "Find Anomalies" button runs the back-end anomaly finder. It takes the user-assigned labels into account, and outputs a new ranked list of anomalous objects. Once it terminates, the display changes to reflect the new order. The anomaly finder currently used is described in Chapter 5. It builds a model which is a mixture of dependency trees. The mixture components generally match the specified labels; a heuristic may split a label class into several mixture classes, all having the same name, if that improves the fit. After building the model, each objects is scored by it

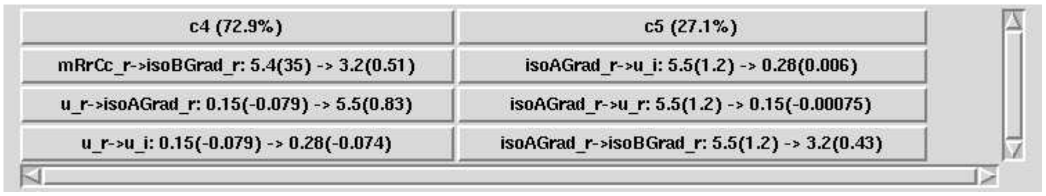

c4 (72.9%)	c5 (27.1%)
mRrCc_r->isoBGrad_r: 5.4(35) -> 3.2(0.51)	isoAGrad_r->u_i: 5.5(1.2) -> 0.28(0.006)
u_r->isoAGrad_r: 0.15(-0.079) -> 5.5(0.83)	isoAGrad_r->u_r: 5.5(1.2) -> 0.15(-0.00075)
u_r->u_i: 0.15(-0.079) -> 0.28(-0.074)	isoAGrad_r->isoBGrad_r: 5.5(1.2) -> 3.2(0.43)

Figure 6.3: The object explanation window.

according to the “interleave” order as described in Chapter 5.

If a model was constructed, clicking on an object’s photo brings up an “explanation” window which helps understand why the object is anomalous. Refer to Figure 6.3 for an example. We see that this objects is “split” between classes c4 and c5 (with weights 72.9% and 27.1%, respectively). For each component, a selection of three pairwise correlations is shown. Each one is a tree edge, and the display shows the values this particular object takes for them, as well as the average values for the whole data. For example, the first edge shown for class c4 is from “mRrCc_r” to “isoBGrad_r”. The average values for them are 35 and 0.51, respectively. The selected object has the values 5.4 and 3.2, respectively.

Additionally, each pair of attributes displayed can be selected for a plot. An example is shown in Figure 6.4. It shows the scatter-plot of the two attributes (“mRrCc_r” vs. “isoBGrad_r” in this case). The black points indicate objects that are mostly in the current class (here it is c4). Grey and light grey points indicated objects which mostly belong to other classes in varying degrees. A green regression line is also shown. The red dot indicates the current object. We can see that has an unusually high value for isoBGrad_r. This gives a clear visual explanation for selecting a particular edge. We often saw objects which have normal values for each of the (linearly correlated) attributes, but their joint value was highly unusual. This kind of anomaly is made very clear with a scatter-plot, and is hard to spot when examining any single parameter.

Another view of the selected object is a world wide web page for it on an online database. See Figure 6.5. It shows query results from the SkyServer. They include the photo, measured values for the object, cross-reference to observations of the same object in other surveys, and, if available, spectrographic data.

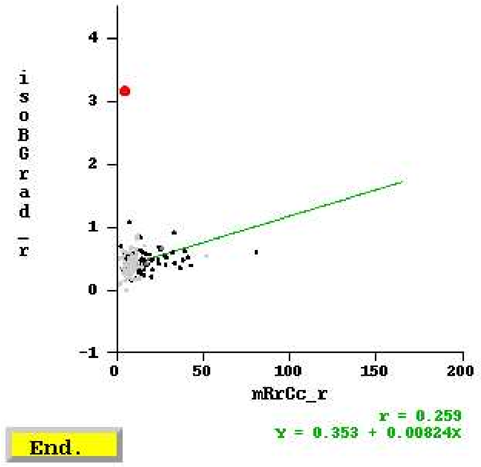

Figure 6.4: The scatterplot window.

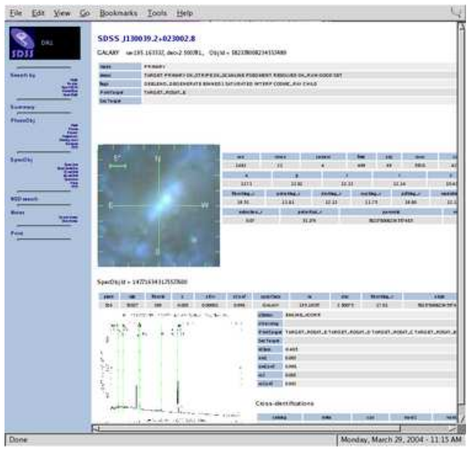

SDSS J130039.2+023002.8

Figure 6.5: The web window.

6.3 Case Study

I conducted an experiment where an astrophysicist used the tool to find anomalies in real SDSS data. The task is to identify objects with measurements that cannot be explained by current theories. For example, telescope time can be budgeted for these objects for further examination. Hopefully, they can provide insights into existing cosmological theories, and help form new ones.

The data is a derived from the SDSS Data Release 1 (Abazajian et al., 2003). Pre-processing steps include removing the objects which the existing software flagged as anomalous according to several known conditions. At the beginning of the experiment we noticed several anomalies (as defined by our program) had a value of 9999 in some attributes. This turned out to mark unknown values. Since only a small number of such objects existed, we removed them manually and the rest of the experiment, described below, was run on the cleaned data. The timeline for the experiment follows.

09:45:	Start of experiment.
10:00:	Spotted a low surface brightness object.
10:00:	Spotted a possible star/galaxy superimposition.
10:23:	Added a class "c0" for low surface brightness galaxies (keyed off mCr4_r vs. petrorad_r).
10:40:	Spotted an amorphous object.
10:40:	Spotted point sources around galaxy (possibly lensed).
10:39:	Added a class "c1".
10:55:	Spotted three sources in a row.
11:03:	Added a class "c2" for red point sources (keyed off q_q vs. q_r).
11:39:	Spotted a possible supernova.
11:40:	Spotted many edge-on galaxies; class "c4" created for them.
11:45:	Spotted a spiral galaxy with knots.
11:46:	Manual inspection of objects labeled by the model as c4: all but one of 5 or 6 of them are good.
11:55:	Added a class "c5" for bright blue objects.
12:30:	The c5 class is determined to be about 60% accurate.
12:31:	Added a class "c6" for any kind of point source.
13:00:	End of experiment.

All in all, the user inspected the details of about 500 objects over the course of the experiment. Of them, he gave labels to 216 objects. In addition, he noted 17 objects as "anomalous" (many of which marked as "spotted" in the timeline above) and intends to continue exploring them.

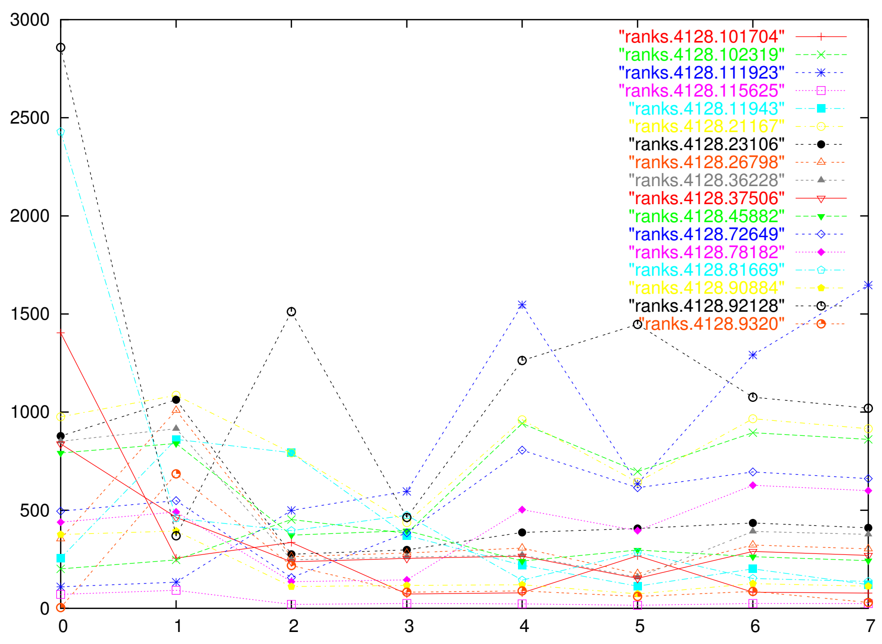

Figure 6.6: Ranks of each of 17 special objects, when analyzed by each of seven consecutive models.

After the experiment ended, I marked the 17 "special" objects to examine how their rankings changed over the course of the experiment. I used the same inputs given to the model learner to reconstruct each of the seven refinements built during the experiment. For each one, I recorded the rank of each of the special objects. See Figure 6.6. We can see that many objects achieve a high (top) ranking at one point or another. Remember that an anomaly only needs to be seen once by the expert.

6.3.1 Requested Features

A discussion followed the interaction with the program. Here are the features the user said would be beneficial in future versions:

- A view for all the objects in a given class (currently there exists a "search by class" functionality, but it only shows one object at a time).
- Ability to track the class size distribution.
- Ability to checkpoint label sets, to support experimentation with new labels and easily backtrack out of bad ones.

- The only criterion for displaying an object is its ranking on the anomaly list. This does not give the user direct control over objects to be excluded. A flag is needed that would inhibit the display of an object. Presumably such an object is some kind of boring anomaly that is not being modeled correctly even after labeling.

- Once a model is built, there needs to be an easy way to carry it over and apply it to a different data set. For example, a new batch of data from the same source might be available. It will have the same properties as the existing batch, so just the anomaly detection phase is needed.

6.4 Conclusion

The anomaly hunting application helps aggregate different kinds of information into a single view. This, combined with the anomaly finding back-end make it an efficient way to spot anomalies. Using it, a domain expert was able to spot, within the course of three hours, anomalies in data set containing half a million objects. By his judgment, this set includes all of the anomalies in this data. This statement is strengthened by the plot of object rankings over time and the timeline. Both indicate an overfitting effect and stabilization of model usefulness before the experiment ended.

When work on this tool started, there was very little support for viewing so much of the available data in one place. This step was done semi-manually and was time consuming. Now, new tools like the SkyServer help alleviate this problem. However, we are unaware of similar ways to incorporate feedback from the expert directly into the model. In this respect this is a unique tool.

Conclusion

I do not claim to have solved the data mining problem. For a start, we still lack a good definition of that problem. What can be said is that the research community successfully tackled several different tasks, arrived at crisp definitions for others, and is still attempting to come up with a grand view of everything. Here, I described a suite of related subproblems for cluster-based data mining.

It is undeniable that researchers generally have made huge progress in our ability to mechanically process raw data. This holds for our hardware, software, and mathematical foundations. But an often overlooked fact is that the human ability to grasp the information as presented did not change. Regardless of how big and complex the data is, we always need to reduce it to bite-size pieces. For example, traditional applications of clustering involved hundreds or thousands of biological measurements, and the output consisted of a (flat or nested) hierarchy of species, with up to a dozen or two elements. However, modern methods, such as microarrays, require processing of thousands of different elements, often resulting in complex structures that require new organization and visualization tools. The same happens in astronomical data, where scientists now manipulate high-order functions of large scale observations. A typical reduction in cosmology is processing of tens or hundreds of thousands of objects into the 2-point correlation function which succinctly describes their structure (Gray, 2003).

In the future, we can only expect this trend to continue. For instance, plans for new astronomical surveys call for data collection at the rate of a full SDSS survey equivalent — currently taking five years to complete — streaming in twice a week. While we can probably build hardware and software to process this much data in time, we cannot rely on a new breed of genius scientists to be able to read today's output repeated 1000-fold. So a big part of the success of such an endeavor would be algorithms that can summarize how the universe, as observed last night, is different from last week's version.

The bottom line is that we are still far from a Grand Unified Theory of data mining. But we approach it as fast as we can by solving collections of smaller issues, all seemingly arising from some common need.

Specifically, I concentrate on clustering. Its main advantage is its generality. Separating data into groups of similar objects reduces the perception problem significantly. The classical example is measurements of a population of several hundred crabs. After clustering, two similar — but different — species can be identified and each specimen labeled. Published work on the statistical foundations of this kind of modeling dates back more than 100 years (Pearson, 1894). A huge body of work follows to improve and expand the methods. Consequently, nowadays we can apply fast methods to simulate the creation of a universe, and then we can use results such as those presented here to cluster the resulting millions of galaxies in an attempt to better understand theories behind dark matter.

Relating back to contributions of this work, my fast K-means algorithm presented in Chapter 1 gives a two orders of magnitude speedup in low-dimensional data, and influenced similar works in high dimensions. I extended it into an efficient framework to choose the number of clusters in Chapter 2. My implementation of both of these was made available to researchers and was downloaded by over 200 users. It was used in numerous published and unpublished works. Among them:

- cDNA microarray data. K-means is run repeatedly on a small subset of the total data (Bainbridge, 2004).
- DNA microarray gene expression levels (Ballini, 2003; Qian, 2001).
- Prediction of functional RNA genes in genomic sequences. The data is clustered for the purpose of drawing negative examples for the training set. There are about 700 clusters and more than a million data points (Meraz, 2002).
- Music information retrieval (Logan & Salomon, 2001; Zissimopoulos, 2003). Multiple features vectors are extracted for each one of 8500 songs. A specialized inter-cluster distance metric is used to determine a distance matrix for song similarity.
- Computer program analysis in the Daikon package (Ernst et al., 2001). Likely invariants for a program are detected dynamically. To determine conditional properties of the program, X-means clustering is performed on the invariants.
- Computer architecture (Sherwood et al., 2002). A large trace (several billion instructions) of a computer program is taken. Instructions are grouped into

basic blocks. Time intervals of a program's execution are represented by a vector of counts of the times each basic block was executed. The vectors are clustered to determine phases in the program's execution.

- Natural language processing (Kruengkrai, 2004).
- Financial data analysis (Kallur, 2003).
- Multi-objective optimization with evolutionary algorithms (Koch, 2002).
- Molecular biology (Zhang, 2000).
- Image segmentation (Kruengkrai, 2004).
- Speaker identification.

In Chapter 3 I presented a novel mixture model to produce highly readable clusters. I also show how to fit it efficiently in the EM framework. I gave evidence that it makes the output of clustering easy for people to comprehend. It was used to aid in anomaly finding for highway traffic data (Raz et al., 2004). For example, a common misclassification failure was detected where the low-level software would determine some trucks had one axle. Another observation made clear was that a system-wide change occurred around November 1999. Later it was discovered that a vendor of one of the software components made unreported configuration changes at that date.

In Chapter 4 I applied a "probably approximately correct" approach to dependency-tree construction for numeric and categorical data. This allows quick processing of huge inputs with minimal loss of quality. Empirical evidence showed run time which is constant regardless of the input size, and depends only on intrinsic properties of the data.

In Chapter 5 I examined the issue of active learning for general mixtures, when applied to data containing very rare classes of anomalies. I showed that some of the popular methods for active learning perform poorly in realistic active-learning scenarios. I also proposed a model-agnostic framework which lets each component "nominate" its favorite queries, and gave evidence that it is superior to existing methods. The goal is to quickly find anomalies in large and noisy data sets. The active-learning "oracle" is a human expert which can tell useful anomalies from plain errors and known classes of irregularities. The challenge — which was met according to the empirical evaluation — is accurate classification without over-burdening the expert.

In Chapter 6 I combined principles from Chapters 4 and 5 and presented a graphical application that interacts with a human domain expert to find anomalies in complex and voluminous data sets. A case study showed its effectiveness on SDSS data.

In the final anomaly-hunting application, I used only models based on dependency trees. This does not imply that the other models mentioned cannot be used similarly. In fact, the active-learning technique described in Chapter 5 is component-agnostic. The only assumption it makes on the model is that it is a mixture model, with components that are probability density estimators. It is straightforward to substitute a K-means component from Chapter 1 or a rectangle-based model from Chapter 3. In fact, the mixture does not even have to be homogeneous, and can have components with different forms. The main message is that PDEs that can be estimated from data can also be combined into mixture models in the EM framework. In addition, the components are also useful in anomaly detection by appropriate use of the density function.

This raises the question of which model to use and when. I presented several different models, and each has its strong and weak points. I now give some rules-of-thumb to help choose an appropriate model.

- If the data is all numeric, and Euclidean distances in the induced space are meaningful, K-means is appropriate. Often, different dimensions have hugely varying ranges. If this is the case then pre-normalization should be performed. An easy way to do this is the linear transformation to make data in each dimension have zero mean and unit variance.
- If the number of clusters is not known in advance, then X-means can help find it autonomously. Another option is to use the anomaly finding tool to manually add or remove classes until a reasonable model is generated.
- If human perception of the generated model and the clusters is important, mixture of rectangles is the obvious choice.
- The K-means implementation is the most widely deployed and most robust. It is also very fast, especially with large numbers of data points and clusters, and low dimensionality.
- The fast dependency learner is most suited for learning high-dimensional numeric data. It is also appropriate for very large numbers of records.

This work opens several avenues for further progress. Below I list several which promise the most benefit.

- Explore various approaches to the "semi-supervised" learning stage. This is the part of the anomaly-hunting loop which considers a small set of labeled points and a much larger unlabeled set to build a PDE.
- Extend the dependency-tree learner so it can handle both continuous and discrete attributes in the same tree.
- Develop an X-means-inspired algorithm for mixtures of Gaussians. Like the algorithm discussed in Chapter 2, it will perform structure search based on local decisions. However the mixture components will be generalized Gaussians.
- Investigate alternative approaches to the hint-nomination stage of the anomaly detector from Chapter 5.
- Accelerate the mixture-of-rectangles algorithm from Chapter 3. The sufficient statistics needed for the function optimization step are, at most, the one-dimensional projections of each attribute. It seems possible to leverage this fact into a fast algorithm. It would also benefit from a public release of the code so it can be used by researchers.
- Apply the technology introduced in Chapter 4 to the full problem of Bayes Net structure search.
- Make the fast dependency-tree algorithm in Chapter 4 more disk-access friendly. This can be achieved by splicing the input into several files, one per attribute, and keeping a memory buffer of segments of the files.
- Improve the anomaly hunting process from Chapter 6 by incorporating the suggested improvements identified in the case study. The tool itself is rather prototypical. Therefore it might be worthwhile to design new tool from scratch. This also has the advantage of allowing better integration with the data views and APIs currently offered by the SDSS project's SkyServer.
- Improve the perceived latency in the anomaly finding stage of the anomaly hunter tool. Once the user instructs the tool to find anomalies, a set of anomalies is chosen from a small sample of the data. This sample can be random, but should also include anomalies previously flagged. Processing of the full data set will occur in the background. Whenever it finds anomalies better than currently on display, the front end will be notified and updated.

Bibliography

Abazajian, K., Adelman-McCarthy, J., Ageros, M., Allam, S., Anderson, S., & et al (2003). The first data release of the sloan digital sky survey. *Astronomical Journal*, *126*.

Agrawal, R., Gehrke, J. E., Gunopulos, D., & Raghavan, P. (1998). Automatic subspace clustering of high dimensional data for data mining applications. *Proc. ACM SIGMOD Int. Conf. Management of Data*, *27*, 94–105.

AlSabti, K., Ranka, S., & Singh, V. (1999). An efficient space-partitioning based algorithm for the K-means clustering. *Proceedings of the 3rd Pacific-Asia Conference on Methodologies for Knowledge Discovery and Data Mining (PAKDD-99)* (pp. 355–359). Berlin: Springer.

Bainbridge, M. (2004). Personal communication.

Ballini, M. (2003). Personal communication.

Baram, Y., El-Yaniv, R., & Luz, K. (2003). Online choice of active learning algorithms. *Proceedings of the Twentieth International Conference on Machine Learning*.

Basu, S., Banerjee, A., & Mooney, R. J. (2004). Active semi-supervision for pairwise constrained clustering. *Proceedings of the SIAM International Conference on Data Mining (SDM-2004)*. Lake Buena Vista, FL.

Bentley, J. L. (1980). Multidimensional Divide and Conquer. *Communications of the ACM*, *23*, 214—229.

Bezdek, J. C. (1981). *Pattern recognition with fuzzy objective function algorithms.* Plenum Press.

Bishop, C. M. (1995). *Neural networks for pattern recognition.* Oxford: Clarendon Press.

Blake, C., & Merz, C. (1998). UCI repository of machine learning databases. `http://www.ics.uci.edu/∼mlearn/MLRepository.html`.

Bradley, P. S., & Fayyad, U. M. (1998). Refining initial points for K-Means clustering. *Proceedings of the Fifteenth International Conference on Machine Learning* (pp. 91–99). Morgan Kaufmann, San Francisco, CA.

Bradley, P. S., Fayyad, U. M., & Reina, C. (1998). Scaling clustering algorithms to large databases. *Proceedings of the Fourth International Conference on Knowledge Discovery and Data Mining (KDD-98)* (pp. 9–15). New York: AAAI Press.

Brinker, K. (2003). Incorporating diversity in active learning with support vector machines. *Proceedings of the Twentieth International Conference on Machine Learning*.

Chow, C. K., & Liu, C. N. (1968). Approximating discrete probability distributions with dependence trees. *IEEE Transactions on Information Theory*, *14*, 462–467.

Cohn, D., Atlas, L., & Ladner, R. (1994). Improving generalization with active learning. *Machine Learning*, *15*, 201–221.

Cohn, D. A., Ghahramani, Z., & Jordan, M. I. (1995). Active learning with statistical models. *Advances in Neural Information Processing Systems* (pp. 705–712). The MIT Press.

Cormen, T. H., Leiserson, C. E., & Rivest, R. L. (1989). *Introduction to algorithms*. McGraw-Hill.

Cozman, F. G., Cohen, I., & Cirelo, M. C. (2003). Semi-supervised learning of mixture models and bayesian networks. *Proceedings of the Twentieth International Conference on Machine Learning*.

Dasgupta, S. (2000). Experiments with random projection. *Proceedings of the 16th Conference in Uncertainty in Artificial Intelligence* (pp. 143–151). San Francisco, CA: Morgan Kaufmann.

Deng, K., & Moore, A. W. (1995). Multiresolution instance-based learning. *Proceedings of the Twelfth International Joint Conference on Artificial Intelligence* (pp. 1233–1242). San Francisco: Morgan Kaufmann.

Domingos, P., & Hulten, G. (2000). Mining high-speed data streams. *Proceedings of 6th International Conference on Knowledge Discovery and Data Mining* (pp. 71–80). N. Y.: ACM Press.

Domingos, P., & Hulten, G. (2001a). A general method for scaling up machine learning algorithms and its application to clustering. *Proceedings of the Eighteenth International Conference on Machine Learning*. Morgan Kaufmann.

Domingos, P., & Hulten, G. (2001b). Learning from infinite data in finite time. *Advances in Neural Information Processing Systems 14*. Vancouver, British Columbia, Canada.

Duda, R. O., & Hart, P. E. (1973). *Pattern Classification and Scene Analysis.* John Wiley & Sons.

Elkan, C. (2003). Using the triangle inequality to accelerate k-means. *Proceedings of the Twentieth International Conference on Machine Learning (ICML 2003)* (pp. 147–153). AAAI Press.

Eppstein, D. (2000). Fast hierarchical clustering and other applications of dynamic closest pairs. *J. Experimental Algorithmics*, *5*, 1–23.

Ernst, M., Cockrell, J., Griswold, W., & Notkin, D. (2001). Dynamically discovering likely program invariants to support program evolution. *IEEE Transactions on Software Engineering (TSE)*, *27*, 1–25.

Ester, M., Kriegel, H.-P., & Xu, X. (1995). A database interface for clustering in large spatial databases. *Proceedings of First International Conference on Knowledge Discovery and Data Mining.* Menlo Park: AAAI.

Farnstrom, F., Lewis, J., & Elkan, C. (2000). Scalability for clustering algorithms revisited. *SIGKDD Explorations*, *2*, 51–57.

Fasulo, D. (1999). An analysis of recent work on clustering algorithms. `http://www.cs.washington.edu/homes/dfasulo/clustering.ps`.

Friedman, J., & Fisher, N. (1999). Bump hunting in high-dimensional data. *Statistics and Computing*, *9*, 1–20.

Friedman, N., Goldszmidt, M., & Lee, T. J. (1998). Bayesian Network Classification with Continuous Attributes: Getting the Best of Both Discretization and Parametric Fitting. *Proceedings of the Fifteenth International Conference on Machine Learning.* Morgan Kaufmann, San Francisco, CA.

Friedman, N., Nachman, I., & Peér, D. (1999). Learning bayesian network structure from massive datasets: The "sparse candidate" algorithm. *Proceedings of the 15th Conference on Uncertainty in Artificial Intelligence (UAI-99)* (pp. 206–215). Stockholm, Sweden.

Gersho, A., & Gray, R. (1992). *Vector quantization and signal compression.* Kluwer Academic Publishers; Dordrecht, Netherlands.

Gray, A. (2003). *Bringing tractability to generalized n-body problems in statistical and scientific computation.* Doctoral dissertation, Carnegie-Mellon University.

Guha, S., Rastogi, R., & Shim, K. (1998). CURE: An efficient clustering algorithm for large databases. *Proceedings of the ACM SIGMOD International Conference on Management of Data (SIGMOD-98)* (pp. 73–84). New York: ACM Press.

Hamerly, G. (2003). *Learning structure and concepts in data through data clustering.* Doctoral dissertation, University of California, San Diego.

Hamerly, G., & Elkan, C. (2002). Alternatives to the k-means algorithm that find better clusterings. *Proceedings of the 2002 ACM CIKM International Conference on Information and Knowledge Management* (pp. 600–607). McLean, VA, USA: ACM.

Hamerly, G., & Elkan, C. (2003). Learning the k in k-means. *Advances in Neural Information Processing Systems 17*. MIT Press.

Hettich, S., & Bay, S. D. (1999). The UCI KDD archive. `http://kdd.ics.uci.edu`.

Hofmann, T., & Buhmann, J. M. (1997). Pairwise data clustering by deterministic annealing. *IEEE Transactions on Pattern Analysis and Machine Intelligence*, *19*, 1–14.

Kallur, S. (2003). Personal communication.

Kass, R., & Wasserman, L. (1995). A reference Bayesian test for nested hypotheses and its relationship to the Schwarz criterion. *Journal of the American Statistical Association*, *90*, 773–795.

Kearns, M., Mansour, Y., & Ng, A. Y. (1997). An information-theoretic analysis of hard and soft assignment methods for clustering. *Proceedings of the 13th Conference on Uncertainty in Artificial Intelligence (UAI-97)* (pp. 282–293). San Francisco: Morgan Kaufmann Publishers.

Koch, T. E. (2002). Personal communication.

Kruengkrai, C. (2004). Personal communication.

LCRS (1998). *Las campanas redshift survey.* LCRS. `http://manaslu.astro.utoronto.ca/∼lin/lcrs.html`.

Lewis, D. D., & Catlett, J. (1994). Heterogeneous uncertainty sampling for supervised learning. *Proceedings of the Eleventh International Conference on Machine Learning* (pp. 148–156). New Brunswick, US: Morgan Kaufmann.

Liu, B., Xia, Y., & Yu, P. (2000). *Clustering through decision tree construction* (Technical Report RC21695). IBM Research.

Logan, B., & Salomon, A. (2001). A music similarity function based on signal analysis. *IEEE International Conference on Multimedia and Expo.*

Maass, W., & Warmuth, M. K. (1995). Efficient learning with virtual threshold gates. *Proc. 12th International Conference on Machine Learning* (pp. 378–386). Morgan Kaufmann.

MacKay, D. (1992). Information-based objective functions for active data selection. *Neural Computation*, *4*, 590–604.

Maron, O., & Moore, A. W. (1994). Hoeffding races: Accelerating model selection search for classification and function approximation. *Advances in Neural Information Processing Systems* (pp. 59–66). Denver, Colorado: Morgan Kaufmann.

Mehta, M., Agrawal, R., & Rissanen, J. (1996). SLIQ: A fast scalable classifier for data mining. *5th Intl. Conf. on Extending Database Technology.*

Meila, M. (1999a). An accelerated chow and liu algorithm: fitting tree distributions to high dimensional sparse data. *Proceedings of the Sixteenth International Conference on Machine Learning.*

Meila, M. (1999b). *Learning with mixtures of trees.* Doctoral dissertation, Massachusetts Institute of Technology.

Meila, M., & Heckerman, D. (1998). *An experimental comparison of several clustering and initilalization methods* (Technical Report 98-06). Microsoft Research, Redmond, WA.

Meraz, R. (2002). Personal communication.

Miller, D. J., & Uyar, H. S. (1997). A mixture of experts classifier with learning based on both labeled and unlabelled data. *Advances in Neural Information Processing Systems 9.*

Moore, A. (1998). Very fast EM-based mixture model clustering using multiresolution kd-trees. *Advances in Neural Information Processing Systems 10* (pp. 543–549). Morgan Kaufmann.

Moore, A. (2000). The anchors hierarchy: Using the triangle inequality to survive high dimensional data. *Proceedings of the 16th Conference on Uncertainty in Artificial Intelligence* (pp. 397–405). San Francisco, CA: Morgan Kaufmann.

Moore, A. W. (1991). *Efficient memory-based learning for robot control.* Doctoral dissertation, University of Cambridge. Technical Report 209, Computer Laboratory, University of Cambridge.

Moore, A. W., & Lee, M. S. (1994). Efficient algorithms for minimizing cross validation error. *Proceedings of the Eleventh International Conference on Machine Learning* (pp. 190–198). New Brunswick, US: Morgan Kaufmann.

Moore, A. W., & Lee, M. S. (1998). Cached sufficient statistics for efficient machine learning with large datasets. *Journal of Artificial Intelligence Research*, *8*, 67–91.

Nagesh, H., Goil, S., & Choudhary, A. (1999). *MAFIA: Efficient and scalable subspace clustering for very large data sets* (Technical Report 9906-010). Northwestern University.

Ng, R. T., & Han, J. (1994). Efficient and effective clustering methods for spatial data mining. *Proceedings of VLDB.*

Nichol, R. C., Collins, C. A., & Lumsden, S. L. (2000). The Edinburgh/Durham southern galaxy catalogue — IX. Submitted to the Astrophysical Journal.

P.Brazdil, & J.Gama (1991). StatLog. `http://www.liacc.up.pt/ML/statlog`.

Pearson, K. (1894). Contributions to the mathematical theory of evolution. *Philosophical Transaction A*, *185*, 71–110.

Pelleg, D. (2003). Hunting anomalies in sloan data. *Proc. 7th Great Lakes Cosmology Workshop.*

Pelleg, D., & Moore, A. (1999). Accelerating exact k-means algorithms with geometric reasoning. *Proceedings of the Fifth ACM SIGKDD International Conference on Knowledge Discovery and Data Mining* (pp. 277–281). New York, NY: AAAI Press. An extended version is available as Technical Report CMU-CS-00-105.

Pelleg, D., & Moore, A. (2000a). *Accelerating exact k-means with geometric reasoning* (Technical Report CMU-CS-00-105). Carnegie Mellon University. Also available from `http://www.cs.cmu.edu/∼dpelleg/`.

Pelleg, D., & Moore, A. (2000b). X-means: Extending K-means with efficient estimation of the number of clusters. *Proc. 17th International Conf. on Machine Learning* (pp. 727–734). Morgan Kaufmann, San Francisco, CA.

Pelleg, D., & Moore, A. (2001). Mixtures of rectangles: Interpretable soft clustering. *Proc. 18th International Conf. on Machine Learning* (pp. 401–408). Morgan Kaufmann, San Francisco, CA.

Pelleg, D., & Moore, A. (2002). Using Tarjan's red rule for fast dependency tree construction. *Advances in Neural Information Processing Systems 15* (pp. 801–808). Cambridge, MA: MIT Press.

Plutowski, M., & White, H. (1993). Selecting concise training sets from clean data. *IEEE Transactions on Neural Networks*, *4*, 305–318.

Press, W. H., Teukolsky, S. A., Vetterling, W. T., & Flannery, B. P. (1992). *Numerical recipes in C, 2nd. edition.* Cambridge University Press.

Qian, Y. (2001). Personal communication.

Raz, O., Buchheit, R., Shaw, M., Koopman, P., & Faloutsos, C. (2004). Detecting semantic anomalies in truck weigh-in-motion traffic data using data mining. *Journal of Computing in Civil Engineering.*

Reza, F. (1994). *An introduction to information theory*, 282–283. New York: Dover Publications.

SDSS (1998). *The sloan digital sky survey.* SDSS. `www.sdss.org`.

Seeger, M. (2000). *Learning with labeled and unlabeled data* (Technical Report). Institue for Adaptive and Neural Computation, University of Edinburgh.

Seung, H. S., Opper, M., & Sompolinsky, H. (1992). Query by committee. *Computational Learning Theory* (pp. 287–294).

Shafer, J. C., Agrawal, R., & Mehta, M. (1996). SPRINT: A scalable parallel classifier for data mining. *Proc. 22nd Int. Conf. Very Large Databases* (pp. 544–555). Mumbai (Bombay), India: Morgan Kaufmann.

Shahshashani, B., & Landgrebe, D. A. (1994). The effect of unlabeled examples in reducing the small sample size problem. *IEEE Trans Geoscience and Remote Sensing*, *32*, 1087–1095.

Sherwood, T., Perelman, E., Hamerly, G., & Calder, B. (2002). Automatically characterizing large scale program behavior. *10th International Conference on Architectural Support for Programming Languages and Operating Systems.*

Stephens, M. A. (1974). EDF statistics for goodness of fit and some comparisons. *Journal of the American Statistical Association*, *69*, 730–737.

Szalay, A., Gray, J., Thakar, A., Boroski, B., Gal, R., Li, N., Kunszt, P., Malik, T., O'Mullane, W., Nieto-Santisteban, M., Raddick, J., Stoughton, C., & vandenBerg, J. (2004). The SDSS DR1 skyserver. To be published. `http://skyserver.sdss.org/`.

Tarjan, R. E. (1983). *Data structures and network algorithms*, vol. 44 of *CBMS-NSF Reg. Conf. Ser. Appl. Math.* SIAM.

Ueda, N., & Nakano, R. (1998). Deterministic annealing em algorithm. *Neural Networks*, *11*, 271–282.

Wasserman, L. (1997). *Bayesian model selection and model averaging* (Technical Report TR666). Carnegie Mellon University, Pittsburgh, PA. Also available from `http://www.stat.cmu.edu/www/cmu-stats/tr/tr666/tr666.html`.

Wiratunga, N., Craw, S., & Massie, S. (2003). Index driven selective sampling for CBR. *Proceedings of the Fifth International Conference on Case-Based Reasoning.* Trondheim, Norway: Springer-Verlag.

Witten, I. H., & Frank, E. (2000). *Data mining: Practical machine learning tools with java implementations.* San Francisco: Morgan Kaufmann.

Zhang, B., Hsu, M., & Dayal, U. (2000). *K-harmonic means - a data clustering algorithm* (Technical Report). Hewlett-Packard Labs.

Zhang, M. (2000). Personal communication.

Zhang, T., Ramakrishnan, R., & Livny, M. (1995). BIRCH: An efficient data clustering method for very large databases,. *Proceedings of ACM SIGMOD* (pp. 103–114).

Zissimopoulos, B. (2003). Personal communication.